AD-A087 656 NAVAL POSTGRADUATE SCHOOL MONTEREY CA F/G 4/1
OPTICAL AEROSOL SPECTROMETERS FACTORS AFFECTING OPTICAL EXTINCT--ETC(U)
APR 80 G E SCHACHER, K L DAVIDSON
UNCLASSIFIED NPS-61-80-013 NL

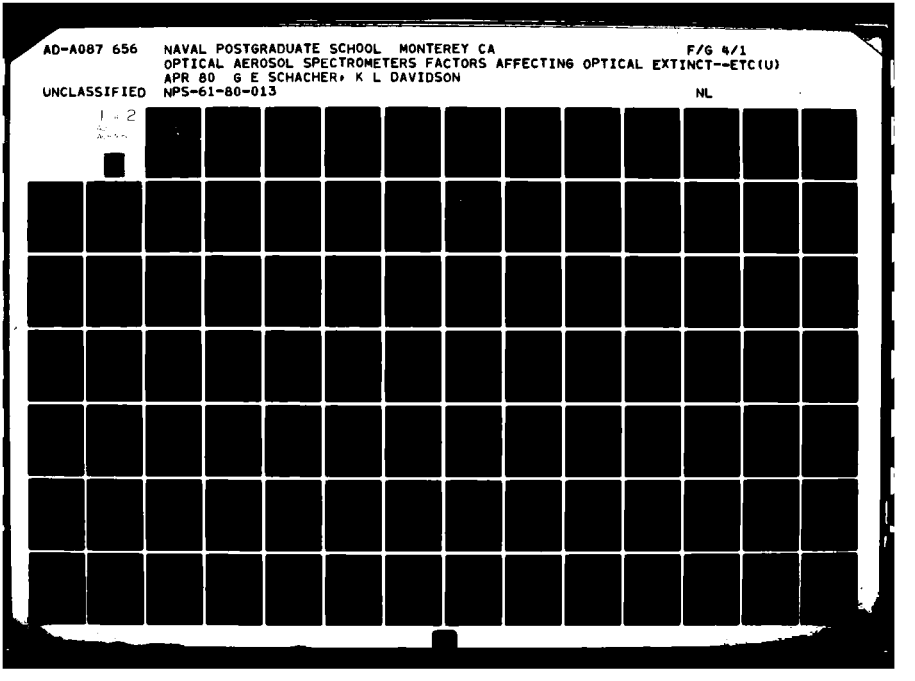

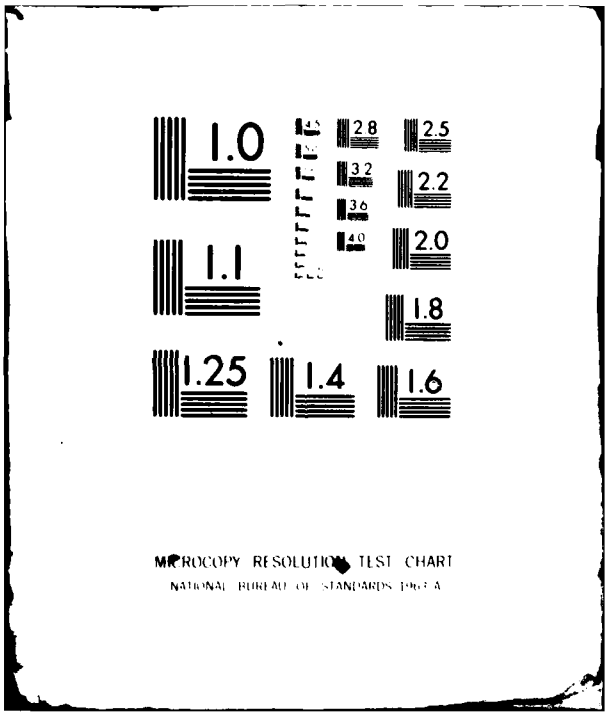
1.0
1.1
1.25
1.4
1.6
1.8
2.0
2.2
2.5
2.8
3.2
3.6
4.0
MICROCOPY RESOLUTION TEST CHART
NATIONAL BUREAU OF STANDARDS 1963-A

NPS 61-80-013

NAVAL POSTGRADUATE SCHOOL

Monterey, California

OPTICAL AEROSOL SPECTROMETERS
FACTORS AFFECTING OPTICAL
EXTINCTION PREDICTIONS

G. E. Schacher and K. L. Davidson
Environmental Physics Group
and C. W. Fairall, BDM Corporation

April 1980

Prepared for: Naval Ocean System Center
San Diego, California 92152

NAVAL POSTGRADUATE SCHOOL
Monterey, California

Rear Admiral J. J. Ekelund
Superintendent

J. R. Borsting
Provost

The work reported herein was supported in part by the California Air Resources Board, Sacramento, California.

This report was prepared by

Gordon E Schacher
G. E. Schacher
Professor of Physics

Kenneth L Davidson
K. L. Davidson
Associate Professor of Meteorology

C W Fairall
C. W. Fairall
BDM Corporation

Approved by:

J N Dyer
J. N. Dyer, Chairman
Department of Physics & Chemistry

G. J. Haltiner
G. J. Haltiner, Chairman
Department of Meteorology

William M. Tolles
William M. Tolles
Dean of Research

SECURITY CLASSIFICATION OF THIS PAGE (When Data Entered)

REPORT DOCUMENTATION PAGE

READ INSTRUCTIONS BEFORE COMPLETING FORM

1. REPORT NUMBER: NPS-61-80-013	2. GOVT ACCESSION NO.: AD-A087 656
3. RECIPIENT'S CATALOG NUMBER	
4. TITLE (and Subtitle): Optical Aerosol Spectrometers Factors Affecting Optical Extinction Predictions	5. TYPE OF REPORT & PERIOD COVERED: May 1978 - June 1979 Technical Report
6. PERFORMING ORG. REPORT NUMBER	
7. AUTHOR(s): G. E. Schacher, K. L. Davidson, C. W. Fairall	8. CONTRACT OR GRANT NUMBER(s): 19 Apr 80
9. PERFORMING ORGANIZATION NAME AND ADDRESS: Naval Postgraduate School, Code 61Sq, Monterey, California 93940	10. PROGRAM ELEMENT, PROJECT, TASK AREA & WORK UNIT NUMBERS: 97
11. CONTROLLING OFFICE NAME AND ADDRESS: Naval Ocean System Center (Code 532), San Diego, CA 92152	12. REPORT DATE: April 19, 1980
	13. NUMBER OF PAGES
14. MONITORING AGENCY NAME & ADDRESS (if different from Controlling Office): Technical Report, May 78-June 79	15. SECURITY CLASS. (of this report): Unclassified
	15a. DECLASSIFICATION/DOWNGRADING SCHEDULE

16. DISTRIBUTION STATEMENT (of this Report)

Approved for Public Release, Distribution Unlimited

17. DISTRIBUTION STATEMENT (of the abstract entered in Block 20, if different from Report)

18. SUPPLEMENTARY NOTES

19. KEY WORDS (Continue on reverse side if necessary and identify by block number)

Aerosols, Aerosol Spectrometers, Optical Extinction

20. ABSTRACT (Continue on reverse side if necessary and identify by block number)

Optical aerosol counters are used to measure aerosol spectra and thence to calculate the aerosol contribution of optical extinction. This report contains the results of field experiments and laboratory investigations of the performance of the NPS spectrometers. Areas of concern in the use of these spectrometers and the subsequent calculations are identified and discussed. In general the spectrometer performance is adequate for use in predicting the performance of overocean optical systems.

DD FORM 1 JAN 73 1473 EDITION OF 1 NOV 68 IS OBSOLETE S/N 0102-014-6601

Unclassified

SECURITY CLASSIFICATION OF THIS PAGE (When Data Entered)

OPTICAL AEROSOL SPECTROMETERS FACTOR AFFECTING OPTICAL EXTINCTION PREDICTIONS

by

G. E. Schacher, K. L. Davidson, and

C. W. Fairall

ABSTRACT

Optical aerosol counters are used to measure aerosol spectra and thence to calculate the aerosol contribution of optical extinction. This report contains the results of field experiments and laboratory investigations of the performance of the NPS spectrometers. Areas of concern in the use of these spectrometers and the subsequent calculations are identified and discussed. In general the spectrometer performance is adequate for use in predicting the performance of overocean optical systems.

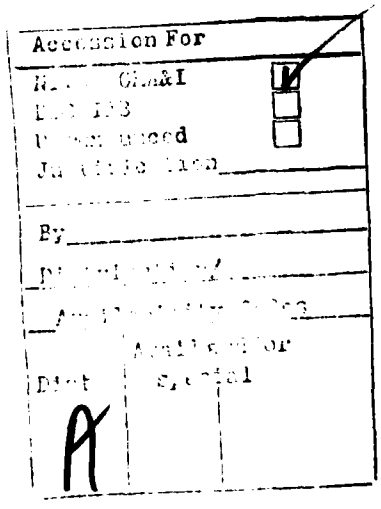

OUTLINE

List of Tables

Figure Captions

Figure 1. Spectrometer response vs particle radius for indices of refraction of 1.5 and 1.33 for ASASP and CSASP spectrometers. Shaded areas are ambiguity zones.

Figure 2. ASASP and CSASP spectrometer bin configurations. The bins for each range are shown as boxes. Bins for which there is overlap are shown partially shaded. The size ranges for the ambiguity zones for each instrument are indicated by the shaded areas.

Figure 3. Comparison of data for various size bins. X-ASASP range zero. 0-Bins for which there is range overlap. The data is from a one-half hour average during the SNI intercomparison experiment.

Figure 4. Location of shoal with respect to SNI and positions at which aerosol data was taken abord the R/V ACANIA. Circled numbers are location of R/V ACANIA aerosol measurements. M indicates the meteorological tower location.

Figure 5. Aerosol spectra obtained at locations 1 and 5 in neighborhood of SNI offshore breaker line. Dashed line is the difference between the spectra.

Figure 6. Calculated aerosol contribution to extinction for NOSC (x) and NPS (-) data as a function of time. Data was obtained during the NOSC-NPS intercomparison.

Figure 7. Relative counts per bin for CSASP-range 1 spectrometer using 2.7 μm diameter latex spheres.

Figure 8. Relative counts per bin for ASASP-range 1 spectrometer using 2.05 μm latex spheres.

Figure 9. Relative counts per bin for ASASP-range 0 spectrometer using 1.1 μm diameter latex spheres.

Figure 10. Relative counts per bin for ASASP-range 0 spectrometer using 2.7 μm diameter latex spheres.

Figure 11. Relative counts per bin for ASASP-range 0 spectrometer using 2.05 μm diameter latex spheres.

Figure 12. Relative counts per bin for ASASP-range 2 spectrometer using 0.43 μm diameter latex spheres.

Figure 13. Upper figure: plot of idealized spectrum showing assumed (solid vertical lines) and actual (dashed vertical lines) bin edges.

Lower figure: shift of dN/dr spectrum due to wide bin.

Figure 14. Particle size calibration for NPS, ●, and Garmisch, 0, spectrometers. The solid line shows correct sizing. The solid squares enclose the ambiguity zones for the spectrometers.

Figure 15. Extinction calculated from NPS aerosol measurements (solid line) and Calspan nephelometer (dashed line) as functions of time for 5/9. The shaded blocks show times when the wind direction was good.

Figure 16. Extinction calculated from NPS aerosol measurements (solid line) and Calspan nephelometer (dashed line) as functions of time for 5/10. The A's are NOSC aircraft measurements. The shaded areas show times when the wind direction was good.

Figure 17. Extinction calculated from NPS aerosol measurements (solid line) and Calspan nephelometer as functions of time for 5/15 on an expanded scale. The X's are values measured with a 6328 laser. The A's are NOSC aircraft measurements.

Figure 18. Extinction calculated from NPS aerosol measurements (solid line) and Calspan nephelometer (dashed line) as functions of time for 5/15. Triangles are the Wells, et al. prediction.

Figure 19. Extinction calculated from NPS aerosol measurements compared to Wells' model, Δ, 6328 laser measurements, x, and 4880 laser measurements, 0.

Figure 20. Extinction calculated from NPS aerosol measurements compared to Wells' model

Figure 21. Comparison of PMTC measured optical extinction (0), extinction calculated from NPS aerosol measurements (x), and Wells' model (Δ). Results are presented for wavelength of 1.06, 3.75, and 10.59 μm.

Figure 22. log(dN/dr) vs log(r) for 5/15/78 - 1646. The solid line is the 7th order polynomial fit to the data.

Figure 23. log(dV/dr) vs log(r) for 5/15/78 - 1646. The solid line is the 7th order polynomial fit to the dN/dr data.

Figure 24: log(dN/dr) vs log(r) for 5/15/58 - 2046. The solid line is the seventh order polynomial fit to the data.

Figure 25a-25d: log(dV/dr) vs log(r) for 5/15/78 - 2046. The solid line is the seventh order polynomial fit to the data. The extrapolation methods used were:

a. polynomial extrapolation
b. linear extrapolation
c. constant extrapolation
d. cut off

Figure 25a-26b: Log(dV/dr) vs log(r) for 5/8/78 - 0835. The solid line is the seventh order polynomial fit including polynomial extrapolation (a) and linear extrapolation (b).

Figure 27. Comparison of aerosol contribution to extinction as determined optically and from measured aerosol spectra.

I. Introduction

The capability to make accurate and reliable aerosol measurements has been a major concern of the EO/MET program. For the purposes of this program the word "accurate" means accurate enough to predict the performance of optical systems. Since the relative importance of the aerosol concentration varies with the optical wavelength, the required accuracy depends on particle size. Two methods are used to determine the usefulness of a particular instrument: 1) comparison to other spectrometers, and 2) comparison of optical parameters predicted from aerosol measurements to those measured directly. One of the major efforts undertaken in the FY79 EO/MET program has been to compare and assess the aerosol spectrometers that are used in the various experimental programs.

The Naval Postgraduate School (NPS) has performed a number of experiments with two Particle Measurement Systems (PMS) optical spectrometers over the past two years. The data obtained can be used to determine the accuracy of these instruments and how best to use this class of spectrometer in general. Program spectrometer intercomparisons are being done by the EO/MET group as a whole and therefore is not a subject of this report. The purpose here is to present, in one document, the NPS measurements and several results that should be useful to the EO/MET program.

Results from the following experiments are presented here:

1. CEWCOM-78, comparison of aerosol measurements with Calspan visiometer, NPS ship to shore optics, NOSC aircraft, and Wells' model.

2. CEWCOM-78, affect of offshore breaker line (~1/2 mi.) on aerosol distribution at San Nicolas Island (SNI).
3. SNI spectrometer intercomparison
4. CTQ-79, comparison of aerosol measurements with NPS 13 mi. overwater optical range.
5. NOSC-NPS intercomparison at San Diego
6. Calibration and spectrometer intercomparison with Max Planck Institute fűr Chemie, Mainz, F.R.G.

II. Equipment and Data Handling

NPS operates two aerosol spectometers: the PMS models ASASP and CSASP. They are sensitive to aerosol particles with radii from approximately 0.1 μm to 3 μm and 3 μm to 15 μm radius, respectively. The spectrometers operate in conjunction with a DAS-32 data acquisition system. For almost all measurements the slowest DAS mode is used, for which it collects data for 40 sec then dumps, changes ranges, and resets. The data is collected for 30 minute periods then averaged by a Hewlett Packard 9825 computer.

Most of the experiments were performed aboard the NPS ship R/V ACANIA. The spectrometers were mounted on a mast placed approximately 15 feet aft of the tip of the bow so that the sampled air was not conditioned by the ship. The mounting was 36 feet above the deck, 43 feet above mean sea level. (Note that for the CTQ cruise the mounting was 18 feet lower.) The spectrometers air inlets are pointed directly toward the bow, with fixed orientation requiring that, as a precautionary measure, we only accept data when the relative wind is within 30° of the bow. Normal operation is to head the ship into the wind during times of data acquisition.

Both spectrometers have size regions where sizing uncertainty exists, called ambiguity zones.[1] In these zones the optical sizing cannot be expected to be reliable because the Mie scattering curve is not monotonic. This leads to a situation where a given intensity of scattered light corresponds to three particle sizes. In Figure 1 we show the spectrometers responses vs particle radius for 1.33 and 1.5 indices of refraction. (1) zones for which there is

ambiguity are shown as shaded, for both the ASASP, and CSASP spectrometers.

The full output of both spectrometers consists of 6 ranges, 15 points per range, for a total of 90 points. Due to natural fluctuations, counting errors, ambiguity zones, etc. all points are subject to uncertainties, even though one half hour averaging is used. Because of the uncertainties associated with individual points the correct manner to reduce the data is to use some averaging technique, and we have chosen a fit using a 7th order polynomial for $\log(dn/dr)$ vs $\log(r)$. An odd order was chosen because the data is odd in log space, and order 7 because this essentially treats each range as a single point.

Some of the individual data points are discarded before forming the polynomial fit. There are two reasons for excluding data: 1) inherent inaccuracies in the small size bins for each range and 2) the ambiguity zones. Figure 2 shows the bin configurations of the various spectrometer ranges and the location of the ambiguity zones. The shaded bins show regions of overlap between the ranges.

We have used two schemes for handling the data, both of which are compromises between eliminating ambiguity and rejecting data from small size bins. The methods are:

1. Reject those small size bins which overlap with large size bins from the next smaller size range. The bins eliminated for each range are:

ASASP					CSASP	
3	2	1	0	Range	1	0
3	3	6	3	# of Bins Rejected	5	3

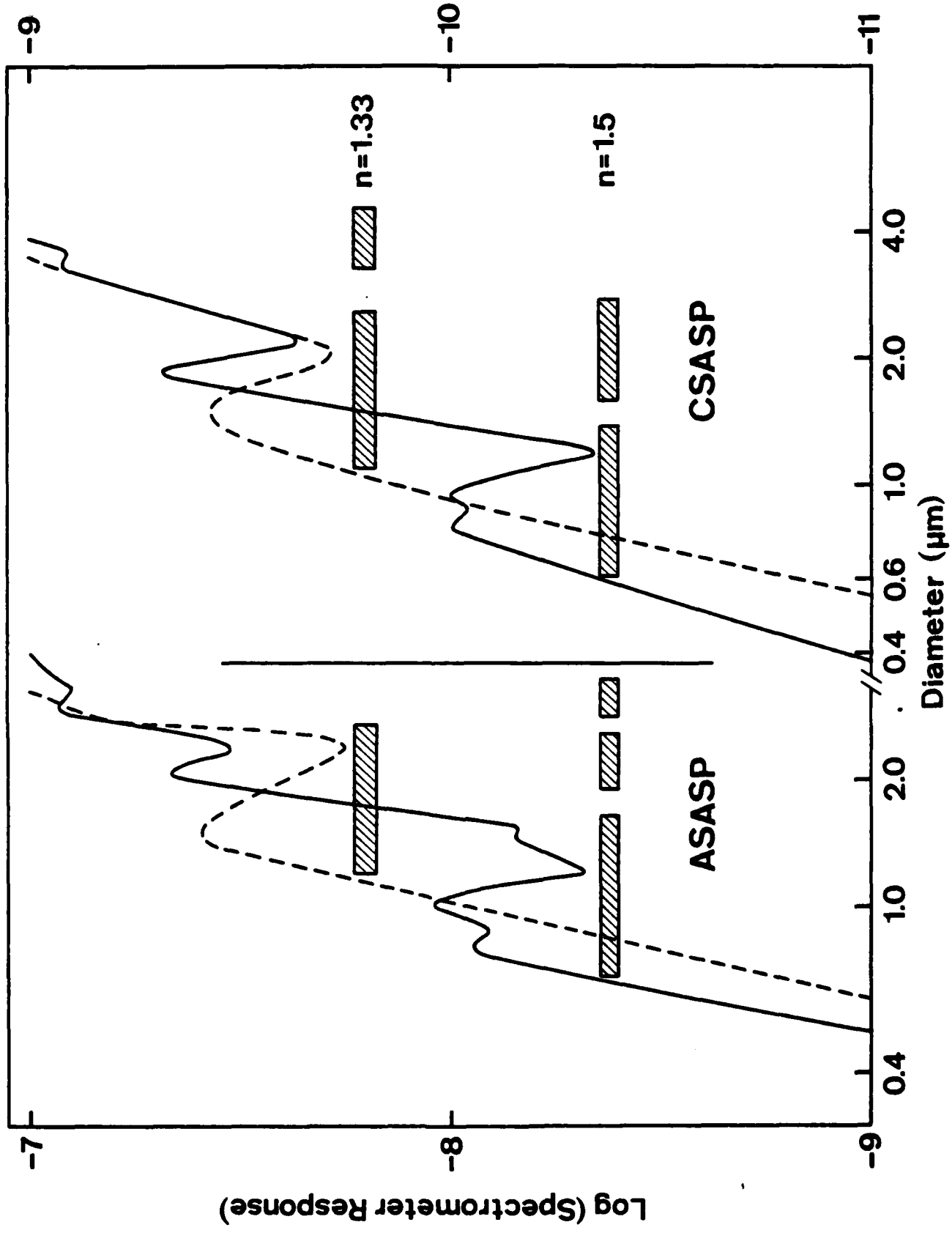
-9
-10
-11
n=1.33
n=1.5
CSASP
ASASP
0.4
0.6
1.0
2.0
4.0
Diameter (μm)
-7
-8
-9
Log (Spectrometer Response)

Figure 1

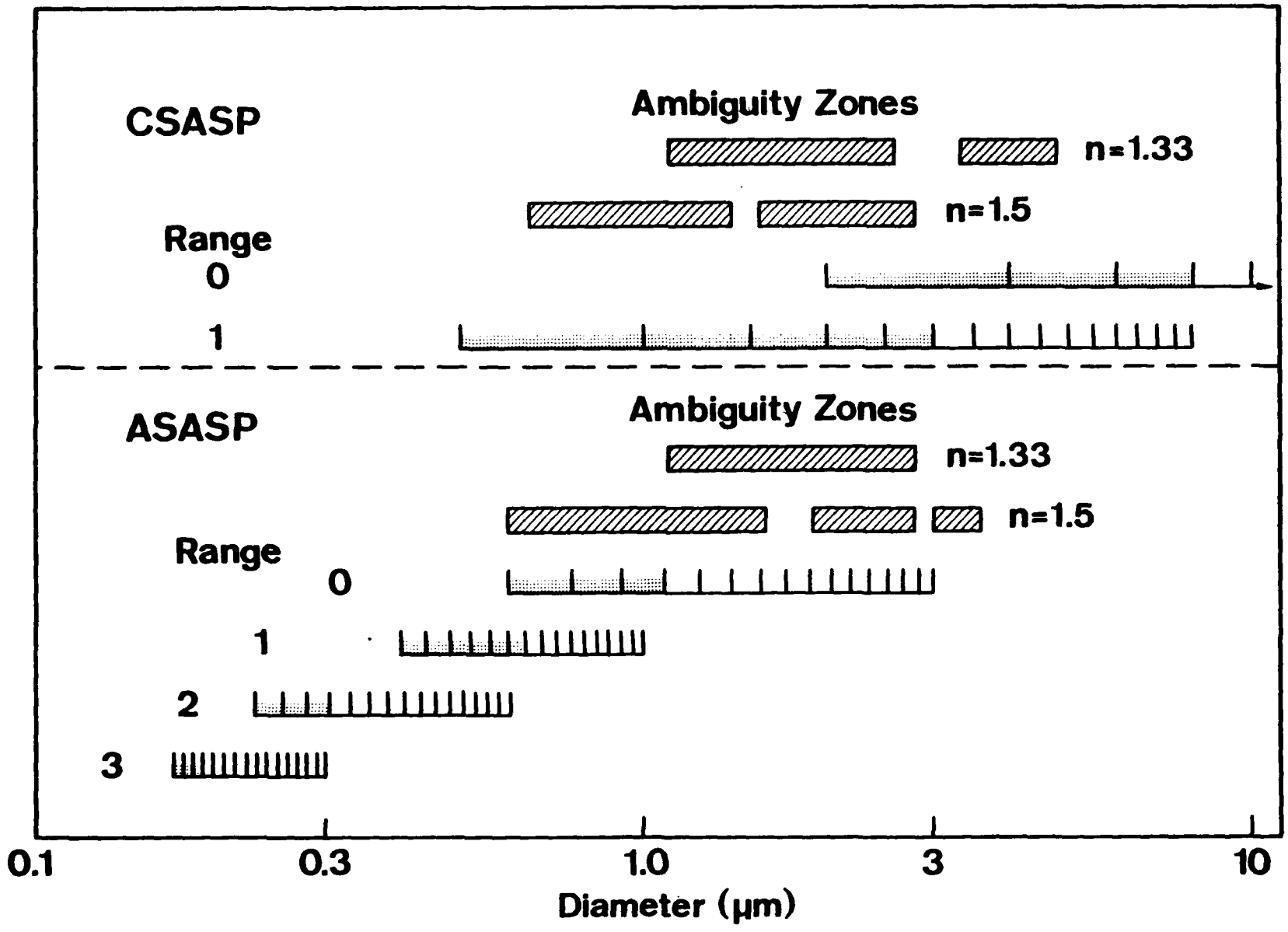
CSASP
Ambiguity Zones
n=1.33
n=1.5
Range
0
1
ASASP
Ambiguity Zones
n=1.33
n=1.5
Range
0
1
2
3
0.1
0.3
1.0
3
10
Diameter (μm)

Figure 2
12

2. Reject smallest size bins and all of ASASP Range 0 to eliminate its ambiguity zone. The bins eliminated for each range are:

ASAP					CSASP	
3	2	1	0	Range	1	0
3	3	3	All	# of Bins Rejected	1	1

Method 1 was originally used to evaluate SNI Intercomparison data. Method 2 was developed using an independent data set from the JASIN experiment. When method 2 was applied to the SNI data the calculated extinction at the visible was increased by about 10% and no change resulted at 10.6 μm. Method 2 was used to calculate the extinctions for the SNI Intercomparison report.

Figure 3 shows data points for a one half hour average period plotted on a log(dN/dr) vs log(r) scale. The plot compares the two methods. The solid dots are data points used in both methods, the x's data points from ASASP range 0 which are not used for method 2, and the open circles data points that overlap other bins that are not used for method 1. The figure shows that method 2 eliminates the errors that can be introduced by the ASASP ambiguity zone in the 1 μm region, otherwise there is little difference between the two methods.

One further note on the polynomial fit is in order. The highest order polynomial term will always dominate the fit for large argument. If the coefficient of the highest order term is positive then the fit will ultimately go to large positive log(dN/dr) for positive log(r) and vice-versa for negative log(r). This turnover in the curve will cause erroneous results if it occurs within the size range of interest (which often happens). We prevent this from occurring within the size range

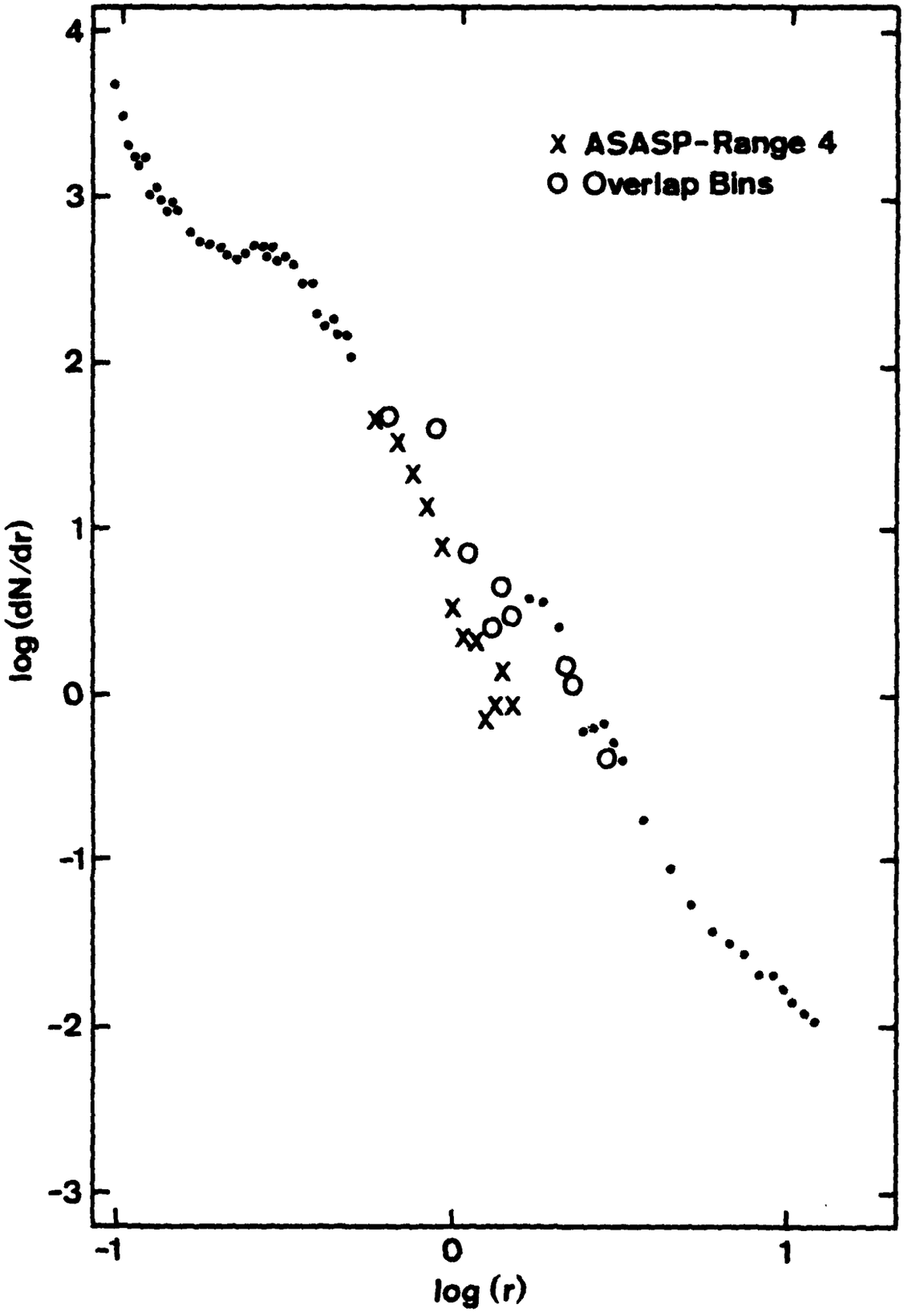

Figure 3

used by generating two points outside the range of data, at log(r) = $\pm$1.5, and adding them to the data. For -1.5 the point is generated by using the average slope of the first five points accepted in ASASP range 3. For +1.5 all points in the CSAP range 0 are used to generate an average slope. The polynomial fit uses all accepted data points and the two ficticious points. Additional discussion on the effect of the added point at +1.5 will be found in a later section.

Extinction calculations are performed using the polynomial fit, not the original data. The range defined by log(r) equal -1.0 to +1.4 is divided into 48 bins, with equal width of 0.05 in log(r). The average dN/dr in each bin is calculated from the polynomial then the contribution to the scattering is calculated using the appropriate Mie coefficient.

III. San Nicolas Island Breaker Line

We present these results first since they impact directly on ongoing programs. SNI is used for many EO/MET and Optical Signature Programs (OSP) experiments. It was chosen partially because the island is located approximately 90 miles from the coast of California and could fairly closely represent open ocean conditions. An optical range and tower for meteorological measurements are located at the north end of the island which is the location used for the SNI Intercomparison reported below.

Shoals are located approximately 1/2 N mile offshore, to the W of the range (see Figure 4) and an exposed rock is located 8 N miles to the NW. We have been concerned that the frequent breakers across the shoals could introduce a significant quantity of sea spray droplets into the atmosphere and compromise shoreline measurements.

During CEWCOM-78 the NPS ship R/V ACANIA operated in the SNI area. The ship was equipped with a complete suite of meteorological equipment and the two spectometers.[2] One of the purposes of the cruise was to test the respresentativeness of SNI to open conditions. Results for small scale properties (ε and C_T^2) have been reported previously.[3] The particular test reported here was designed to assess the effects of the breaker line and not the influence of the island itself. In order to determine the influence of the island it is necessary to make measurements at sea and on the island, preferably with the same instrument. Some of the results presented later in this report could be used to check for island influence on the aerosol spectrum but lack of

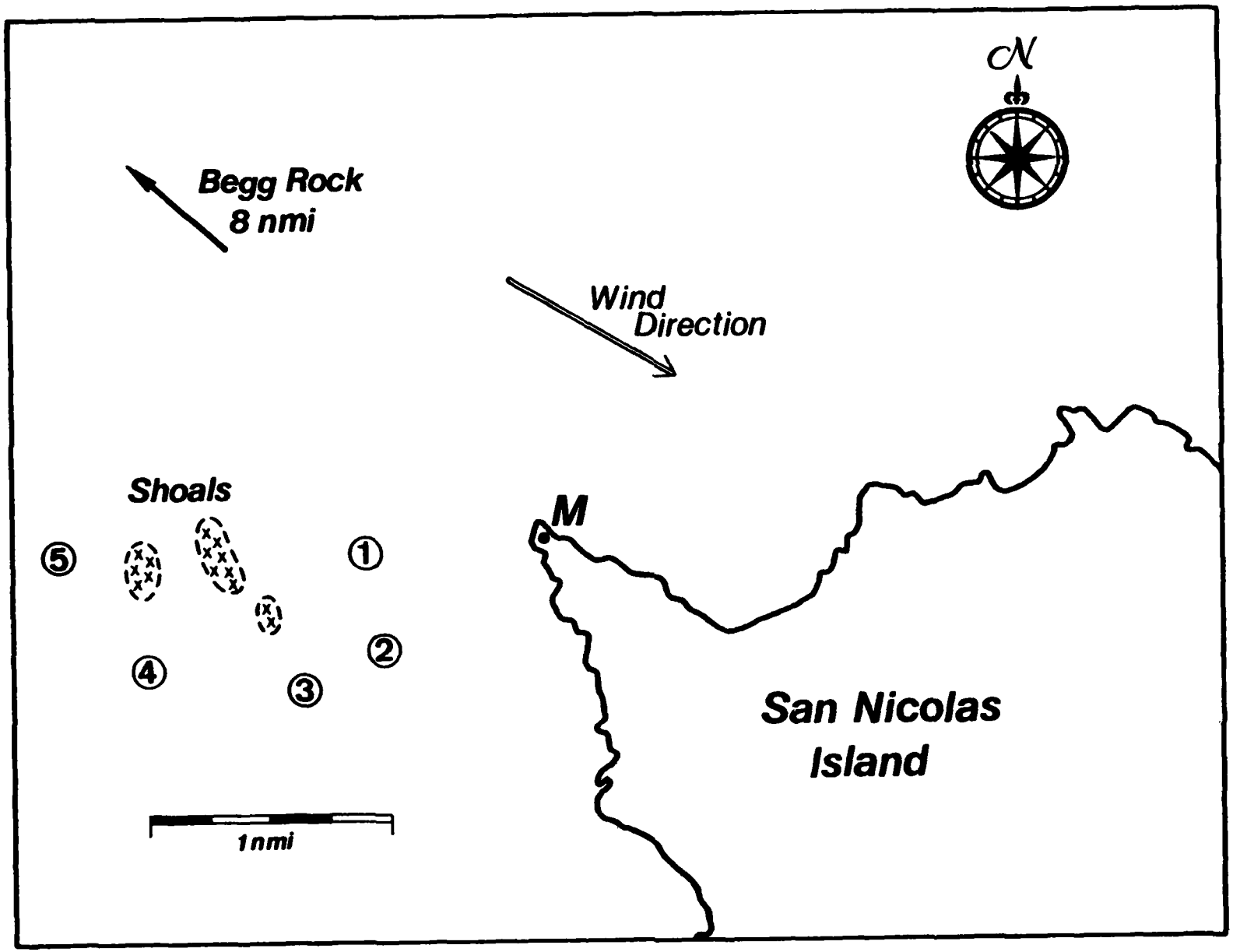
N
Begg Rock
8 nmi
Wind
Direction
Shoals
M
San Nicolas
Island
1nmi

Figure 4

cross calibration between shore and ship instruments would make the comparison of dubious value.

In Figure 4 we show the orientation of the island, the location of the shoal and five positions at which the ship was stationed for aerosol measurements. In Figure 5 we show aerosol spectra obtained at positions 1 and 5, and the difference between the spectra. The measurements were made when there was a light wind (6 knts, 300°) approximately from the shoal toward the island. The occurance of light winds was fortunate since local generation from surface waves is then minimal and the breaker effect would be easily observed. At position 1 there was a large increase in the number of particles with sizes of 3 μ and above relative to position 5. These are the sizes expected for the local generation contribution to the aerosol spectrum and are obviously generated at the breaker line.

These results appear to be very serious with regard to the representativeness of the island to open ocean conditions. Since the prevailing wind is roughly in a quadrant about NW one can expect the horizontal transport of aerosols generated at the breakers to influence the aerosol spectrum at the island a significant fraction of the time. We draw this conclusion from the fact that, with the ship directly between the island meteorological tower and the shoal, and the local wind at 300°, the ship detected significant shoal influence. When the wind is more westerly the effect should be worse. When the wind is more northerly, the effect should disappear, but this is the wind direction for which continental influence from Pt. Conception

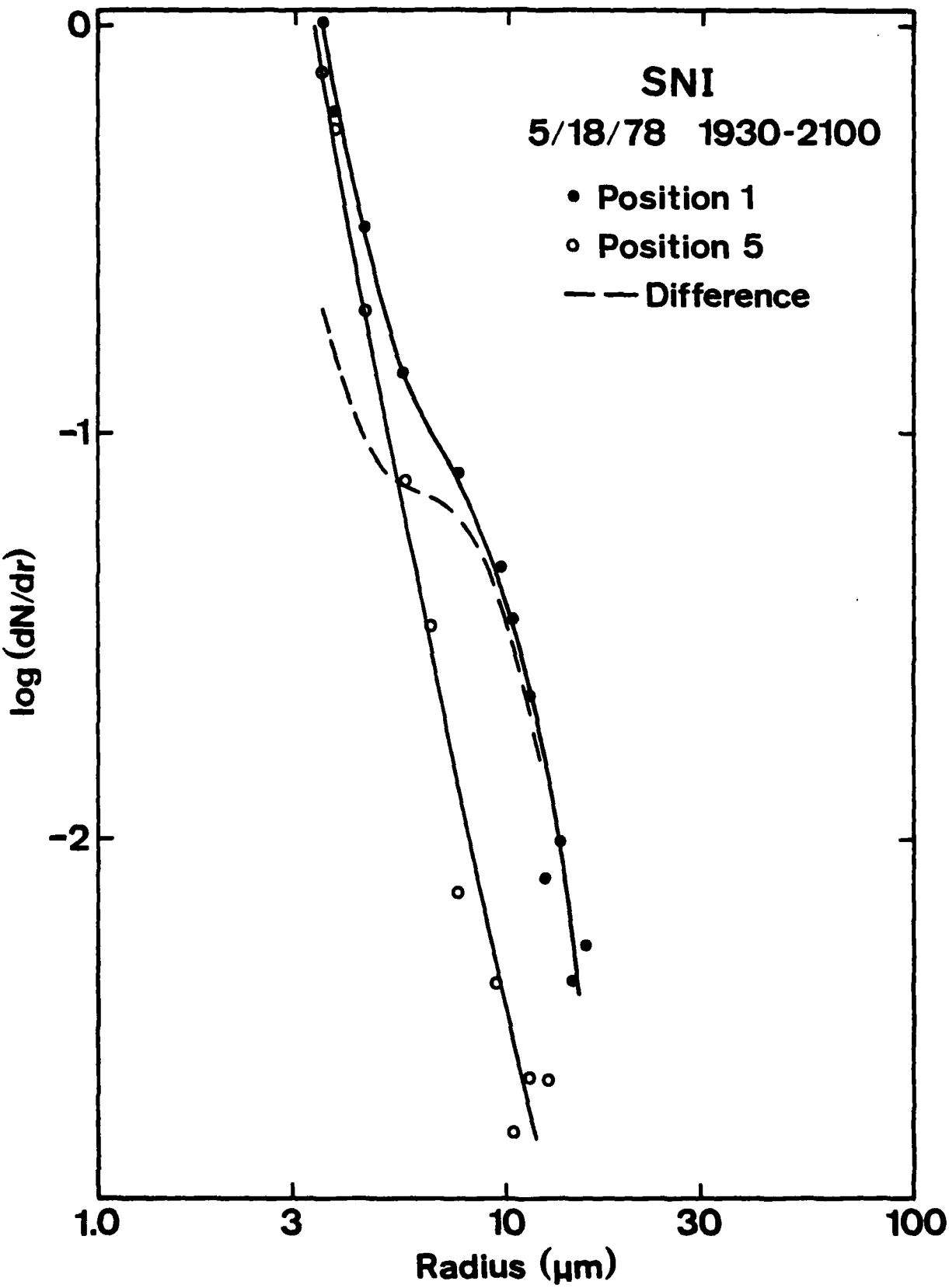
SNI
5/18/78 1930-2100
• Position 1
o Position 5
— — Difference
0
-1
-2
log (dN/dr)
1.0
3
10
30
100
Radius (μm)

Figure 5

will most likely occur. It is also possible that for a NW wind the influence of Begg rock could be important. Obviously, no definite conclusions can be made as to the seriousness of the shoal and Begg rock influences without extensive testing.

These results also suggest another comparison that should be made: coincident aerosol measurements at the meteorological tower and in the cove near the optical paths. The meteorological tower at SNI is on the tip of the island and the optical range is in a cove where local breakers could influence the optical measurements.

IV. San Diego Intercomparison

As a preliminary to the San Nicolas Island Intercomparison NPS and Naval Ocean System Center (NOSC) performed an intercomparison of their spectrometers at San Diego. The spectometers were installed side by side on the roof of building 323 at NOSC and operated for four days, 1/22 to 1/25 1979. The roof is approximately 30 ft high and the building is located on a shoreline bluff approximately 100 ft above the sea surface.

The results of the intercomparison are shown in Figure 6. The extinction was calculated from the measured aerosol spectra by each laboratory for their respective data for a wavelength of 0.53 μm.[4] Figure 6 shows extinction plotted as a function of time, with a solid line for NPS and X for NOSC. The results are quite good. There is a systematic discrepancy of approximately a factor of 2 during the morning of 1/25. This was a time when high winds were experienced, the wind exceeding 20 knts from 0400 on. No explanation is offered as to why a high wind would cause a systematic difference in measurements made by the two types of spectrometers. For the remainder of the measurement period there was no systematic error. A wide variety of wind speeds and directions, except high winds, were experienced and the spectrometers always operated satisfactorily.

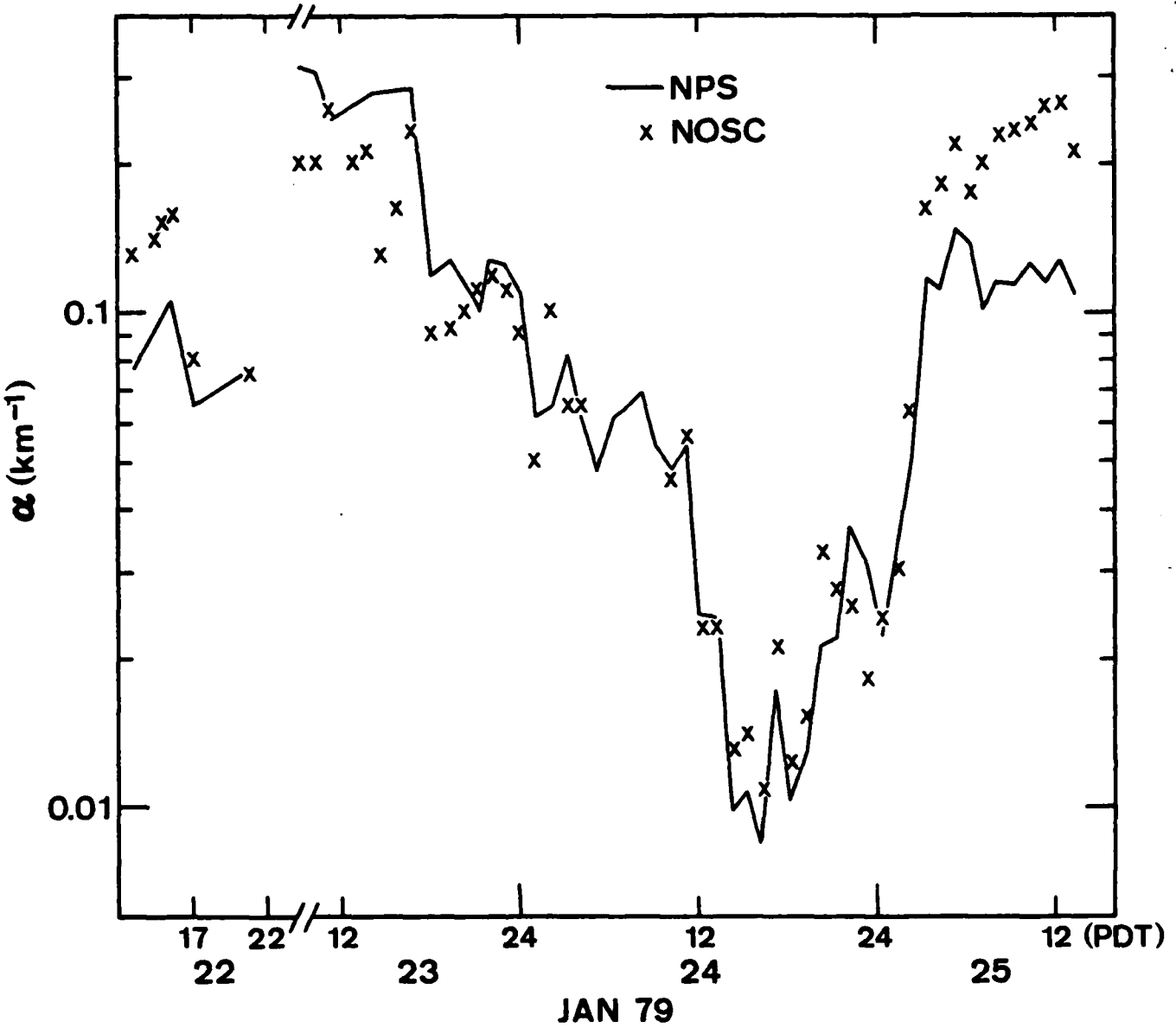

Figure 6

V. San Nicolas Island Intercomparison

During the first two weeks of May, 1979, several laboratories installed equipment at SNI to perform optical extinction and aerosol measurements. The purpose of this intercomparison was to try some new optical techniques and to determine the validity of the aerosol spectrometer results. The NPS aerosol results are too voluminous to be reproduced here. They are in a special project report which is available to anyone interested.[5] Sample outputs of intercomparison data are presented in Figure 7 and Table 1. The table lists bin center radii, the measured values of dn/dr and the 7th order polynomial coefficients, where

$$\log(dN/dr) = \sum_{i=0}^{7} a_i (\log r)^{7-i}$$

The figure shows the data points plotted as log(dn/dr) vs log(r), with the points alternating between + and 0 to delineate ranges. The solid line is the polynomial fit.

The test of the aerosol spectometers is to be made in two ways: 1) direct comparison of the spectra produced by the various spectrometers, 2) comparison of spectrometer extinction predictions and optically measured values. Comparisons will be presented in a report on results for all instruments which is being prepared by NOSC.

Table 2 lists the NPS determined extinctions as a function of time which are to be used for the intercomparison.

r and dN/dr

0.096	4.82E 03	0.159	2.51E 02	0.330	7.21E 01
0.100	3.49E 03	0.171	1.93E 02	0.350	5.45E 01
0.104	2.55E 03	0.184	1.49E 02	0.370	4.65E 01
0.109	1.90E 03	0.196	7.69E 01	0.390	4.01E 01
0.113	1.65E 03	0.209	5.71E 01	0.410	4.49E 01
0.118	1.45E 03	0.221	8.79E 01	0.430	3.53E 01
0.123	1.08E 03	0.234	5.05E 01	0.450	1.92E 01
0.128	8.85E 02	0.246	9.01E 01	0.470	2.72E 01
0.133	8.24E 02	0.259	6.37E 01	0.490	1.28E 01
0.138	6.43E 02	0.271	1.08E 02	0.250	0.00E 00
0.143	5.82E 02	0.284	7.91E 01	0.000	0.00E 00
0.148	5.49E 02	0.296	6.59E 01	0.000	0.00E 00
0.580	1.55E 01	1.479	9.44E-01	3.685	8.71E-02
0.660	9.62E 00	1.671	1.16E 00	4.452	3.83E-02
0.740	7.03E 00	1.863	1.29E 00	5.219	2.32E-02
0.820	4.81E 00	2.055	1.05E 00	5.986	1.09E-02
0.900	2.96E 00	2.246	5.45E-01	6.753	1.05E-02
0.980	2.40E 00	2.438	2.46E-01	7.520	7.00E-03
1.060	5.55E-01	2.630	2.86E-01	8.287	6.77E-03
1.140	1.85E-01	2.822	3.00E-01	9.054	4.51E-03
1.220	1.85E-01	3.013	2.71E-01	9.821	4.18E-03
1.300	1.85E-01	3.205	1.91E-01	10.588	1.92E-03
1.380	3.70E-01	1.651	0.00E 00	11.355	2.14E-03
1.460	5.55E-01	0.000	0.00E 00	12.122	2.03E-03

Order 7 Polynomial Fit

a1	3.027E-01	a2	-2.855E 00	a3	4.983E-01
a4	1.773E 00	a5	-7.277E-01	a6	-2.804E 00
a7	4.042E-01	a8	8.813E-01		

Table 1

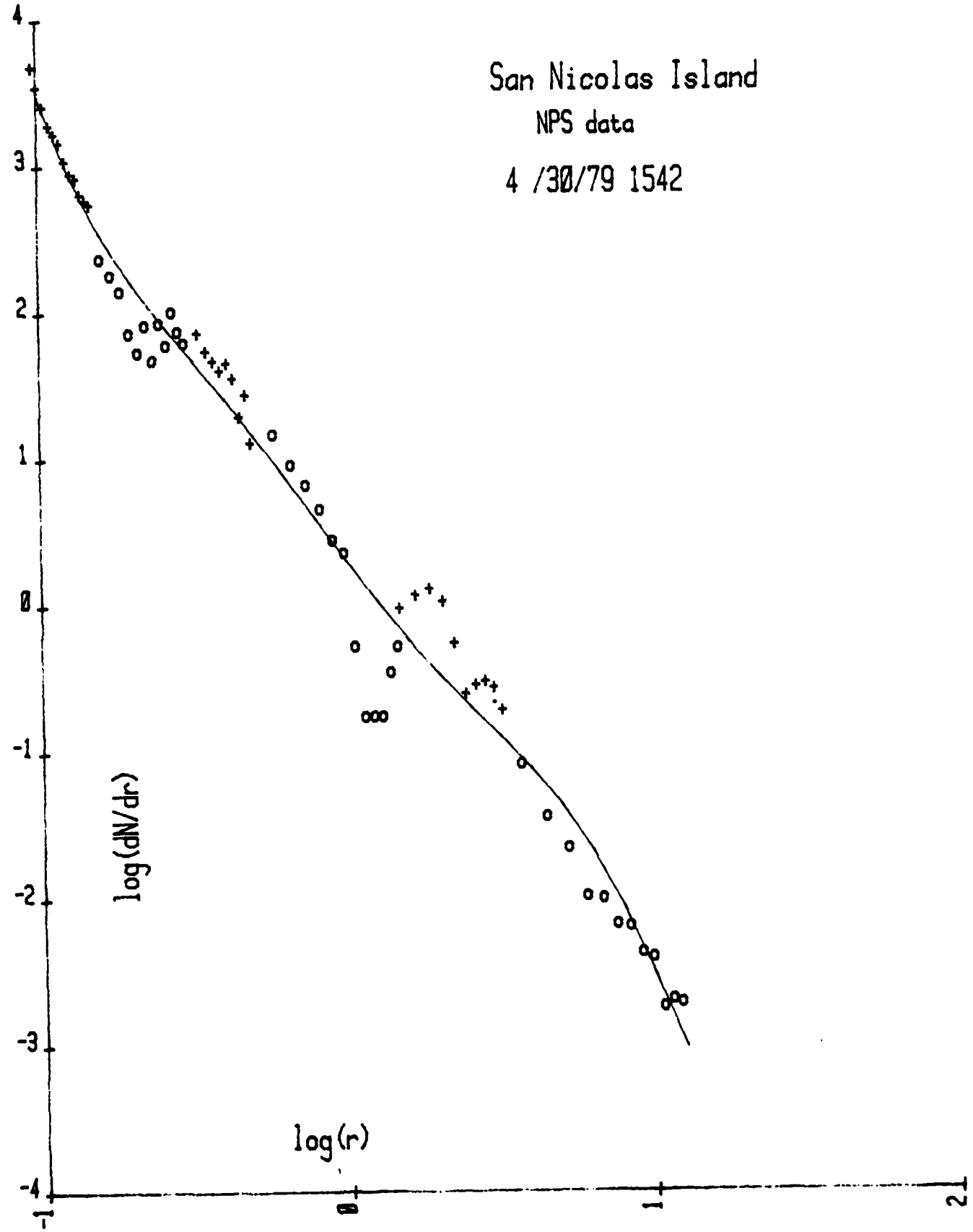
San Nicolas Island
NPS data
4 /30/79 1542
log(dN/dr)
log(r)
4
3
2
1
0
-1
-2
-3
-4
-1
0
1
2

Figure 7

Table 2

SNI Intercomparison Extinctions (m^{-1})

Date/Time	λ	0.530	1.060	3.750	10.590
4 /30/79 1542		1.205E-04	1.227E-04	9.245E-05	3.834E-05
4 /30/79 1607		1.240E-04	1.156E-04	9.689E-05	5.174E-05
4 /30/79 1638		1.623E-04	1.596E-04	1.390E-04	9.681E-05
4 /30/79 1703		1.392E-04	1.366E-04	1.170E-04	7.076E-05
4 /30/79 1727		1.102E-04	1.067E-04	8.877E-05	3.961E-05
4 /30/79 1752		1.103E-04	1.075E-04	8.409E-05	3.481E-05
4 /30/79 1859		1.203E-04	1.220E-04	9.253E-05	3.248E-05
4 /30/79 1932		1.104E-04	1.128E-04	8.431E-05	2.668E-05
4 /30/79 2005		1.151E-04	1.178E-04	8.919E-05	2.807E-05
4 /30/79 2129		1.150E-04	1.182E-04	8.684E-05	2.180E-05
4 /30/79 2159		1.186E-04	1.237E-04	8.710E-05	2.020E-05
4 /30/79 2230		1.042E-04	1.070E-04	7.061E-05	1.404E-05
4 /30/79 2258		1.092E-04	1.107E-04	7.022E-05	1.364E-05
4 /30/79 2329		1.113E-04	1.125E-04	7.383E-05	1.556E-05
4 /30/79 2337		1.078E-04	1.082E-04	6.762E-05	1.405E-05
4 /30/79 2344		1.002E-04	1.010E-04	6.372E-05	1.321E-05
5 /1 /79 843		4.248E-05	3.729E-05	2.742E-05	6.175E-06
5 /1 /79 927		4.523E-05	3.893E-05	2.502E-05	4.018E-06
5 /1 /79 957		3.932E-05	3.463E-05	2.158E-05	3.569E-06
5 /1 /79 1031		5.125E-05	4.696E-05	3.019E-05	9.935E-06
5 /1 /79 1102		5.303E-05	4.871E-05	3.226E-05	7.174E-06
5 /1 /79 1132		4.935E-05	4.427E-05	3.037E-05	9.948E-06
5 /1 /79 1202		4.905E-05	4.371E-05	3.093E-05	8.765E-06
5 /1 /79 1230		5.154E-05	4.478E-05	3.136E-05	8.042E-06
5 /1 /79 1258		7.505E-05	6.722E-05	4.871E-05	1.923E-05
5 /1 /79 1329		7.937E-05	6.860E-05	5.375E-05	2.795E-05
5 /1 /79 1300		1.324E-04	1.222E-04	1.027E-04	5.780E-05
5 /1 /79 1430		8.032E-05	7.816E-05	5.515E-05	2.166E-05
5 /1 /79 1458		9.992E-05	9.830E-05	7.214E-05	3.013E-05
5 /1 /79 1526		1.103E-04	1.098E-04	7.843E-05	3.628E-05
5 /1 /79 1554		9.997E-05	9.989E-05	7.076E-05	3.220E-05
5 /1 /79 1622		1.167E-04	1.167E-04	7.703E-05	3.509E-05

SNI Intercomparison Extinctions (m^{-1})

Date/Time	λ	0.530	1.060	3.750	10.590
5 /1 /79 1650		1.178E-04	1.170E-04	7.620E-05	3.309E-05
5 /1 /79 1718		1.308E-04	1.317E-04	8.846E-05	4.035E-05
5 /1 /79 1746		1.569E-04	1.581E-04	1.041E-04	4.827E-05
5 /1 /79 1814		1.727E-04	1.745E-04	1.146E-04	5.379E-05
5 /1 /79 1842		1.736E-04	1.749E-04	1.177E-04	5.363E-05
5 /1 /79 1910		1.987E-04	2.007E-04	1.297E-04	6.259E-05
5 /1 /79 1941		1.700E-04	1.690E-04	1.089E-04	4.440E-05
5 /1 /79 2012		1.977E-04	1.996E-04	1.269E-04	5.386E-05
5 /1 /79 2042		2.223E-04	2.241E-04	1.438E-04	7.089E-05
5 /1 /79 2110		2.237E-04	2.249E-04	1.511E-04	7.564E-05
5 /1 /79 2138		2.107E-04	2.137E-04	1.412E-04	6.755E-05
5 /1 /79 2206		2.012E-04	2.019E-04	1.321E-04	6.206E-05
5 /2 /79 108		2.071E-04	2.026E-04	1.439E-04	8.023E-05
5 /2 /79 136		2.402E-04	2.364E-04	1.693E-04	1.027E-04
5 /2 /79 204		2.573E-04	2.565E-04	1.774E-04	9.320E-05
5 /2 /79 232		2.583E-04	2.548E-04	1.743E-04	9.042E-05
5 /2 /79 300		2.669E-04	2.636E-04	1.746E-04	8.636E-05
5 /2 /79 328		3.045E-04	3.046E-04	2.021E-04	9.981E-05
5 /2 /79 356		3.133E-04	3.133E-04	2.062E-04	1.004E-04
5 /2 /79 424		2.801E-04	2.769E-04	1.812E-04	9.297E-05
5 /2 /79 452		2.644E-04	2.611E-04	1.725E-04	8.798E-05
5 /2 /79 520		2.552E-04	2.510E-04	1.630E-04	7.987E-05
5 /2 /79 548		2.667E-04	2.641E-04	1.703E-04	7.805E-05
5 /2 /79 616		2.782E-04	2.781E-04	1.836E-04	8.613E-05
5 /2 /79 646		2.992E-04	3.002E-04	1.929E-04	9.026E-05
5 /2 /79 717		3.062E-04	3.073E-04	1.965E-04	8.720E-05
5 /2 /79 748		3.159E-04	3.174E-04	2.039E-04	9.547E-05
5 /2 /79 818		2.996E-04	2.990E-04	1.875E-04	8.652E-05
5 /2 /79 849		2.440E-04	2.435E-04	1.528E-04	6.761E-05
5 /2 /79 920		2.192E-04	2.185E-04	1.441E-04	6.437E-05
5 /2 /79 950		2.465E-04	2.431E-04	1.657E-04	8.522E-05
5 /2 /79 1021		2.545E-04	2.517E-04	1.723E-04	8.748E-05

SNI Intercomparison Extinctions (m^{-1})

Date/Time	λ	0.530	1.060	3.750	10.590
5 /2 /79 1052		2.563E-04	2.546E-04	1.654E-04	8.224E-05
5 /2 /79 1122		2.597E-04	2.604E-04	1.631E-04	7.715E-05
5 /2 /79 1153		2.423E-04	2.432E-04	1.558E-04	7.613E-05
5 /2 /79 1224		2.208E-04	2.192E-04	1.345E-04	6.090E-05
5 /2 /79 1252		2.314E-04	2.317E-04	1.468E-04	6.657E-05
5 /2 /79 1320		2.370E-04	2.346E-04	1.457E-04	6.496E-05
5 /2 /79 1348		2.254E-04	2.265E-04	1.352E-04	5.440E-05
5 /2 /79 1416		2.240E-04	2.225E-04	1.370E-04	5.851E-05
5 /2 /79 1512		1.828E-04	1.816E-04	1.108E-04	4.687E-05
5 /2 /79 1542		1.583E-04	1.568E-04	9.615E-05	3.762E-05
5 /2 /79 1613		1.963E-04	1.929E-04	1.227E-04	4.908E-05
5 /2 /79 1644		1.971E-04	1.930E-04	1.241E-04	4.956E-05
5 /2 /79 1712		2.033E-04	2.013E-04	1.258E-04	4.535E-05
5 /2 /79 1740		2.063E-04	2.064E-04	1.302E-04	4.409E-05
5 /2 /79 1808		2.245E-04	2.221E-04	1.382E-04	4.592E-05
5 /2 /79 1836		2.449E-04	2.382E-04	1.570E-04	6.098E-05
5 /2 /79 1904		2.612E-04	2.595E-04	1.744E-04	6.859E-05
5 /2 /79 1932		3.226E-04	3.213E-04	2.156E-04	9.408E-05
5 /2 /79 1900		3.028E-04	3.060E-04	2.043E-04	8.376E-05
5 /2 /79 2030		3.271E-04	3.219E-04	2.320E-04	1.197E-04
5 /2 /79 2101		2.986E-04	2.986E-04	1.913E-04	7.694E-05
5 /2 /79 2129		3.229E-04	3.270E-04	2.228E-04	9.617E-05
5 /2 /79 2157		3.089E-04	3.081E-04	2.002E-04	8.626E-05
5 /2 /79 2225		3.222E-04	3.261E-04	2.164E-04	9.099E-05
5 /2 /79 2253		3.169E-04	3.212E-04	2.143E-04	8.734E-05
5 /2 /79 2321		3.175E-04	3.158E-04	2.046E-04	7.544E-05
5 /2 /79 2349		3.713E-04	3.498E-04	2.722E-04	1.260E-04
5 /3 /79 17		3.810E-04	3.804E-04	2.672E-04	1.070E-04
5 /3 /79 45		3.748E-04	3.764E-04	2.733E-04	1.105E-04
5 /3 /79 113		3.637E-04	3.691E-04	2.569E-04	1.015E-04
5 /3 /79 141		3.515E-04	3.586E-04	2.403E-04	8.572E-05
5 /3 /79 209		3.361E-04	3.419E-04	2.223E-04	7.610E-05

SNI Intercomparison Extinctions (m^{-1})

Date/Time	λ	0.530	1.060	3.750	10.590
5 /3 /79 237		3.342E-04	3.336E-04	2.345E-04	8.851E-05
5 /3 /79 305		3.500E-04	3.406E-04	2.599E-04	1.143E-04
5 /3 /79 333		3.165E-04	3.066E-04	2.265E-04	8.138E-05
5 /3 /79 401		3.319E-04	3.304E-04	2.412E-04	8.948E-05
5 /3 /79 429		3.363E-04	3.418E-04	2.422E-04	8.266E-05
5 /3 /79 457		3.361E-04	3.430E-04	2.447E-04	8.240E-05
5 /3 /79 525		3.322E-04	3.381E-04	2.493E-04	8.874E-05
5 /3 /79 553		2.826E-04	2.821E-04	2.041E-04	6.243E-05
5 /3 /79 621		2.669E-04	2.624E-04	1.938E-04	6.803E-05
5 /3 /79 649		2.283E-04	2.206E-04	1.652E-04	5.237E-05
5 /3 /79 717		3.396E-04	3.340E-04	2.734E-04	1.470E-04
5 /3 /79 745		2.805E-04	2.727E-04	2.165E-04	8.514E-05
5 /3 /79 813		2.417E-04	2.294E-04	1.736E-04	5.676E-05
5 /3 /79 841		1.927E-04	1.807E-04	1.331E-04	3.948E-05
5 /3 /79 909		1.729E-04	1.616E-04	1.204E-04	4.120E-05
5 /3 /79 1052		1.344E-04	1.236E-04	9.144E-05	3.853E-05
5 /3 /79 1122		1.345E-04	1.194E-04	9.179E-05	3.223E-05
5 /3 /79 1153		2.252E-04	2.039E-04	1.634E-04	6.055E-05
5 /3 /79 1224		2.764E-04	2.512E-04	2.052E-04	8.412E-05
5 /3 /79 1254		3.264E-04	3.040E-04	2.610E-04	1.121E-04
5 /3 /79 1325		2.908E-04	2.685E-04	2.208E-04	7.509E-05
5 /3 /79 1356		2.500E-04	2.213E-04	1.686E-04	4.575E-05
5 /3 /79 1426		1.870E-04	1.596E-04	1.201E-04	4.189E-05
5 /3 /79 1457		1.417E-04	1.281E-04	8.917E-05	2.271E-05
5 /3 /79 1528		1.891E-04	1.829E-04	1.390E-04	4.806E-05
5 /3 /79 1556		1.451E-04	1.405E-04	1.003E-04	3.318E-05
5 /3 /79 1624		1.053E-04	9.037E-05	6.451E-05	1.778E-05
5 /3 /79 1652		1.148E-04	1.043E-04	7.535E-05	2.696E-05
5 /3 /79 1720		1.037E-04	9.294E-05	6.721E-05	2.114E-05
5 /3 /79 1748		1.032E-04	9.384E-05	6.525E-05	2.178E-05
5 /3 /79 1816		9.127E-05	8.525E-05	5.740E-05	1.513E-05
5 /3 /79 1844		1.045E-04	9.341E-05	5.875E-05	1.747E-05

SNI Intercomparison Extinctions (m^{-1})

Date/Time	λ	0.530	1.060	3.750	10.590
5 /3 /79 1912		8.909E-05	8.420E-05	5.318E-05	1.460E-05
5 /3 /79 1942		9.198E-05	8.262E-05	5.372E-05	1.579E-05
5 /3 /79 2013		9.761E-05	9.375E-05	6.873E-05	2.696E-05
5 /3 /79 2041		1.122E-04	1.042E-04	8.011E-05	3.633E-05
5 /3 /79 2112		1.070E-04	9.832E-05	7.992E-05	3.810E-05
5 /3 /79 2140		8.946E-05	8.516E-05	6.663E-05	2.853E-05
5 /3 /79 2208		1.090E-04	1.083E-04	8.366E-05	3.605E-05
5 /3 /79 2236		1.074E-04	1.053E-04	7.892E-05	3.012E-05
5 /3 /79 2304		1.473E-04	1.407E-04	1.184E-04	7.029E-05
5 /3 /79 2332		1.327E-04	1.286E-04	1.008E-04	4.770E-05
5 /3 /79 2300		1.482E-04	1.448E-04	1.094E-04	4.576E-05
5 /4 /79 28		2.265E-04	2.209E-04	1.887E-04	1.165E-04
5 /4 /79 56		1.647E-04	1.471E-04	1.172E-04	5.006E-05
5 /4 /79 124		1.824E-04	1.652E-04	1.361E-04	6.618E-05
5 /4 /79 152		1.580E-04	1.406E-04	1.150E-04	4.445E-05
5 /4 /79 320		1.820E-04	1.658E-04	1.328E-04	5.442E-05
5 /4 /79 350		1.869E-04	1.786E-04	1.479E-04	6.273E-05
5 /4 /79 418		1.909E-04	1.839E-04	1.538E-04	6.129E-05
5 /4 /79 446		2.526E-04	2.480E-04	2.120E-04	1.111E-04
5 /4 /79 514		2.510E-04	2.466E-04	2.122E-04	1.111E-04
5 /4 /79 542		2.368E-04	2.294E-04	1.941E-04	1.023E-04
5 /4 /79 610		1.673E-04	1.535E-04	1.239E-04	4.265E-05
5 /4 /79 638		1.357E-04	1.125E-04	8.261E-05	2.260E-05
5 /4 /79 706		1.558E-04	1.384E-04	1.099E-04	3.948E-05
5 /4 /79 734		1.218E-04	9.920E-05	7.127E-05	1.918E-05
5 /4 /79 802		1.404E-04	1.155E-04	8.774E-05	3.054E-05
5 /4 /79 830		1.425E-04	1.193E-04	8.560E-05	2.508E-05
5 /4 /79 858		1.100E-04	8.602E-05	6.019E-05	1.510E-05
5 /4 /79 926		1.224E-04	8.920E-05	5.353E-05	1.568E-05
5 /4 /79 957		1.184E-04	8.918E-05	6.287E-05	1.507E-05
5 /4 /79 1028		1.406E-04	1.009E-04	6.537E-05	1.494E-05
5 /4 /79 1058		1.557E-04	1.129E-04	7.047E-05	1.946E-05

SNI Intercomparison Extinctions (m^{-1})

Date/Time	λ	0.530	1.060	3.750	10.590
5 /4 /79 1126		1.767E-04	1.279E-04	7.180E-05	2.248E-05
5 /7 /79 1201		2.273E-04	2.114E-04	1.224E-04	3.813E-05
5 /7 /79 1232		2.047E-04	2.088E-04	1.289E-04	4.598E-05
5 /7 /79 1303		2.141E-04	2.190E-04	1.332E-04	5.064E-05
5 /7 /79 1333		1.919E-04	1.946E-04	1.213E-04	4.823E-05
5 /7 /79 1404		1.867E-04	1.877E-04	1.127E-04	3.754E-05
5 /7 /79 1435		1.976E-04	2.008E-04	1.272E-04	4.785E-05
5 /7 /79 1505		1.544E-04	1.577E-04	9.933E-05	3.305E-05
5 /7 /79 1536		1.256E-04	1.268E-04	7.650E-05	2.483E-05
5 /7 /79 1607		1.333E-04	1.342E-04	7.878E-05	2.466E-05
5 /7 /79 1637		1.424E-04	1.438E-04	7.333E-05	1.896E-05
5 /7 /79 1708		1.411E-04	1.432E-04	8.042E-05	2.456E-05
5 /7 /79 1739		1.255E-04	1.265E-04	7.001E-05	1.850E-05
5 /7 /79 1809		1.370E-04	1.389E-04	8.509E-05	2.722E-05
5 /7 /79 1840		1.613E-04	1.651E-04	1.046E-04	3.479E-05
5 /7 /79 1911		1.578E-04	1.637E-04	1.025E-04	3.429E-05
5 /7 /79 1941		1.204E-04	1.234E-04	7.961E-05	3.091E-05
5 /7 /79 2012		1.016E-04	1.040E-04	6.929E-05	2.852E-05
5 /7 /79 2043		1.147E-04	1.187E-04	7.928E-05	3.235E-05
5 /7 /79 2111		1.233E-04	1.263E-04	8.697E-05	3.499E-05
5 /7 /79 2139		1.332E-04	1.357E-04	9.460E-05	3.737E-05
5 /7 /79 2207		1.547E-04	1.587E-04	1.084E-04	4.594E-05
5 /7 /79 2235		1.598E-04	1.631E-04	1.127E-04	4.861E-05
5 /7 /79 2303		1.683E-04	1.719E-04	1.161E-04	4.495E-05
5 /7 /79 2331		1.769E-04	1.814E-04	1.176E-04	4.354E-05
5 /7 /79 2359		1.702E-04	1.740E-04	1.127E-04	4.057E-05
5 /8 /79 27		1.784E-04	1.821E-04	1.192E-04	4.235E-05
5 /8 /79 55		1.795E-04	1.857E-04	1.217E-04	4.341E-05
5 /8 /79 123		1.817E-04	1.889E-04	1.230E-04	4.510E-05
5 /8 /79 151		1.524E-04	1.576E-04	1.032E-04	3.423E-05
5 /8 /79 219		1.427E-04	1.450E-04	9.330E-05	2.682E-05
5 /8 /79 247		1.430E-04	1.479E-04	9.167E-05	2.695E-05

SNI Intercomparison Extinctions (m^{-1})

Date/Time	λ	0.530	1.060	3.750	10.590
5 /8 /79 315		1.203E-04	1.232E-04	7.725E-05	2.294E-05
5 /8 /79 343		1.225E-04	1.257E-04	8.305E-05	2.489E-05
5 /8 /79 411		1.237E-04	1.266E-04	8.596E-05	2.547E-05
5 /8 /79 439		1.229E-04	1.274E-04	8.388E-05	2.624E-05
5 /8 /79 507		1.175E-04	1.233E-04	8.055E-05	2.436E-05
5 /8 /79 535		1.094E-04	1.137E-04	7.743E-05	2.486E-05
5 /8 /79 603		1.108E-04	1.150E-04	7.932E-05	2.614E-05
5 /8 /79 631		8.282E-05	8.507E-05	5.253E-05	1.516E-05
5 /8 /79 659		7.436E-05	7.612E-05	5.015E-05	1.821E-05
5 /8 /79 727		8.464E-05	8.668E-05	5.581E-05	2.252E-05
5 /8 /79 755		1.060E-04	1.105E-04	7.021E-05	2.311E-05
5 /8 /79 823		7.188E-05	7.402E-05	4.782E-05	1.821E-05
5 /8 /79 851		8.271E-05	8.443E-05	5.106E-05	1.725E-05
5 /8 /79 919		7.749E-05	7.835E-05	4.904E-05	1.636E-05
5 /8 /79 947		7.885E-05	7.930E-05	4.731E-05	1.582E-05
5 /8 /79 1015		8.214E-05	8.149E-05	5.273E-05	2.017E-05
5 /8 /79 1043		9.759E-05	9.696E-05	6.648E-05	2.948E-05
5 /8 /79 1113		1.033E-04	1.037E-04	6.984E-05	2.976E-05
5 /8 /79 1144		1.270E-04	1.269E-04	8.837E-05	3.957E-05
5 /8 /79 1215		1.529E-04	1.524E-04	1.022E-04	5.224E-05
5 /8 /79 1431		2.370E-04	2.328E-04	1.685E-04	1.042E-04
5 /8 /79 1501		2.703E-04	2.653E-04	1.950E-04	1.279E-04
5 /8 /79 1532		2.684E-04	2.635E-04	1.978E-04	1.326E-04
5 /8 /79 2207		3.224E-04	3.183E-04	2.333E-04	1.533E-04
5 /8 /79 2235		4.381E-04	4.295E-04	3.062E-04	2.049E-04
5 /8 /79 2303		4.588E-04	4.516E-04	3.175E-04	2.100E-04
5 /8 /79 2331		4.685E-04	4.578E-04	3.289E-04	2.247E-04
5 /8 /79 2359		4.746E-04	4.627E-04	3.293E-04	2.268E-04
5 /9 /79 27		4.655E-04	4.539E-04	3.084E-04	1.911E-04
5 /9 /79 55		4.444E-04	4.348E-04	2.879E-04	1.731E-04
5 /9 /79 123		4.579E-04	4.509E-04	3.160E-04	1.988E-04
5 /9 /79 151		4.759E-04	4.684E-04	3.079E-04	1.758E-04

SNI Intercomparison Extinctions (m^{-1})

Date/Time	λ	0.530	1.060	3.750	10.590
5 /9 /79 219		4.878E-04	4.788E-04	3.075E-04	1.682E-04
5 /9 /79 247		4.774E-04	4.690E-04	3.047E-04	1.769E-04
5 /9 /79 315		4.744E-04	4.614E-04	2.998E-04	1.706E-04
5 /9 /79 343		4.622E-04	4.509E-04	2.919E-04	1.685E-04
5 /9 /79 411		4.479E-04	4.410E-04	2.844E-04	1.610E-04
5 /9 /79 439		4.305E-04	4.199E-04	2.668E-04	1.479E-04
5 /9 /79 507		4.140E-04	4.063E-04	2.592E-04	1.422E-04
5 /9 /79 535		3.961E-04	3.900E-04	2.391E-04	1.276E-04
5 /9 /79 610		3.932E-04	3.871E-04	2.382E-04	1.217E-04
5 /9 /79 641		3.866E-04	3.821E-04	2.320E-04	1.139E-04
5 /9 /79 711		3.613E-04	3.565E-04	2.079E-04	9.723E-05
5 /9 /79 742		3.567E-04	3.532E-04	2.004E-04	9.316E-05
5 /9 /79 813		3.400E-04	3.358E-04	1.934E-04	8.668E-05
5 /9 /79 843		3.686E-04	3.643E-04	2.092E-04	9.773E-05
5 /9 /79 914		3.494E-04	3.521E-04	1.997E-04	8.882E-05
5 /9 /79 945		3.158E-04	3.171E-04	1.825E-04	7.807E-05
5 /9 /79 1015		2.891E-04	2.911E-04	1.661E-04	6.729E-05
5 /9 /79 1046		3.169E-04	3.173E-04	1.797E-04	7.469E-05
5 /9 /79 1117		2.919E-04	2.927E-04	1.641E-04	6.367E-05
5 /9 /79 1147		3.353E-04	3.363E-04	1.898E-04	7.596E-05
5 /9 /79 1218		3.591E-04	3.651E-04	1.993E-04	7.970E-05
5 /9 /79 1249		3.604E-04	3.648E-04	2.048E-04	8.313E-05
5 /9 /79 1319		3.265E-04	3.274E-04	1.818E-04	7.703E-05
5 /9 /79 1350		3.274E-04	3.254E-04	1.822E-04	7.569E-05
5 /9 /79 1418		3.611E-04	3.592E-04	2.021E-04	8.694E-05
5 /9 /79 1446		3.539E-04	3.547E-04	2.098E-04	9.474E-05
5 /9 /79 1514		3.425E-04	3.437E-04	2.078E-04	9.468E-05
5 /9 /79 1542		3.519E-04	3.526E-04	2.077E-04	9.433E-05
5 /9 /79 1610		3.509E-04	3.542E-04	2.116E-04	9.733E-05
5 /9 /79 1638		3.153E-04	3.186E-04	1.869E-04	8.340E-05
5 /9 /79 1706		2.759E-04	2.775E-04	1.687E-04	7.321E-05
5 /9 /79 1734		2.852E-04	2.857E-04	1.625E-04	6.904E-05

SNI Intercomparison Extinctions (m^{-1})

Date/Time	λ	0.530	1.060	3.750	10.590
5 /9 /79 1802		3.092E-04	3.092E-04	1.761E-04	7.385E-05
5 /9 /79 1830		3.219E-04	3.230E-04	1.882E-04	8.091E-05
5 /9 /79 1858		3.080E-04	3.050E-04	1.803E-04	8.193E-05
5 /9 /79 1926		3.196E-04	3.191E-04	1.860E-04	8.173E-05
5 /9 /79 1954		3.244E-04	3.291E-04	1.878E-04	7.650E-05
5 /9 /79 2022		3.529E-04	3.546E-04	2.075E-04	9.028E-05
5 /9 /79 2050		3.429E-04	3.444E-04	1.982E-04	7.984E-05
5 /9 /79 2118		3.510E-04	3.543E-04	2.008E-04	7.890E-05
5 /9 /79 2146		3.579E-04	3.652E-04	1.979E-04	7.069E-05
5 /9 /79 2214		3.537E-04	3.586E-04	1.963E-04	7.121E-05
5 /9 /79 2242		3.873E-04	3.918E-04	2.123E-04	7.756E-05
5 /9 /79 2310		4.215E-04	4.286E-04	2.302E-04	8.582E-05
5 /9 /79 2338		3.953E-04	4.037E-04	2.214E-04	8.237E-05
5 /10/79 6		3.851E-04	3.934E-04	2.154E-04	7.717E-05
5 /10/79 34		3.719E-04	3.798E-04	2.066E-04	7.310E-05
5 /10/79 102		4.014E-04	4.232E-04	2.551E-04	9.210E-05
5 /10/79 130		4.999E-04	5.399E-04	3.646E-04	1.406E-04
5 /10/79 158		4.681E-04	4.972E-04	3.150E-04	1.153E-04
5 /10/79 226		5.242E-04	5.626E-04	3.813E-04	1.502E-04
5 /10/79 254		4.016E-04	4.265E-04	2.565E-04	8.043E-05
5 /10/79 322		3.788E-04	4.049E-04	2.323E-04	6.241E-05
5 /10/79 350		3.536E-04	3.788E-04	2.241E-04	5.664E-05
5 /10/79 418		4.006E-04	4.332E-04	2.762E-04	8.071E-05
5 /10/79 446		3.407E-04	3.654E-04	2.309E-04	8.072E-05
5 /10/79 514		3.309E-04	3.539E-04	2.268E-04	6.687E-05
5 /10/79 1110		1.318E-04	1.386E-04	7.293E-05	1.302E-05
5 /10/79 1141		1.303E-04	1.366E-04	7.790E-05	1.419E-05
5 /10/79 1157		1.458E-04	1.557E-04	8.555E-05	1.534E-05

VI. Calibrations at Mainz and Garmisch

One member of the Environmental Physics Group (K. Davidson) spent six months at the Max Planck Institute fur Chemie, Mainz, F.R.G. performing detailed calibrations of the NPS spectometers. The majority of the time was spent working with the group at Mainz, shorter visits being made to Garmisch-Partenkirschen to discuss spectrometer intercomparisons. Investigations were undertaken on:

A. Particle sizing--ambiguity zone effects

B. False sizing due to bin edge shift

C. Particle density calibrations

D. Counting statistics

E. Spectrometer comparison

A. Particle sizing--ambiguity zone effects

Sizing of particles by the spectrometers was calibrated using a generator developed by Jaenicke.[6] The generator produces a monodisperse aerosol using latex particles, the particle size being specified by their manufacturer. The results from several of the calibrations are shown in Figure s-12. Special attention in these measurements was paid to investigating the ambiguity zone effect.

Figure 7 and 8 show results for the CSASP spectrometer, range 1, using 2.7 and 2.05 μm spheres. The sizing was found to be quite good, with the ambiguity zones having little effect. Similarily good results are shown in Figure 9 for ASASP range 0 for 1.1 μm particles.

Quite different results were obtained for the ASASP, range 0,

using larger spheres, 2.05 and 2.7 μm. The results are shown in Figures 10 and 11. The spectrometer placed these particles in bins 3-7, which is 1-1.8 μm. The shift of these sizes to lower bins cannot be accounted for by the ambiguity zones for latex (n = 1.5). However, if the particles had an index of refraction of 1.33 the shift to lower bins could be easily explained. It was noted that during several of the calibrations the humidity was not well controlled, as evidenced by condensation on the walls of the generator. This means that the latex spheres could have been water coated, lowering their index of refraction (n = 1.33 for water).

The final results presented, Figure 12, shows 0.43 μm spheres sized by ASASP range 2. These results are somewhat ambiguous. There appears to be a counting peak at bin 4, ~0.32 μ, and a weaker peak at bin 7, ~0.39 μ. The spectrometer may have sized incorrectly, or, one could interpret the results to be a peak near the correct value false counts in the small size bins.

Finally, note that in all cases there are a large number of false counts in the smallest size bins of each range. This is probably due to the carrier material that is used to suspend the latex spheres. Such effects have been observed at PMS.[7]

B. Bin edge shift

The group at Garmisch has observed significant counting differences between two supposedly identical spectrometers operating side by side. They attribute the differences to errors caused by bin edge shift when measureing very steep slope spectra.

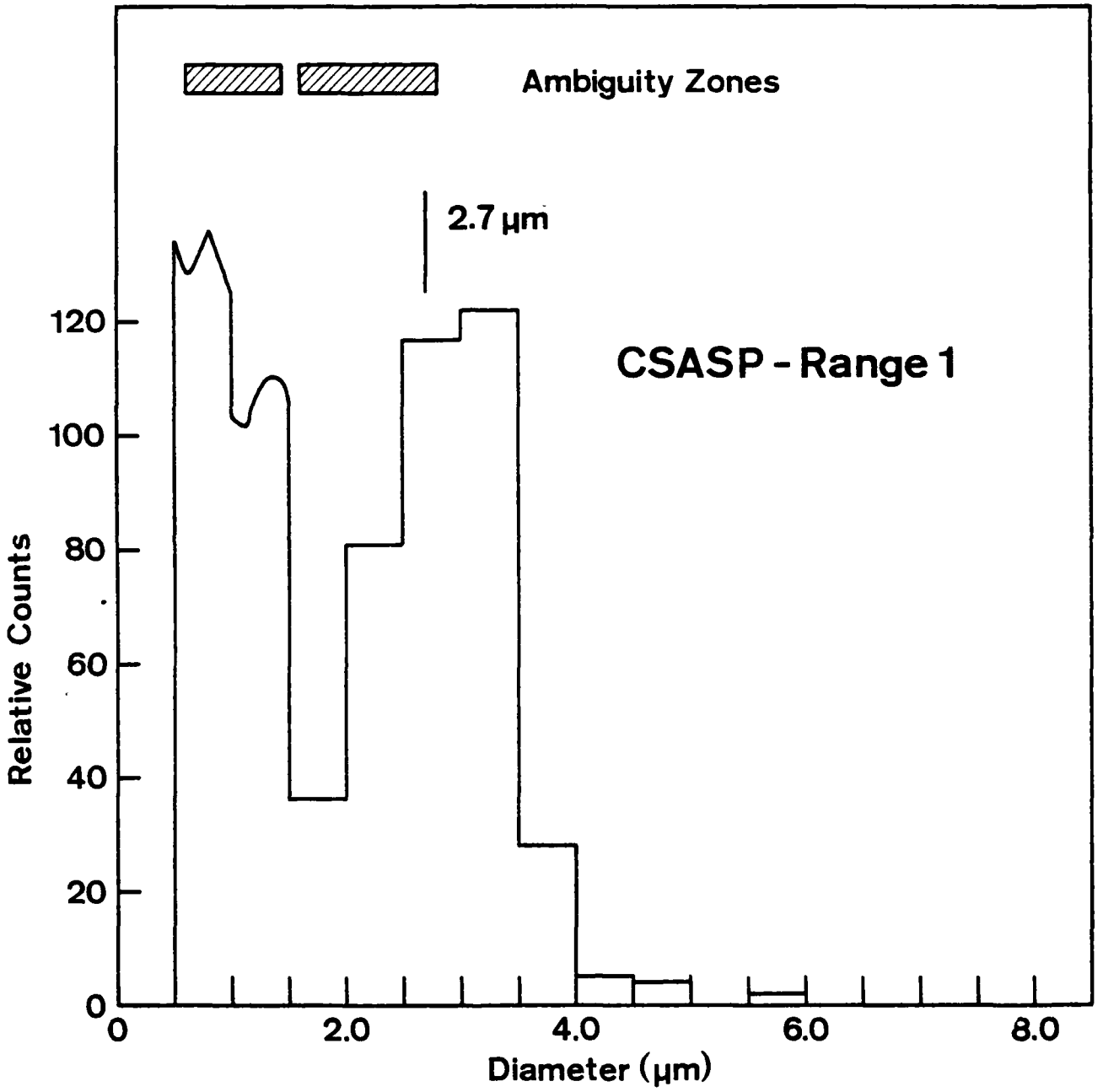
Ambiguity Zones
2.7 µm
CSASP - Range 1
Relative Counts
120
100
80
60
40
20
0
0
2.0
4.0
6.0
8.0
Diameter (µm)

Figure 7

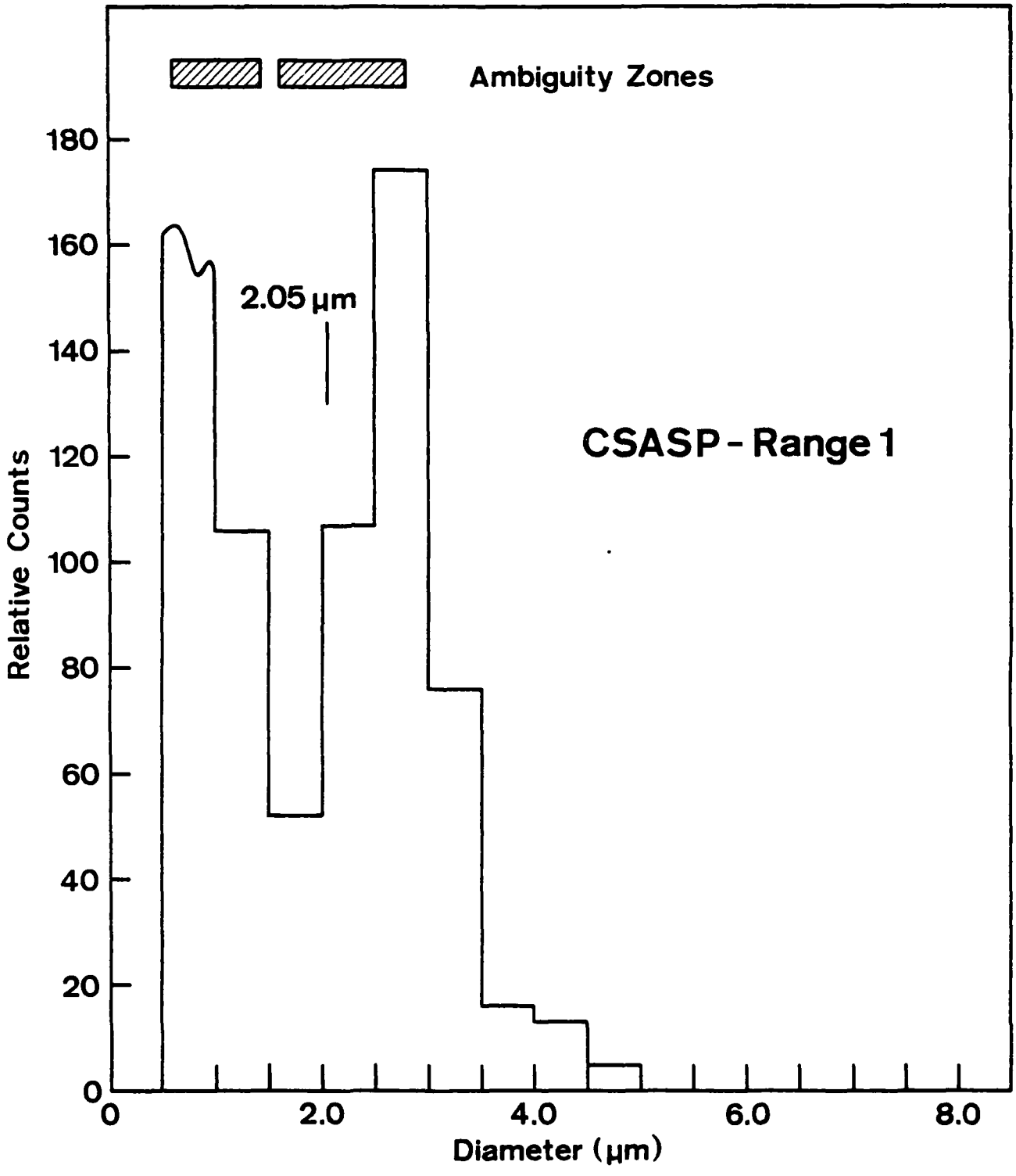
Ambiguity Zones
2.05 µm
CSASP - Range 1
Relative Counts
180
160
140
120
100
80
60
40
20
0
0
2.0
4.0
6.0
8.0
Diameter (µm)

Figure 8

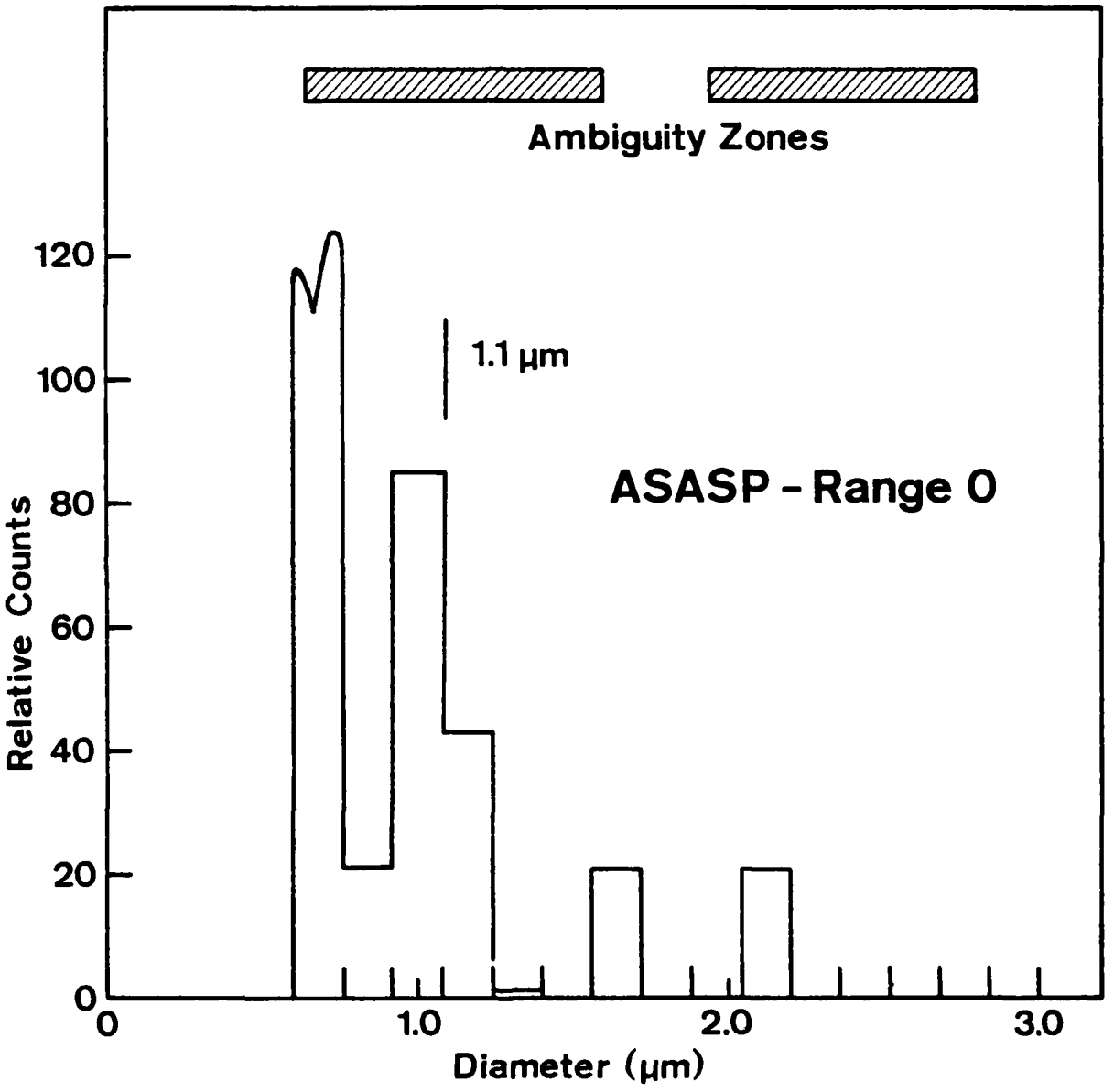
Ambiguity Zones
1.1 µm
ASASP - Range 0
Relative Counts
120
100
80
60
40
20
0
0
1.0
2.0
3.0
Diameter (µm)

Figure 9

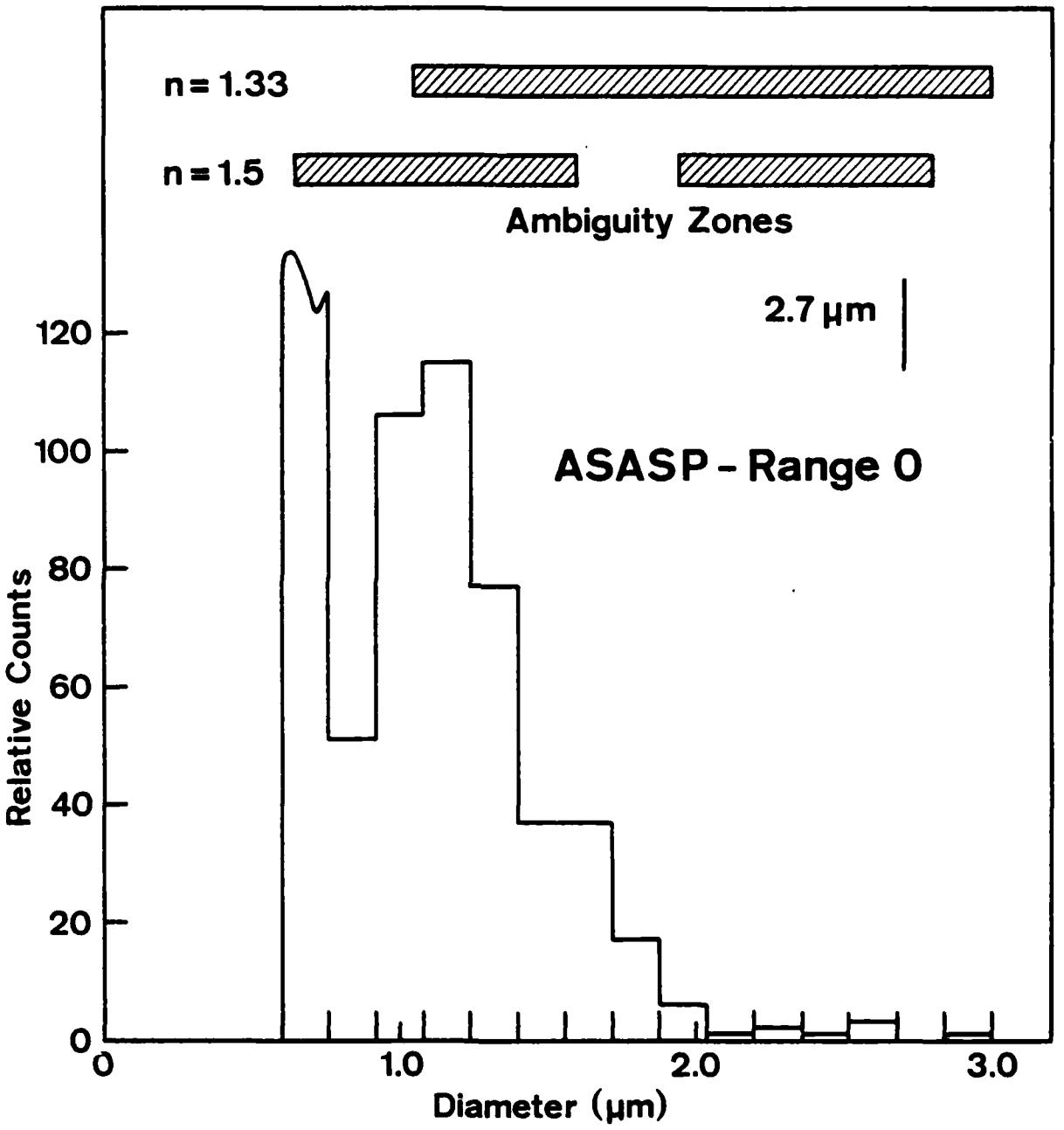
n = 1.33
n = 1.5
Ambiguity Zones
2.7 µm
ASASP - Range 0
Relative Counts
120
100
80
60
40
20
0
0
1.0
2.0
3.0
Diameter (µm)

Figure 10

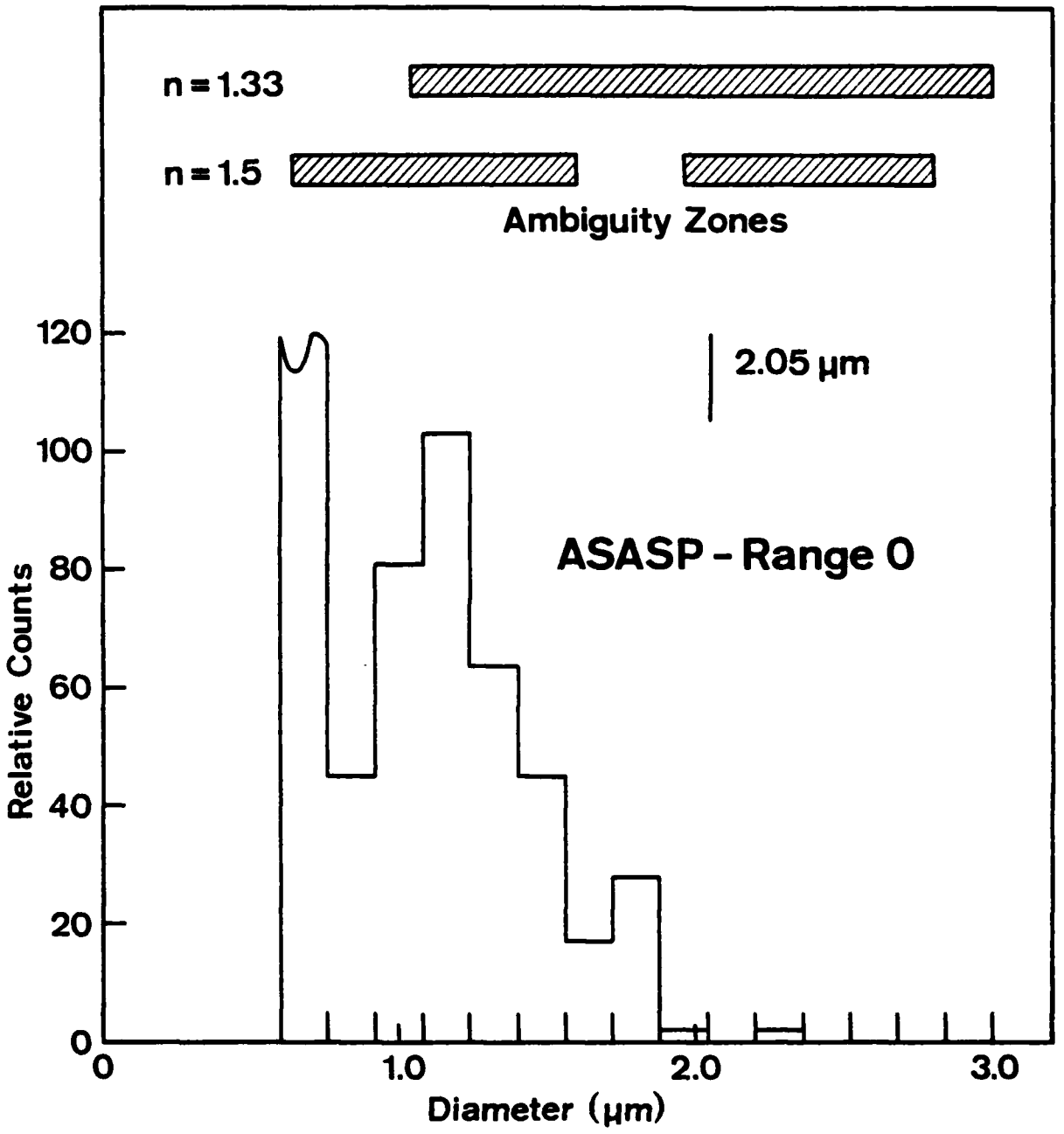
n = 1.33
n = 1.5
Ambiguity Zones
2.05 μm
ASASP - Range 0
Relative Counts
120
100
80
60
40
20
0
0
1.0
2.0
3.0
Diameter (μm)

Figure 11

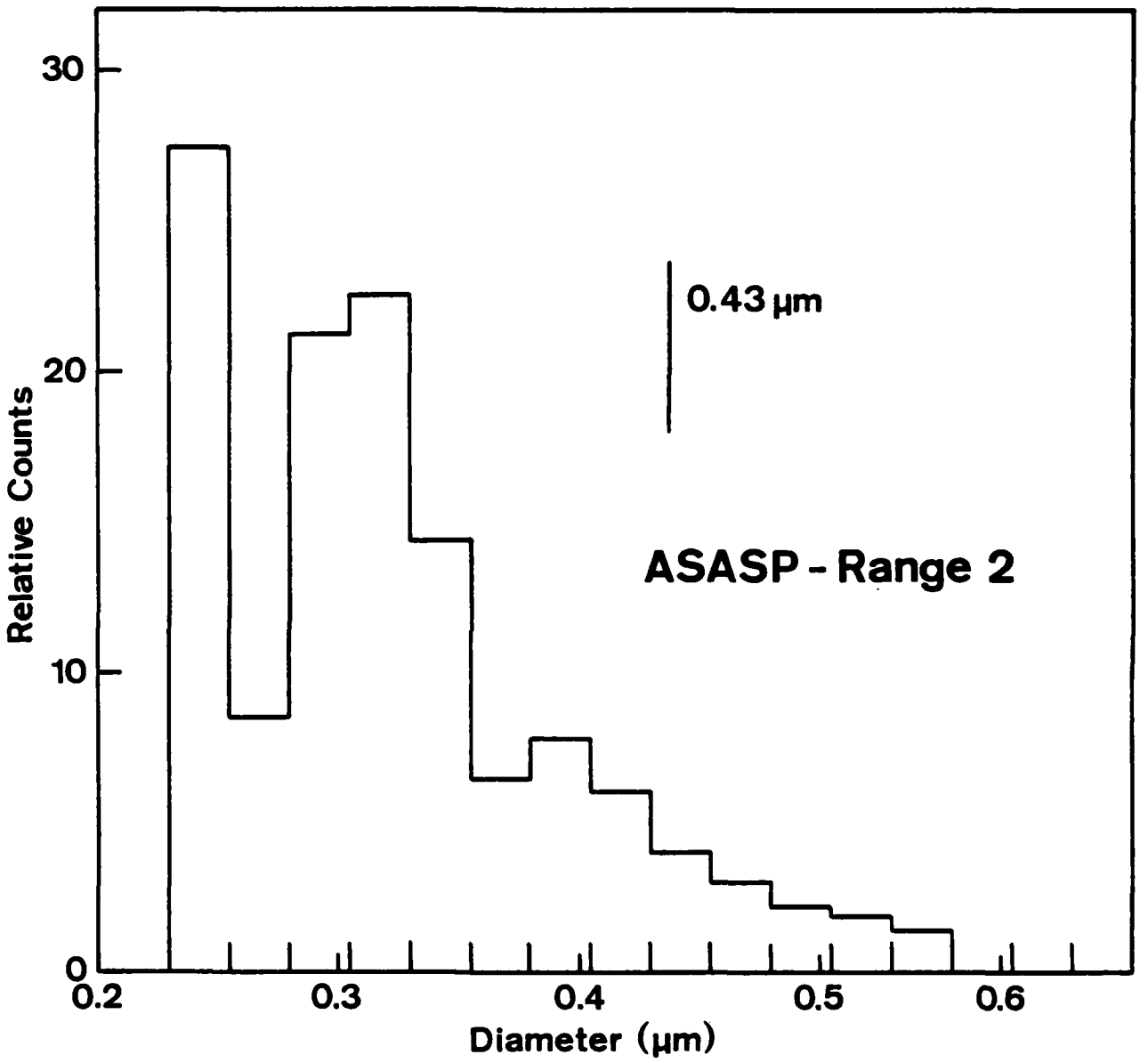
30
20
10
0
Relative Counts
0.43 µm
ASASP - Range 2
0.2
0.3
0.4
0.5
0.6
Diameter (µm)

Figure 12

Figure 13 illustrates the effect. Two assumed bins are shown by solid lines, and the actual bin edges shown with dashed lines. With the edges shifted as shown, smaller sizes, with their corresponding high numbers, will be sized into a larger size bin. This will artificially raise the counts in that bin leading to the spectrum shown by the dashed line in the lower figure.

C. Particle density calibrations

A fair amount of effort was expended on attempting to calibrate the aerosol particle density measurements. We had a nearly complete lack of success for a very simple reason: it is extremely difficult to determine the air flow rate through the optically active volume of the spectrometers, at least with the equipment we have available.

Our experience showed that the method of introducing the aerosol into the spectrometer is extremely critical. If an absolute calibration is to be of any value the aerodynamic flow must be matched to field conditions. In this regard, laboratory calibrations should be made using the horn supplied by the manufacturer with air being drawn from a large volume using the spectrometer fan.

Our limited experience with these laboratory calibrations and with four long duration cruises have identified the following as potential causes of counting errors:

1) The incidence angle of the wind can change the results. This effect is wind speed dependent.
2) Turbulence in the scattering chamber will affect the

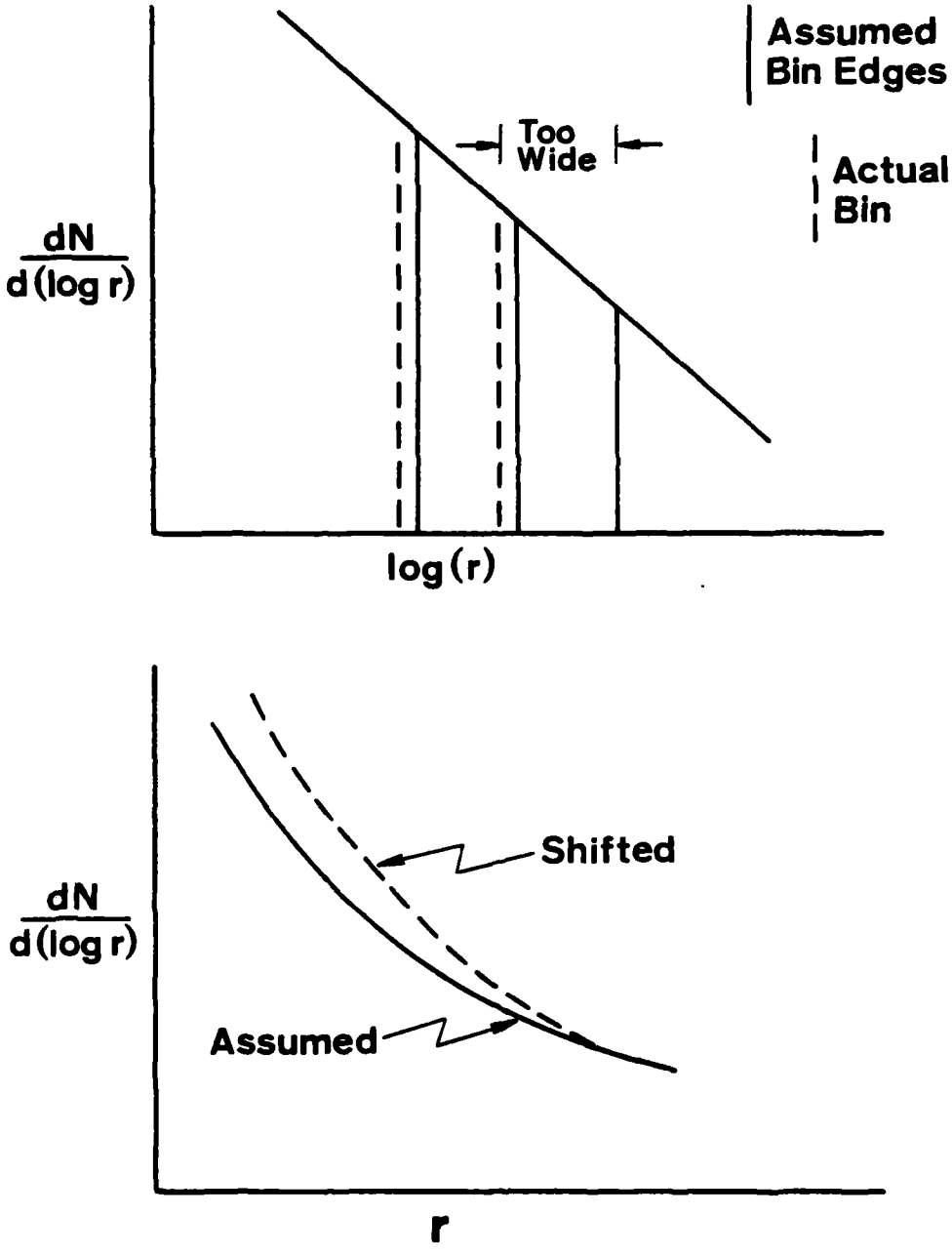
Assumed
Bin Edges
Too
Wide
Actual
Bin
dN
d(log r)
log(r)
Shifted
Assumed
dN
d(log r)
r

Figure 13

calibration. This can occur during high wind situations.

Note that the above shows that a spectrometer designed for aircraft use cannot be used on the ground unless it is aspirated at a rate equal to aircraft speeds. It will not be sufficient to correct for the wind speed difference in order to calculate the total volume of air that has been sampled. (Needed electronics modifications for rejection, etc. are not addressed here.)

D. Sampling statistics

The Garmisch group probably has more continuous experience with the PMS counters than any other. They view the sampling statistics to be very important when describing distributions which change by three orders of magnitudes over the size intervals of interest. Obtaining reasonable statistics for the low concentrations at large sizes requires that sampling times at these sizes must be much longer than at the smaller sizes. A second consideration is that the total sampling time to cover all sizes must not be too long. The present sampling is (for ASASP ranges 0, 1, 2, 3; where range 0 is for the largest particles) as follows:

Range	
0	30 seconds
0	30 seconds
1	30 seconds
2	30 seconds
3	30 seconds
0	30 seconds
0	30 seconds, etc.

This sampling results in 40% of the sampling time being given to the larger sizes. The opinion of the Garmisch group is that the largest sizes should have at least 75% of the sampling time in order to have optimal statistics. (It is important to note that 20 to 30 minute total periods are the most one can expect when the operation modes include other platforms or measurements.) The Garmisch sampling is as follows for a 20 second total period.

Range	
0	14 seconds
1	3 seconds
2	2 seconds
3	1 second

E. Spectrometer comparison

The Garmisch and the NPS spectrometers were calibrated using the aerosol generator at Mainz. All results are shown on a single graph in Figure 14. The results show that the NPS spectrometers tended to size particles slightly too large. In general the results are quite good. The figure shows the ambiguity zones and we see a definite scatter of the sizing in these zones, as expected.

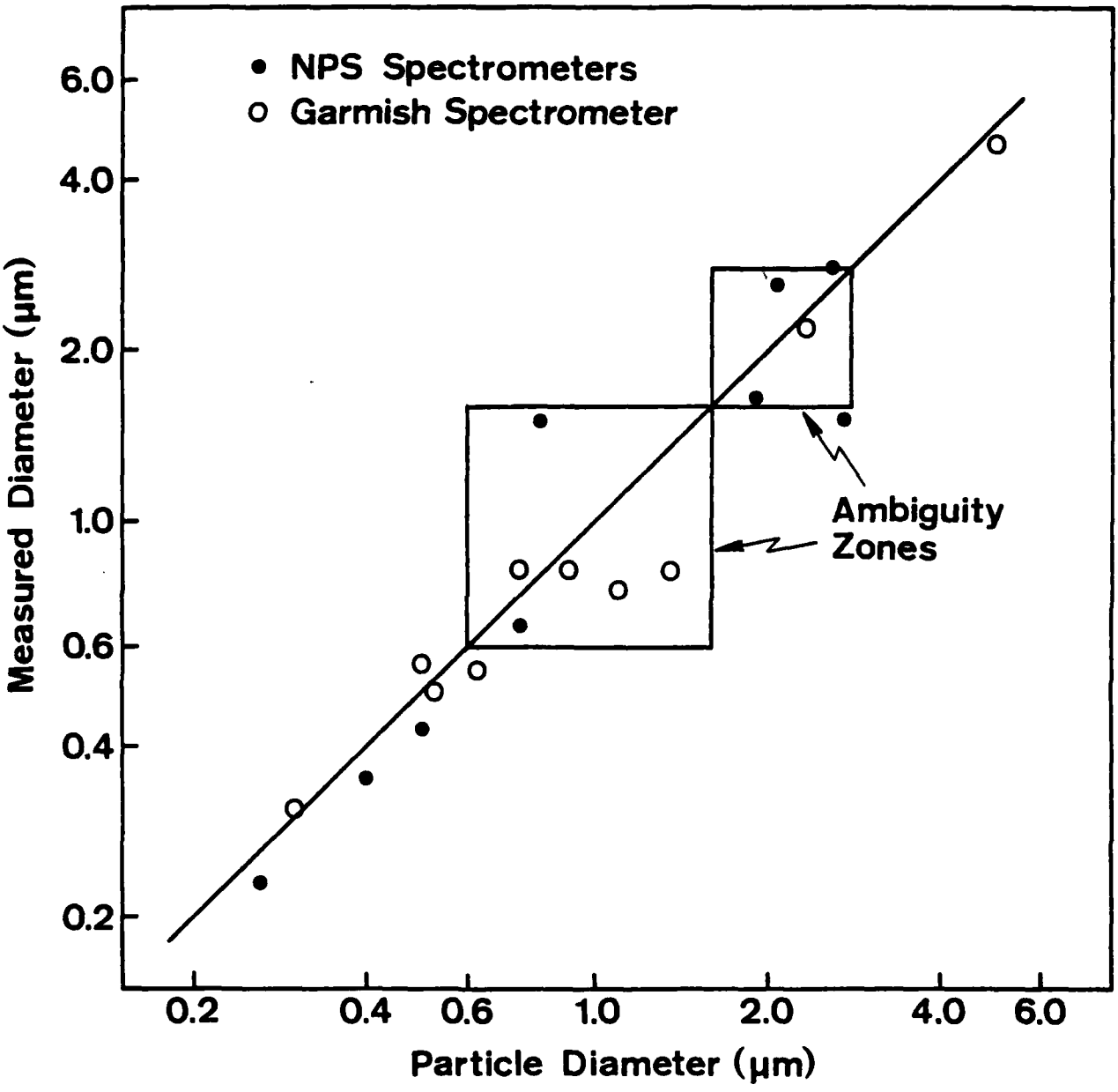
• NPS Spectrometers
o Garmish Spectrometer
Measured Diameter (μm)
6.0
4.0
2.0
1.0
0.6
0.4
0.2
Ambiguity Zones
0.2
0.4
0.6
1.0
2.0
4.0
6.0
Particle Diameter (μm)

Figure 14

VII. CEWCOM-78 COMPARISONS

There were opportunities to compare several instruments, during CEWCOM 78: NPS spectrometers, Calspan nephelometer and particle measuring equipment, NOSC airborn aerosol spectrometer, NPS ship to shore lasers, and PMTC optics. The Calspan equipment was on board for the full cruise, while the laser, aircraft and optics measurements were made only at SNI.

The Calspan equipment on the ship was:

Instrument	Parameter	Height Above Sea Surface
Thermo-Systems Electrical Aerosol Analyzer Mod. 3030	Aerosol size dist. (0.01 - 75 μm)	5.0 m
Royco Model 225 Particle Counter	Aerosol size dist. (0.3 - 5 μm)	5.0 m
Calspan Sea Spray Sampler (gelatin repl.)	Aqueous aerosol spectra (3 - 100 μm)	3.0m
Gardner Small Particle Detector	Total aerosol conc. (>0.0025 μm)	5.0m
Thermo-Sys. Electrostatic Aerosol Sampler, Mod. 3100	Aerosol chemistry by size (>0.02 μm)	5.0 m
Hi-Vol and Lo-Vol Filter Samplers (2)	Bulk aerosol chemistry	5.0 m
Calspan Fog Droplet Sampler (gelatin repl.)	Fog drop size dist.	3.0 m
EG&G Forward Scatter Meter, Mod. 107	Visibility (60-6000 m)	7.5 m
MRI Integrating Nephelometer, Model 2050	Scattering Coeff. (0.1 - $100 \times 10^{-4} m^{-1}$) Visibility (5-80 km)	5.0 m

We list the full compliment of equipment for completeness only. Comparisons have not been made to all of their results.

The NOSC aircraft carried a PMS ASSP-100 spectometer. NPS

optical measurements were made ship to shore using 4880 and 6328 Å wavelength lasers, and an IR broadband source with 3.6-4.0 μm and 9.0-12.0 μm detection filters.

A. Ship and Wind influence

The effect of the ship and wind direction on the measurements are most easily seen by comparing the NPS spectrometers to the Calspan nephelometer.[8] These results are shown in Figs 15-18, where the spectrometer (solid line) calculated extinction and nephelometer (dashed line) measured extinction results are plotted as functions of time. The measured extinction is for visible and the calculated is for 0.488 μm.

Figs 15 and 16 show the wind direction effect. The shaded bands in the figures show times of "good" wind direction, where good means within 30° of the bow. We see that with a good wind direction the spectrometer results show a marked increase relative to the nephelometer. This feature was consistent throughout the cruise. Turbulence in the spectometer sample chamber and particle loss due to non-isokinetic sampling could be responsible for the effect. Turbulence could cause reduced flow through the scattering volume even though the average flow is correct. With a good wind direction the air flow will be less distorted.

Ship influence and/or system location also played an important part in the Calspan nephelometer measurements. All figures other than 15 and 16 are for good wind directions. Results in Figs 15-19 show that with good winds the nephelometer gives much lower scattering values than the spectrometers. This is apparently due to the location of the nephelometer

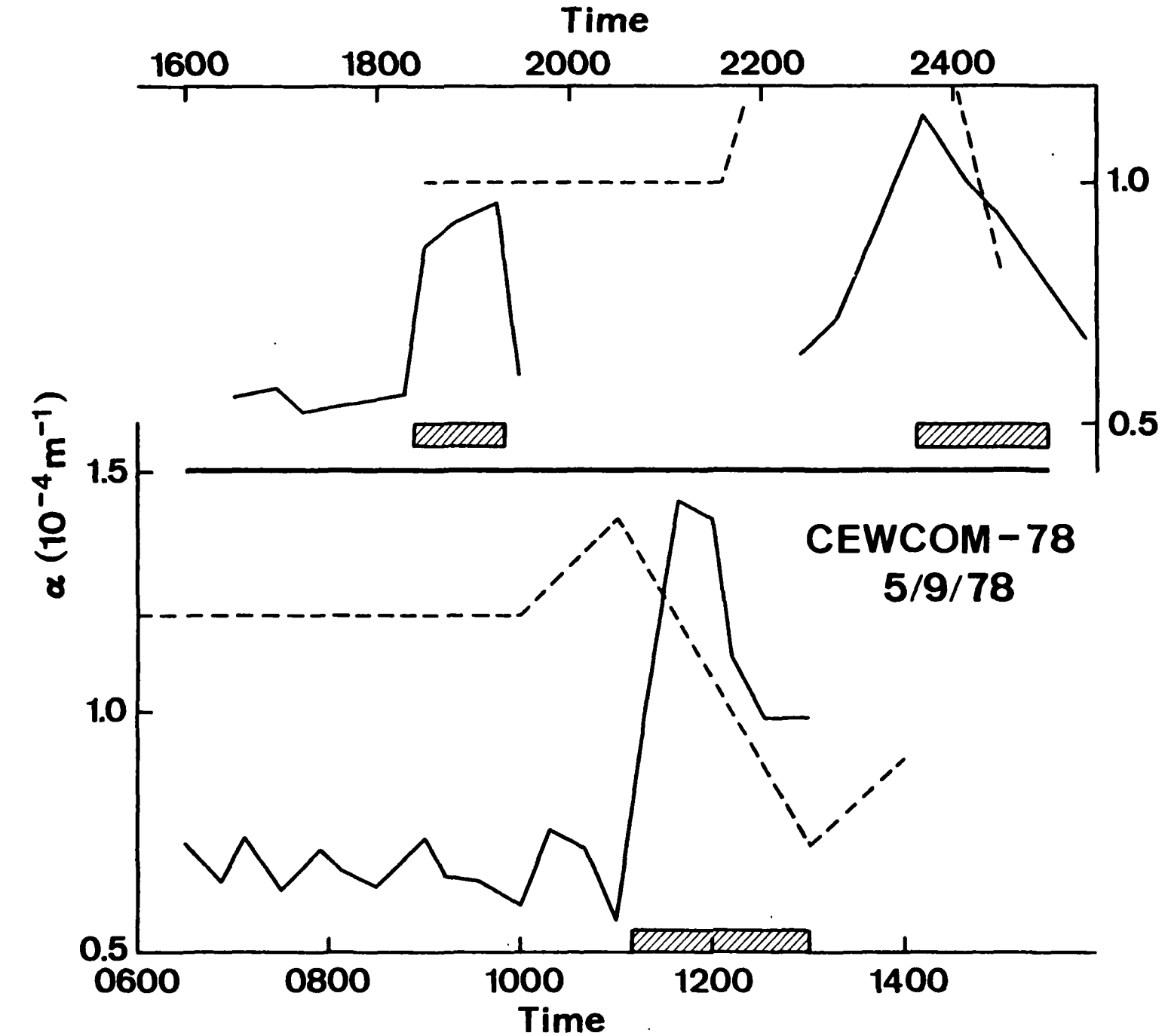
Time
1600
1800
2000
2200
2400
1.0
0.5
α (10⁻⁴m⁻¹)
1.5
1.0
0.5
CEWCOM-78
5/9/78
0600
0800
1000
1200
1400
Time

Figure 15

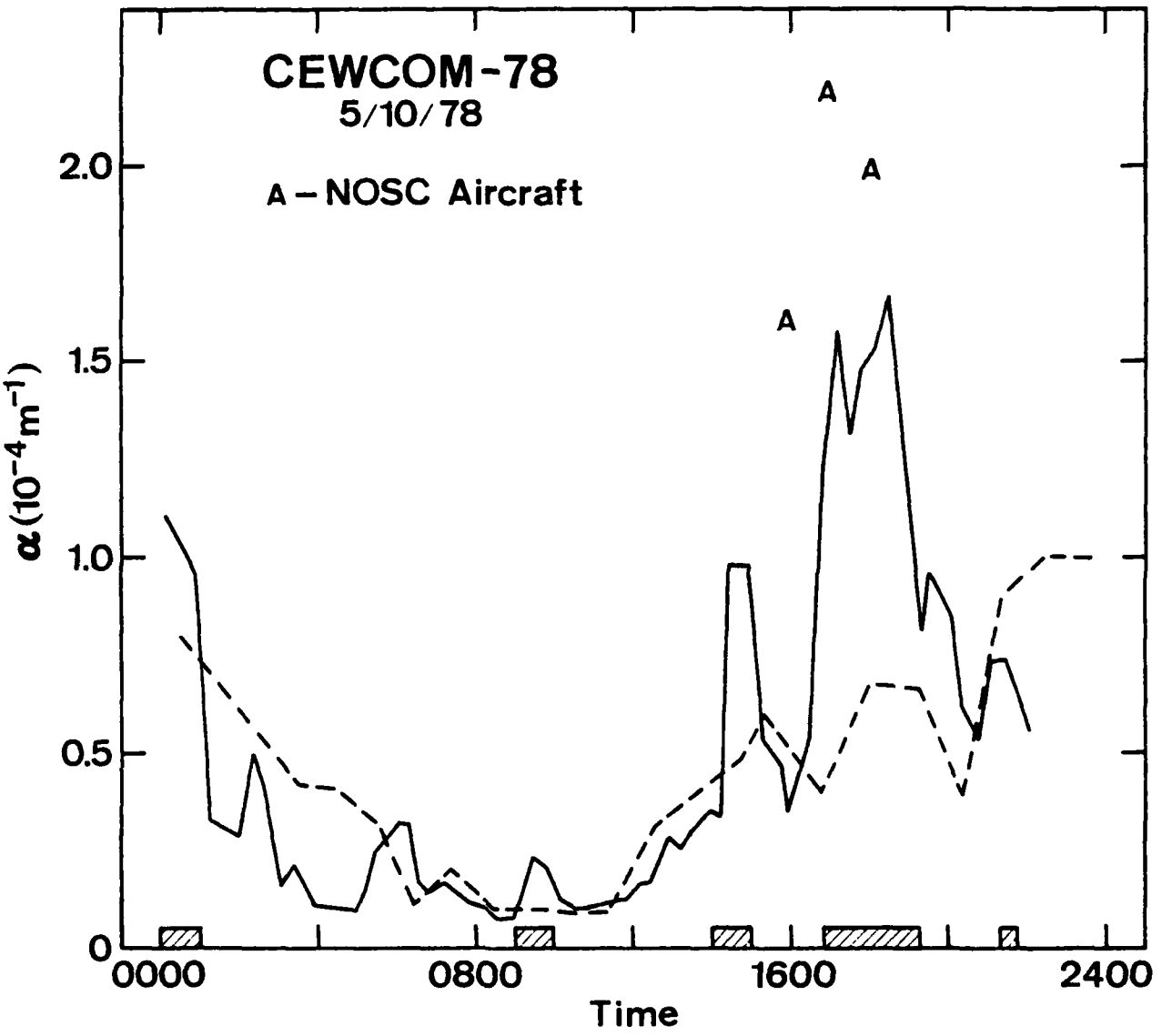
CEWCOM-78
5/10/78
A – NOSC Aircraft
A
A
A
2.0
1.5
1.0
0.5
0
α(10⁻⁴m⁻¹)
0000
0800
1600
2400
Time

Figure 16

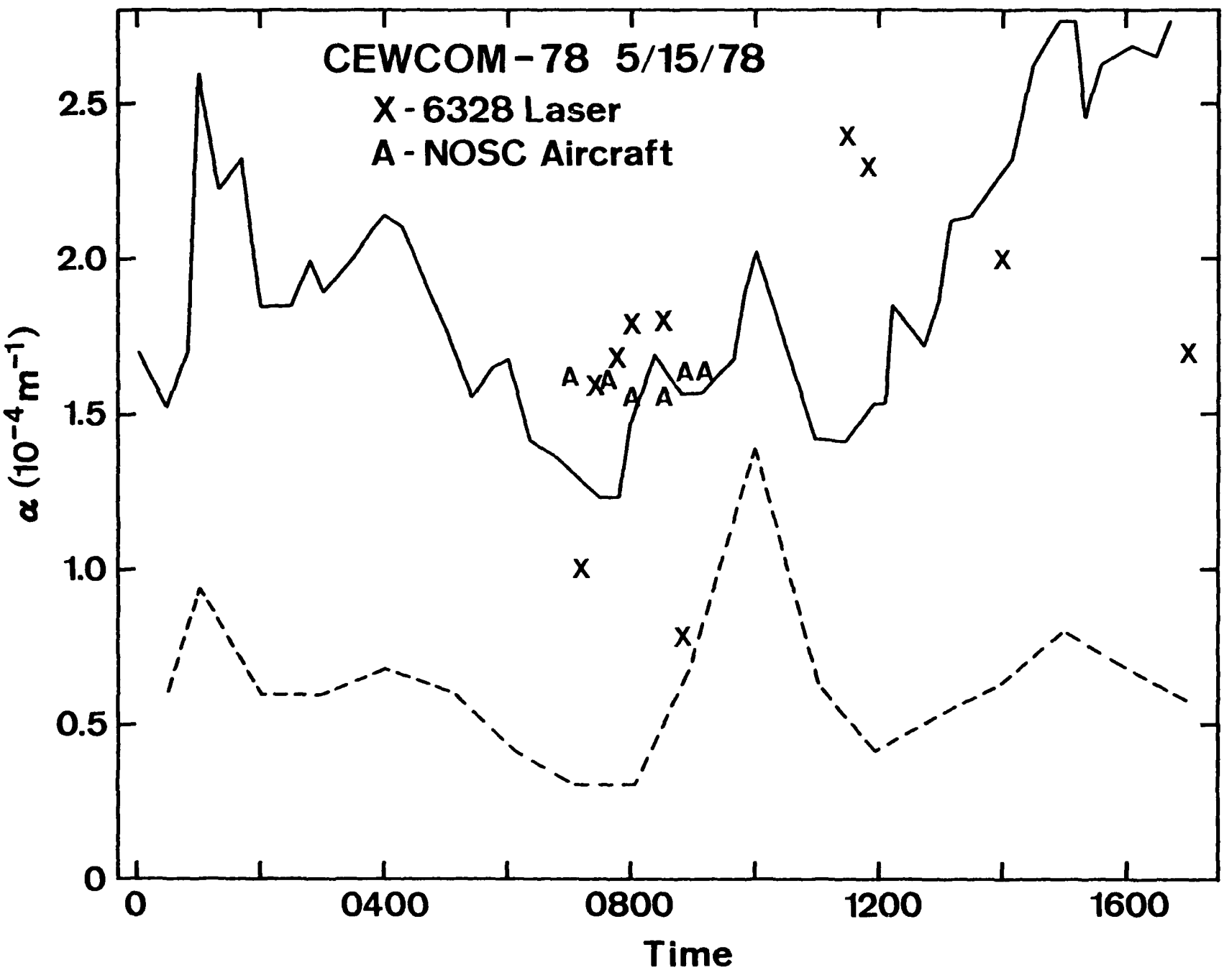
CEWCOM-78 5/15/78
X - 6328 Laser
A - NOSC Aircraft
α (10⁻⁴ m⁻¹)
2.5
2.0
1.5
1.0
0.5
0
0
0400
0800
1200
1600
Time

Figure 17

sampling tube on the ship and the influence of the long inlet tube.[9] This effect is especially apparent later in the day on 5/15. During that time the wind was continually increasing (reaching 60 knts at times) and the Acania continued operation until the anchor chain broke. The spectometers were in an elevated and exposed location and registered a very large increase in aerosol density whereas the protected nephelometer showed no effect.

B. Comparison with NOSC Aircraft

NOSC aircraft measurements are shown in Figs 16 and 17, where they are labeled with an A. The results are summarized below:

	α ($10^{-4}m^{-1}$)	
Date/Time	NPS	NOSC
5/15 0700 - 0900	1.4	1.6
5/10 1600 - 1800	1.5	1.9
5/12 1400	1.4	0.9
5/12 1600	1.4	0.9 (at 100 ft)

C. Comparison with NPS Optics

NPS optically measured extinction for 0.488 μm and 0.6328 μm appear in Figs 17 and 19, with an X for 0.6328 and an 0 for 0.4880. The measurements were made along an approximately 2 km optical path from the RV/Acania to the shore on SNI. In Fig. 19 three or more measurements were made very close together in time and the average and extrema are plotted as a point and error bars. All optically measured values have had 0.2 x $10^{-4}m^{-1}$ subtracted

from the measurement to correct for molecular absorption. This is an adequate approximation to enable comparisons to be made with the aerosol measurements.

There is fairly good agreement between the spectrometer and optical results for all but one point. Further discussion of the optical results is given in other reports.[10] No attempt will be made to use these results to assess aerosol spectrometer performance.

D. Comparison with Wells, Katz, Munn Model.

Figs 18-20 include extinctions calculated from the Well's et al model[11], shown as Δ. We have used the model as modified by Katz, taking the visibility correction term equal to 1, and using the Fitzgerald[12] humidity growth factor. These comparisons of the model and the spectrometer results are made only for times when the wind direction was good.

The model performance was characterized by periods of systematic disagreement and fortuitous agreement in specific instances with the spectrometer measurements. In general the model tended to underestimate the extinction. We will not attempt to discuss model performance here, that will be the subject of a later report. Here we merely present some easily observed points from the CEWCOM-78 data.

1. For wind speeds above 10 m/sec (5/15) the model works fairly well.
2. For low wind speeds the model underestimates the extinction for most cases.
3. For the open ocean conditions of 5/20 and 5/10 (not shown) the model overestimates the extinction.

4. The measurements do not show a sudden increase in extinction for wind speeds greater than 7 m/sec as predicted by the model (5/19, 5/14).
5. The Wells' humidity growth term fits these data better than the Fitzgerald-Ruskin term.

All of these results are for moderate to high wind speeds. For high winds the hydrostatic stability is near neutral. We have found that stability plays an important role in establishing the equilibrium aerosol distribution. We expect to find less agreement with the model for non-neutral stability. This topic is the subject of a report which is in preparation.

E. Comparison with PMTC optics.

During one of the days the RV/Acania was at SNI optical measurements were made by PMTC. Approximately 6 hours of intercomparison data were obtained. The results are shown in Figure 21 for wavelengths of 1.06, 3.75, and 10.59 μm. Wells' model predictions are included for comparison purposes. The optical data was supplied by Mathews of PMTC[13]. Molecular extinction was subtracted from the optical results using LOWTRAN-III, the calculations being performed by NPS.

The agreement between aerosol and optical results is fairly good, especially in view of the optical measurements being made on the shore and the aerosol measurements on the ship. 5/15 was the day when very high winds occured late in the day and the data show a systematic disagreement with high wind speeds, the aerosol results being higher. No conclusive explanation of this effect can be given; acceleration of the airflow

by the land could cause some large particle drop out, resulting in lower extinction being measured near the island.

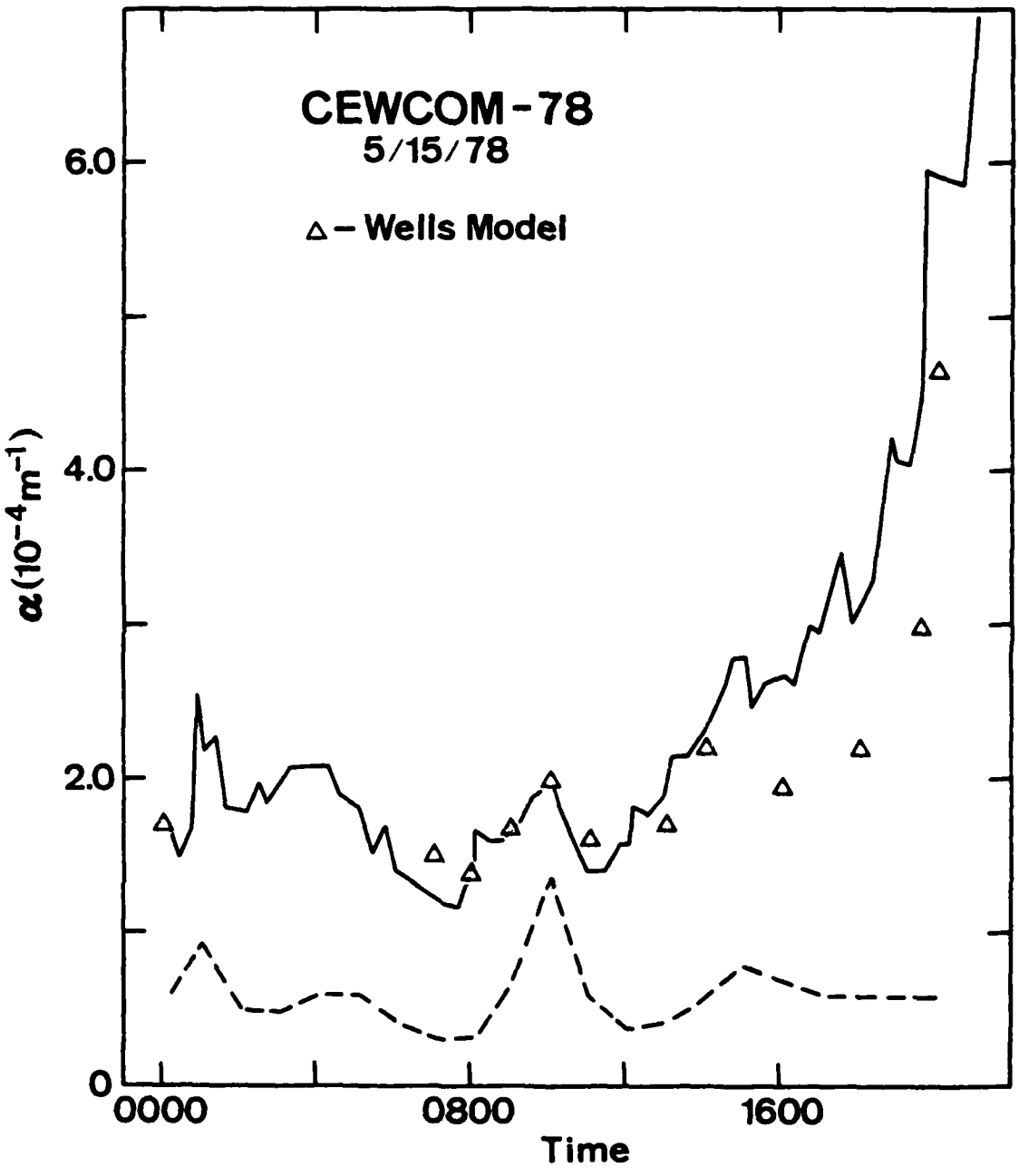
CEWCOM-78
5/15/78
△ – Wells Model
6.0
4.0
2.0
0
α(10⁻⁴m⁻¹)
0000
0800
1600
Time

Figure 18

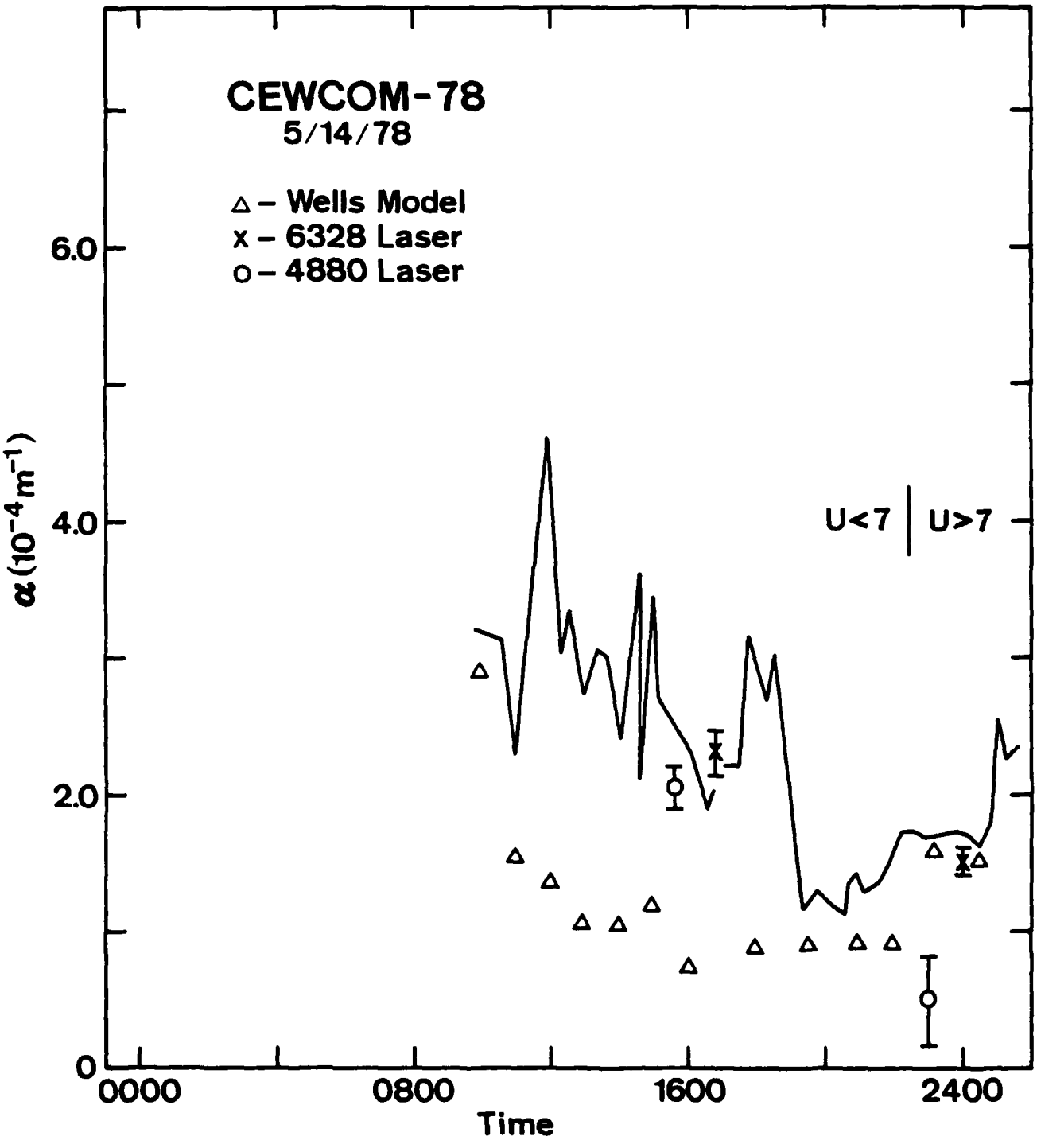
CEWCOM-78
5/14/78
△ – Wells Model
x – 6328 Laser
o – 4880 Laser
U<7 | U>7
α (10⁻⁴m⁻¹)
6.0
4.0
2.0
0
0000
0800
1600
2400
Time

Figure 19

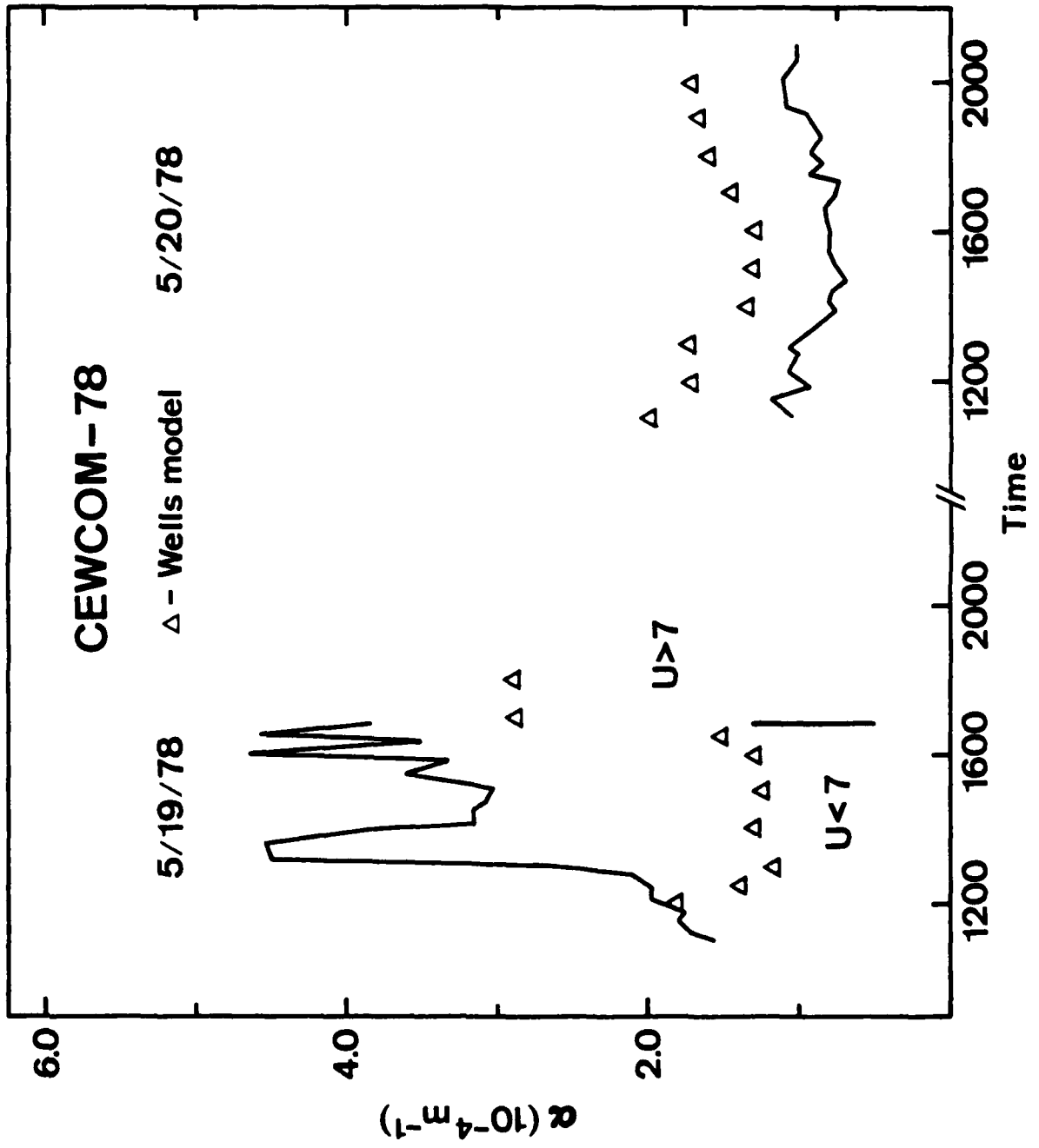
CEWCOM-78
Δ - Wells model
5/19/78
5/20/78
U>7
U<7
6.0
4.0
2.0
α (10⁻⁴m⁻¹)
1200
1600
2000
//
1200
1600
2000
Time

Figure 20

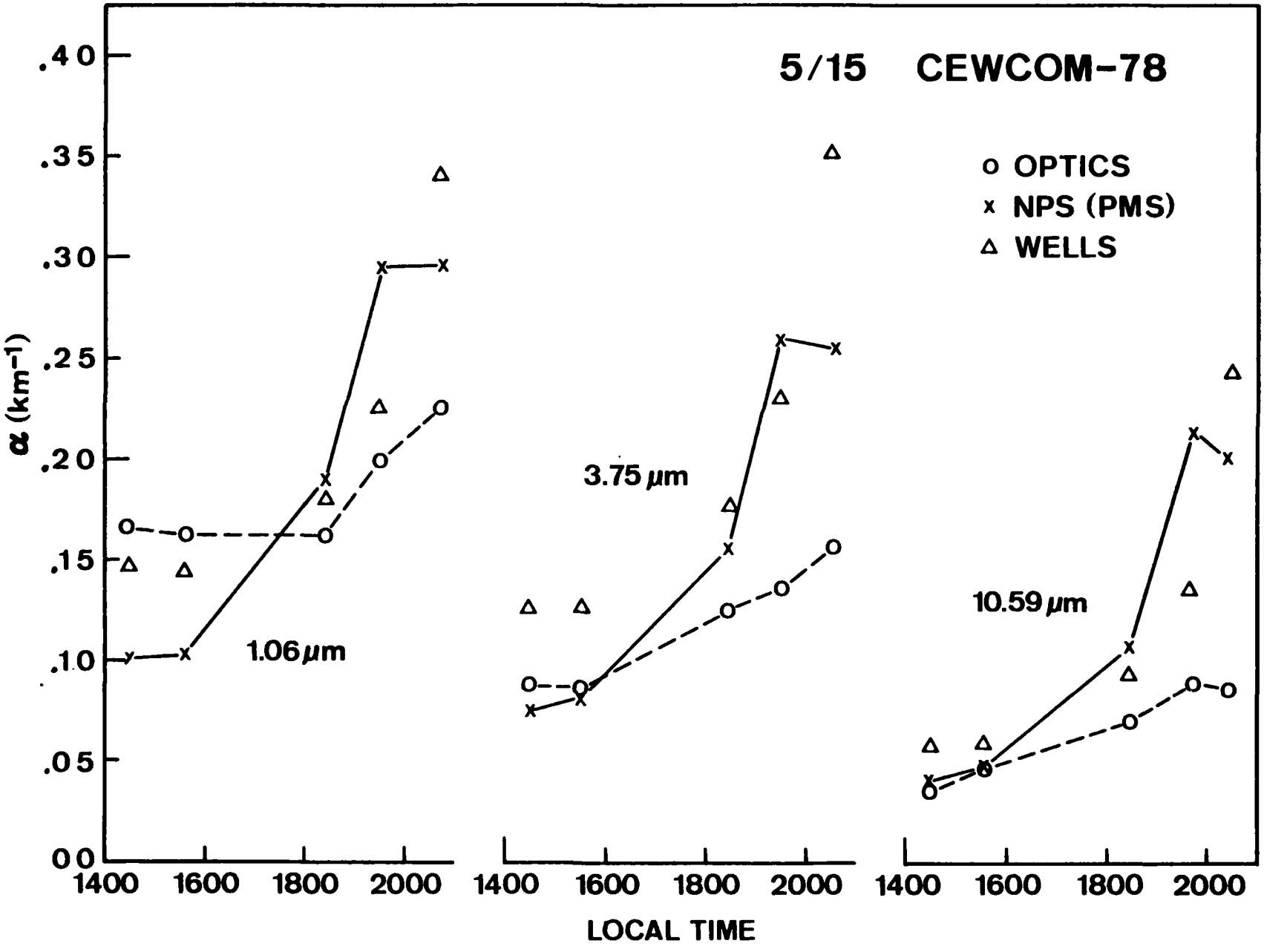
5/15 CEWCOM-78
o OPTICS
x NPS (PMS)
Δ WELLS
α (km⁻¹)
.40
.35
.30
.25
.20
.15
.10
.05
00
1.06 μm
3.75 μm
10.59 μm
1400
1600
1800
2000
LOCAL TIME

Figure 21

VIII. Extrapolation to Large Sizes

Other workers have pointed out that large size droplets contribute significantly to optical extinction for all wavelengths.[14] This is true even when the number density for large sizes is many orders of magnitude smaller than for small sizes. We have investigated this effect for NPS data with particular emphasis on the following:

1. 7th order polynomial fit.
2. Artificial end points to force good behavior of the polynomial fit.
3. Proper extrapolation beyond measurement range.

The best presentation of the data to illustrate the problem is a volume plot. Figures 22 and 23 are plots of log(dN/dr) and log(dV/dr), respectively, vs. log(r) for 1646 on 5/15/78. Both presentations use the same dN/dr polynomial coefficients to fit the data. The polynomial was generated from the raw data plus the artificial end points using method 2. The log(dN/dr) plot looks quite reasonable, showing a monotonically decreasing function that fits the data quite well. The log(dV/dr) plot shows that the end point and the manner in which it is fitted by the polynominal are significant for extinction calculations since dV/dr is highest near the end point.

Table 3a lists the fractional contribution to the extinction for various size ranges. This is done for 9 wavelengths from 0.488 to 10.59 μm. The data used is the same as that for Figures 22 and 23. The contribution shown for a particular size is the total

contribution for all sizes in a bin with upper radius the stated size and lower radius the previous size listed. For 10.6 μm wavelength one expects the larger sizes will be the major contributor and this is what is observed. For 0.488 μm wavelength the large sizes (sizes greater than 8 μm) contribute 30% of the calculated extinction.

The volume plots can be used to obtain an immediate estimate of the relative contribution of the various sizes to the extinction. Ignoring the Mie coefficient the scattering is proportional to

$$\int (dN/dr)A(r)dr$$

where A(r) is the particle cross sectional area. Taking volume $V \alpha A(r)r$ and $dr/r = d(\log r)$, the scattering is proportional to

$$\int (dV/dr)d(\log r)$$

Thus, a constant log(dV/dr) vs log(r) plot shows a roughly constant contribution to scattering with size. Of course a Mie coefficients must be used in an extinction calculation and it does not become appreciable until the particle radius is about one half the wavelength. Thus, smaller sizes do not contribute to the extinction regardless of the magnitude of dV/dr. The data from 2046 on 5/15 has a larger number of particles in the large size ranges and is useful for examining the effects of extrapolation. We have used 4 extrapolation methods to obtain extinction values for this data:

1. Polynomial: This is the standard NPS technique where the 7th order polynomial fits all the data plus the

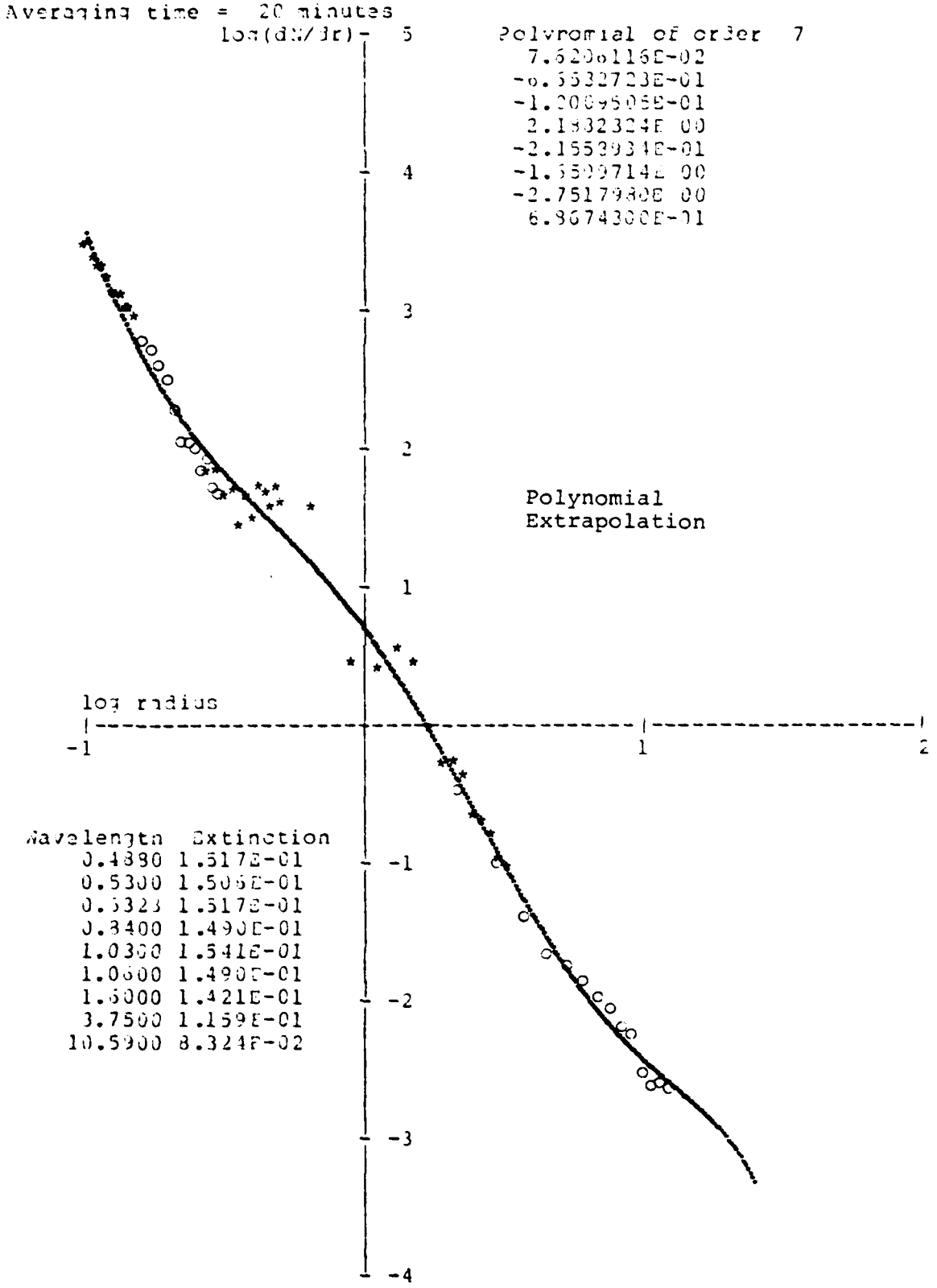
Tape # 0 File #102
Date 5/15/78 Time 16:46
Averaging time = 20 minutes
log(dN/dr)
5
4
3
2
1
-1
-2
-3
-4
Polynomial of order 7
7.6206116E-02
-6.5532723E-01
-1.2006506E-01
2.1832324E 00
-2.1553934E-01
-1.5599714E 00
-2.7517980E 00
6.8674300E-01
Polynomial
Extrapolation
log radius
-1
1
2
Wavelength Extinction
0.4880 1.517E-01
0.5300 1.506E-01
0.5328 1.517E-01
0.8400 1.490E-01
1.0300 1.541E-01
1.0600 1.490E-01
1.6000 1.421E-01
3.7500 1.159E-01
10.5900 8.324E-02

Figure 22

Race # 0 File #102
Date 5/15/78 Time 16:46

Averaging time = 20 minutes

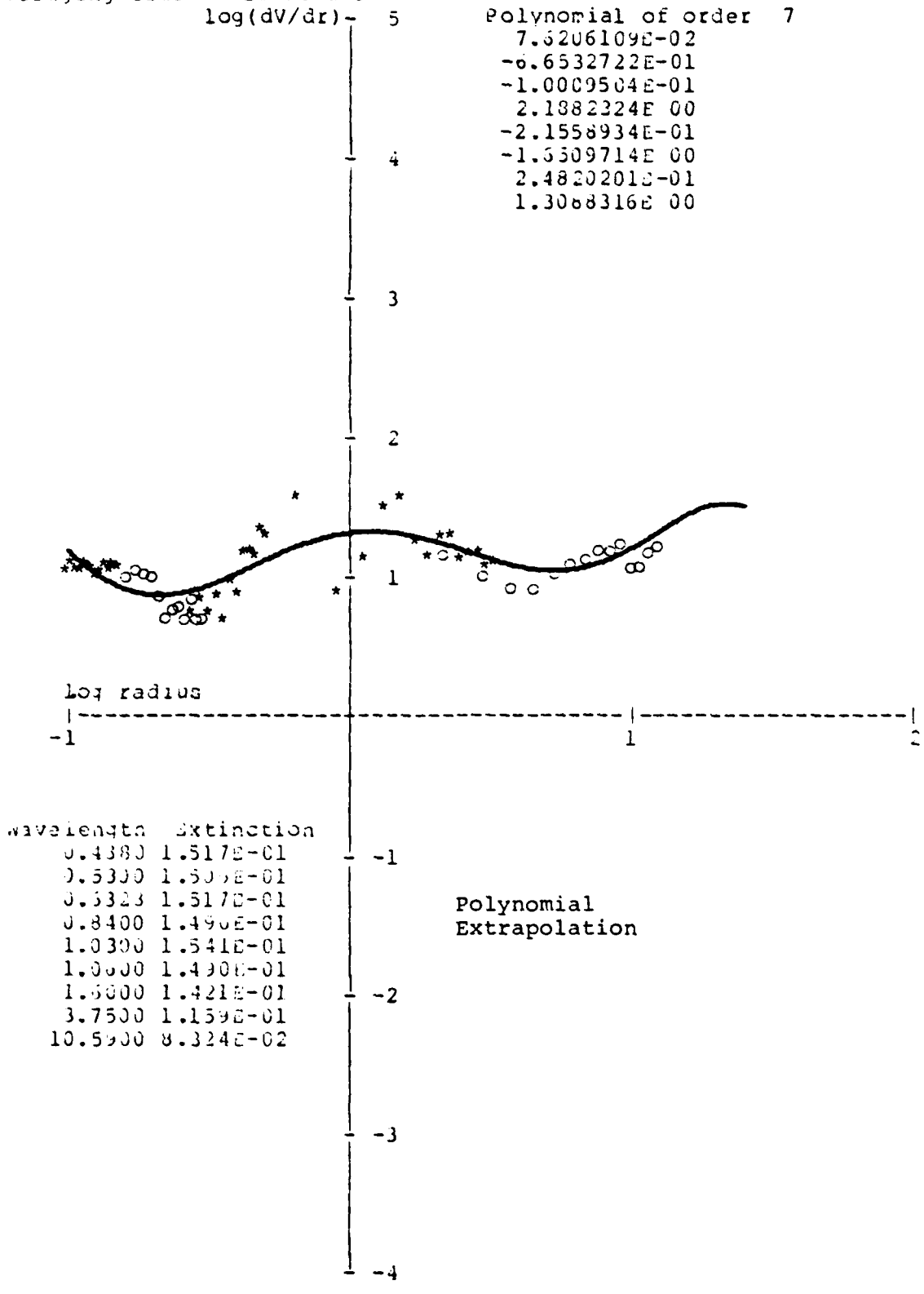

Figure 23

Functional Extinction Contribution

radius	0.49	0.53	0.63	0.84	1.03	1.06	1.60	3.75	10.59	λ
0.10	0.005	0.004	0.002	0.001	0.000	0.000	0.000	0.000	0.000	
0.13	0.008	0.006	0.004	0.002	0.001	0.001	0.000	0.000	0.000	
0.16	0.012	0.010	0.006	0.003	0.001	0.001	0.000	0.000	0.000	
0.20	0.018	0.016	0.010	0.005	0.003	0.003	0.001	0.000	0.000	
0.25	0.027	0.025	0.018	0.010	0.006	0.005	0.002	0.000	0.000	
0.32	0.040	0.039	0.031	0.020	0.012	0.012	0.004	0.000	0.001	
0.40	0.051	0.052	0.048	0.036	0.024	0.024	0.009	0.001	0.001	
0.50	0.050	0.054	0.064	0.058	0.044	0.043	0.020	0.003	0.001	
0.63	0.041	0.045	0.065	0.077	0.068	0.068	0.038	0.007	0.002	
0.79	0.050	0.046	0.049	0.078	0.085	0.087	0.063	0.015	0.003	
1.00	0.061	0.059	0.047	0.058	0.078	0.084	0.086	0.029	0.005	
1.26	0.052	0.052	0.056	0.046	0.055	0.059	0.095	0.048	0.006	
1.58	0.047	0.045	0.047	0.052	0.043	0.041	0.079	0.065	0.009	
2.00	0.041	0.044	0.041	0.045	0.047	0.045	0.050	0.078	0.012	
2.51	0.035	0.038	0.038	0.036	0.038	0.040	0.034	0.081	0.015	
3.16	0.030	0.032	0.034	0.034	0.031	0.033	0.038	0.068	0.021	
3.98	0.027	0.028	0.030	0.029	0.030	0.031	0.033	0.045	0.027	
5.01	0.027	0.026	0.028	0.027	0.028	0.027	0.030	0.032	0.038	
6.31	0.028	0.028	0.029	0.029	0.029	0.029	0.033	0.042	0.054	
7.94	0.033	0.033	0.034	0.034	0.034	0.035	0.038	0.052	0.078	
10.00	0.043	0.042	0.042	0.043	0.041	0.046	0.047	0.059	0.112	
12.59	0.056	0.056	0.056	0.055	0.054	0.059	0.061	0.080	0.146	
15.85	0.071	0.072	0.071	0.072	0.068	0.074	0.076	0.093	0.166	
19.95	0.078	0.079	0.081	0.081	0.085	0.083	0.088	0.106	0.163	
25.12	0.070	0.070	0.070	0.070	0.096	0.071	0.075	0.095	0.139	

Table 3a 1646 - polynomial extrapolation

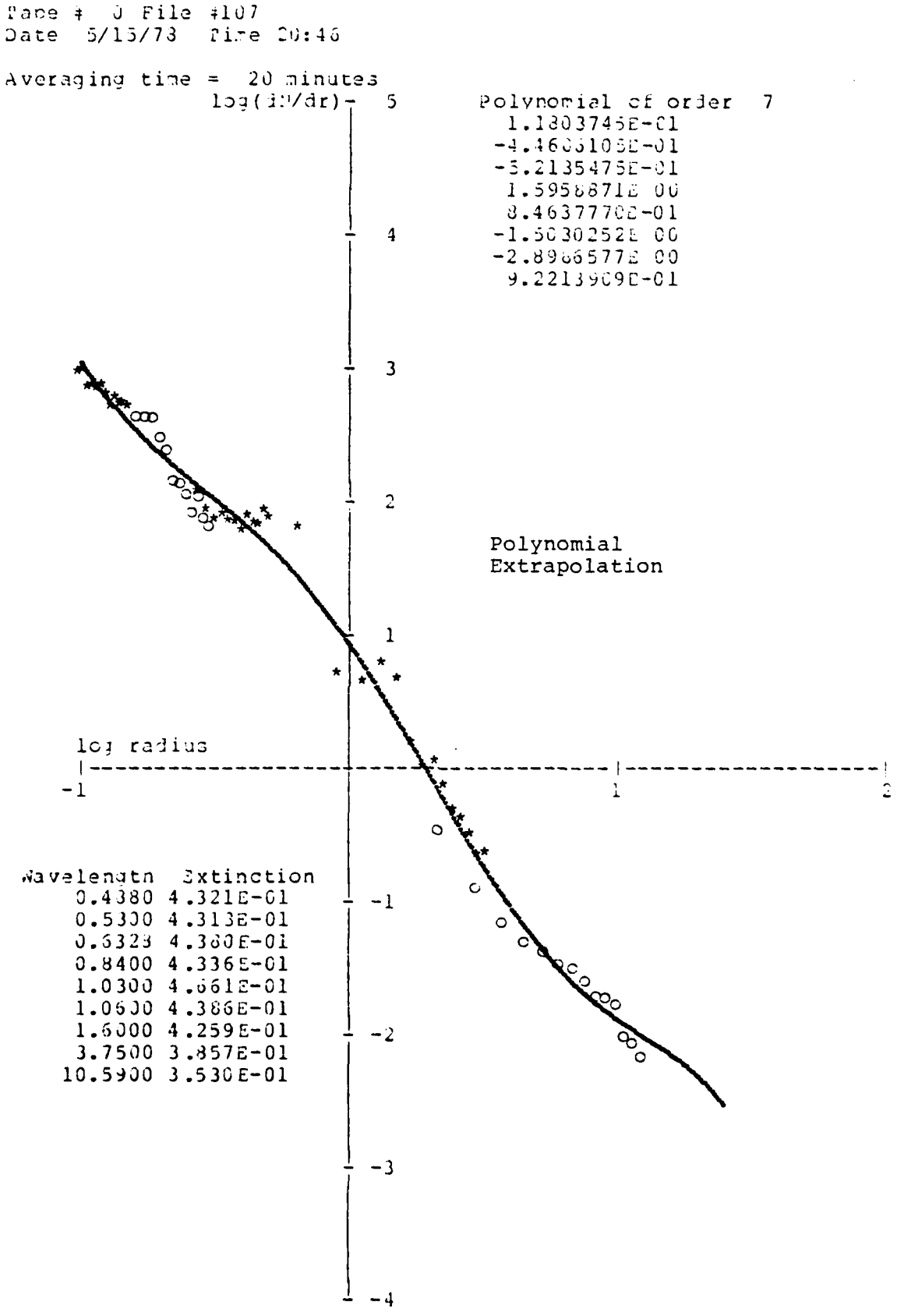
Tape # 0 File #107
Date 5/15/78 Time 20:46
Averaging time = 20 minutes
log(dN/dr)
5
4
3
2
1
-1
-2
-3
-4
Polynomial of order 7
1.1803745E-01
-4.4603105E-01
-5.2135475E-01
1.5958871E 00
8.4637770E-01
-1.5030252E 00
-2.8986577E 00
9.2213909E-01
Polynomial
Extrapolation
log radius
-1
1
2
Wavelength Extinction
0.4380 4.321E-01
0.5300 4.313E-01
0.6328 4.380E-01
0.8400 4.336E-01
1.0300 4.661E-01
1.0600 4.386E-01
1.6000 4.259E-01
3.7500 3.857E-01
10.5900 3.530E-01

Figure 24

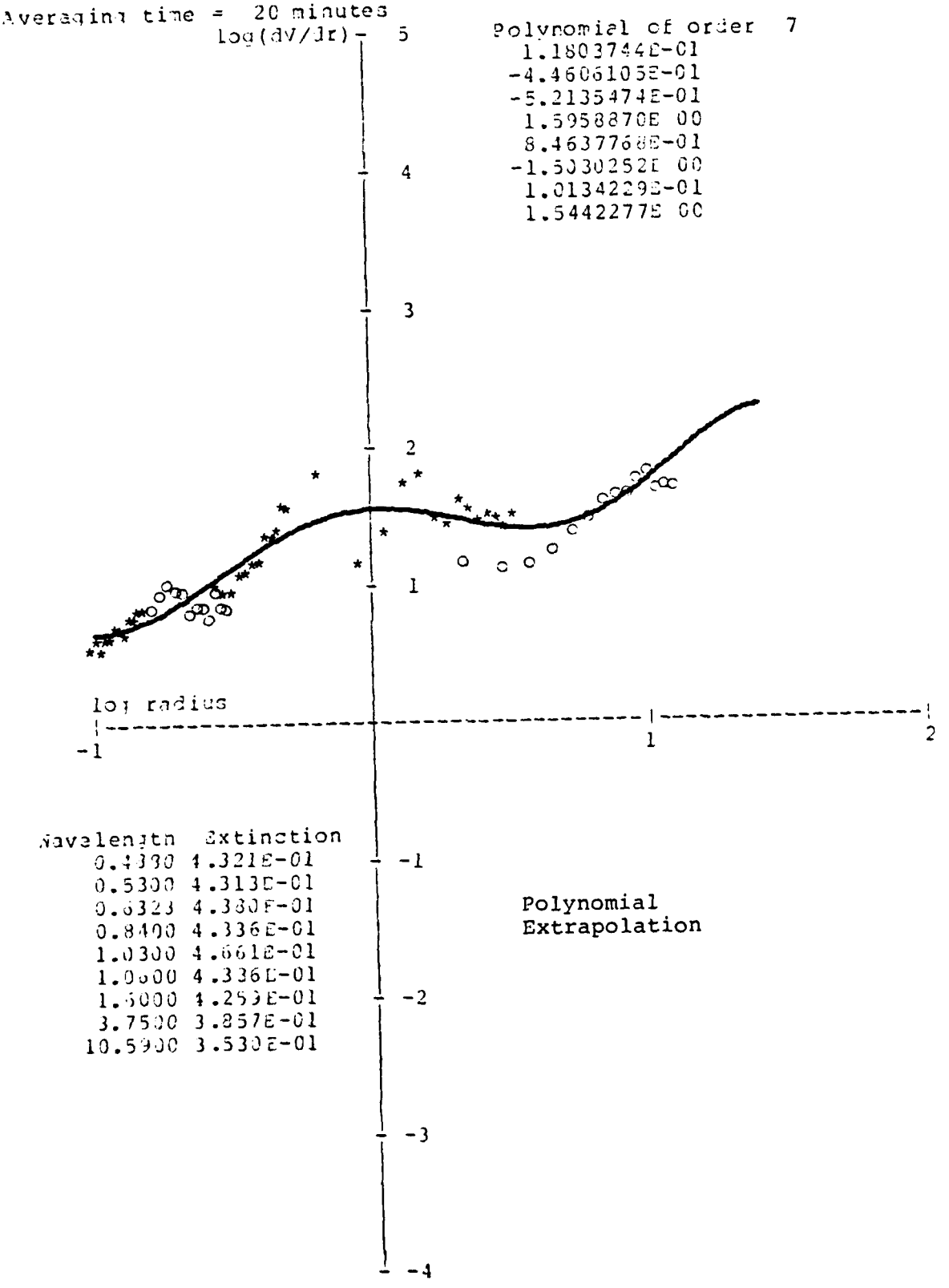
Tape # 35 File #107
Date 5/15/78 Time 20:46
Averaging time = 20 minutes
log(dV/dr)
5
4
3
2
1
-1
-2
-3
-4
Polynomial of order 7
1.1803744E-01
-4.4606105E-01
-5.2135474E-01
1.5958870E 00
8.4637768E-01
-1.5030252E 00
1.0134229E-01
1.5442277E 00
log radius
-1
1
2
Wavelength Extinction
0.4330 4.321E-01
0.5300 4.313E-01
0.6328 4.380E-01
0.8400 4.336E-01
1.0300 4.661E-01
1.0600 4.336E-01
1.6000 4.253E-01
3.7500 3.857E-01
10.5900 3.530E-01
Polynomial
Extrapolation

Figure 25a

Functional Extinction Contribution

radius	0.49	0.53	0.63	0.84	1.03	1.06	1.60	3.75	10.59 λ
0.10	0.001	0.001	0.000	0.000	0.000	0.000	0.000	0.000	0.000
0.13	0.002	0.001	0.001	0.000	0.000	0.000	0.000	0.000	0.000
0.16	0.004	0.003	0.002	0.001	0.000	0.000	0.000	0.000	0.000
0.20	0.007	0.006	0.004	0.002	0.001	0.001	0.000	0.000	0.000
0.25	0.014	0.013	0.009	0.005	0.003	0.003	0.001	0.000	0.000
0.32	0.023	0.022	0.018	0.011	0.007	0.007	0.002	0.000	0.000
0.40	0.032	0.032	0.030	0.022	0.014	0.014	0.005	0.001	0.000
0.50	0.032	0.035	0.040	0.036	0.026	0.027	0.012	0.002	0.001
0.63	0.026	0.028	0.041	0.048	0.040	0.042	0.023	0.004	0.001
0.79	0.030	0.028	0.030	0.047	0.049	0.052	0.037	0.008	0.001
1.00	0.036	0.035	0.028	0.034	0.044	0.048	0.049	0.015	0.002
1.26	0.030	0.030	0.032	0.026	0.030	0.033	0.053	0.024	0.003
1.58	0.027	0.026	0.027	0.030	0.024	0.023	0.044	0.033	0.004
2.00	0.025	0.026	0.025	0.026	0.027	0.026	0.029	0.041	0.005
2.51	0.023	0.024	0.024	0.023	0.023	0.025	0.021	0.045	0.007
3.16	0.022	0.023	0.024	0.023	0.021	0.023	0.026	0.041	0.010
3.98	0.022	0.023	0.023	0.022	0.023	0.024	0.025	0.031	0.015
5.01	0.025	0.023	0.025	0.024	0.024	0.024	0.026	0.025	0.023
6.31	0.029	0.028	0.029	0.029	0.028	0.029	0.032	0.038	0.038
7.94	0.038	0.038	0.039	0.039	0.037	0.039	0.042	0.051	0.062
10.00	0.056	0.054	0.054	0.055	0.050	0.057	0.058	0.066	0.097
12.59	0.080	0.079	0.079	0.078	0.073	0.082	0.083	0.098	0.140
15.85	0.113	0.114	0.112	0.113	0.103	0.114	0.116	0.127	0.177
19.95	0.144	0.145	0.146	0.146	0.150	0.148	0.153	0.167	0.201
25.12	0.159	0.160	0.158	0.158	0.203	0.158	0.164	0.186	0.214

Table 3b 2046 - Polynomial Extrapolation

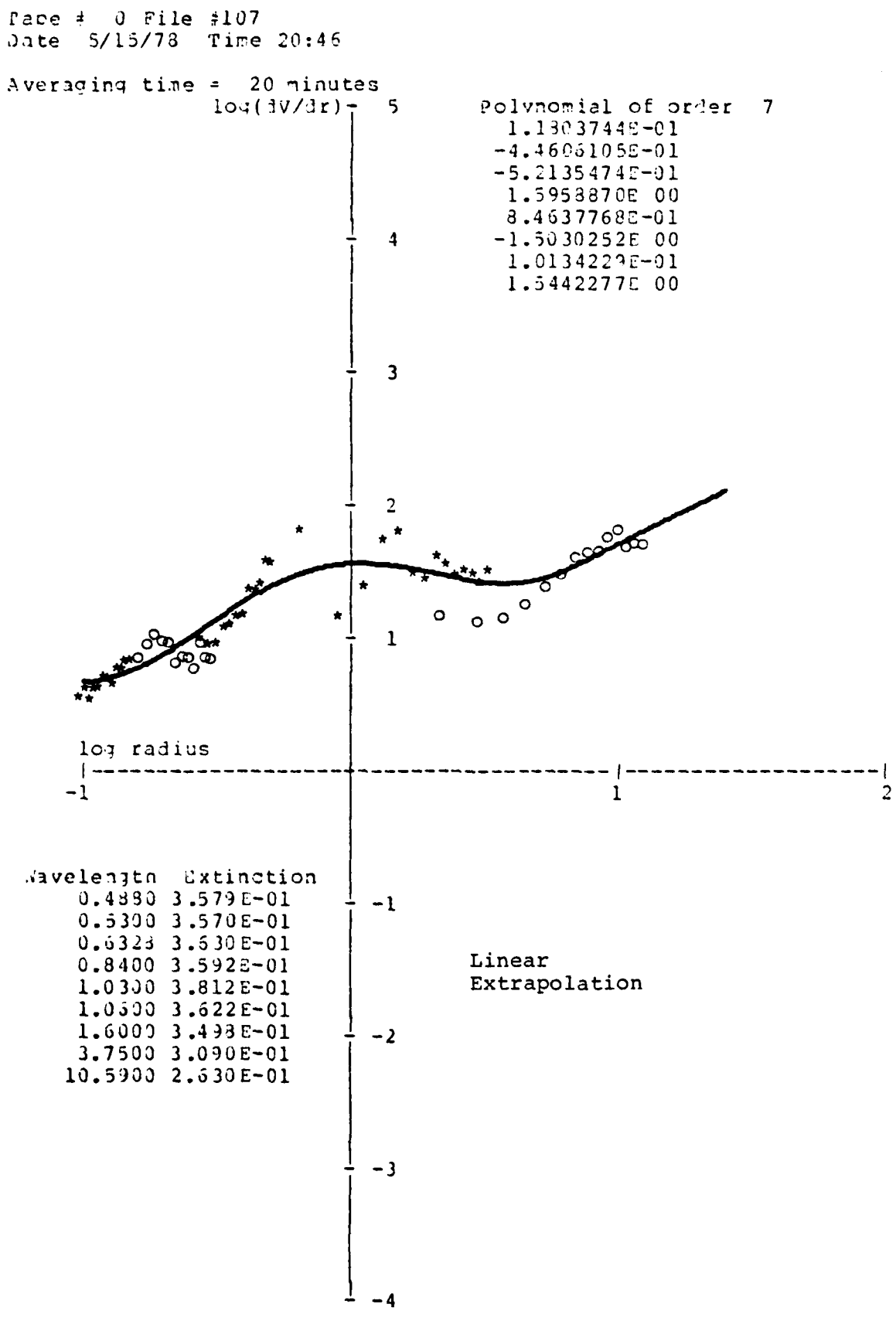
Tape # 0 File #107
Date 5/15/78 Time 20:46
Averaging time = 20 minutes
log(dV/dr)
Polynomial of order 7
1.1303744E-01
-4.4606105E-01
-5.2135474E-01
1.5958870E 00
8.4637768E-01
-1.5030252E 00
1.0134229E-01
1.5442277E 00
5
4
3
2
1
-1
-2
-3
-4
log radius
-1
1
2
Wavelength Extinction
0.4880 3.579E-01
0.5300 3.570E-01
0.6328 3.530E-01
0.8400 3.592E-01
1.0300 3.812E-01
1.0600 3.622E-01
1.6000 3.498E-01
3.7500 3.090E-01
10.5900 2.630E-01
Linear
Extrapolation

Figure 25b

Fraction Extenction Contribution

radius	0.49	0.53	0.63	0.84	1.03	1.06	1.60	3.75	10.59 λ
0.10	0.001	0.001	0.000	0.000	0.000	0.000	0.000	0.000	0.000
0.13	0.002	0.002	0.001	0.000	0.000	0.000	0.000	0.000	0.000
0.16	0.004	0.004	0.002	0.001	0.000	0.000	0.000	0.000	0.000
0.20	0.009	0.008	0.005	0.002	0.001	0.001	0.000	0.000	0.000
0.25	0.017	0.015	0.011	0.006	0.003	0.003	0.001	0.000	0.000
0.32	0.028	0.027	0.022	0.014	0.008	0.008	0.003	0.000	0.000
0.40	0.038	0.039	0.036	0.026	0.018	0.017	0.007	0.001	0.000
0.50	0.039	0.042	0.049	0.044	0.032	0.032	0.015	0.002	0.001
0.63	0.031	0.034	0.049	0.058	0.049	0.050	0.028	0.005	0.001
0.79	0.037	0.034	0.036	0.056	0.060	0.062	0.044	0.010	0.002
1.00	0.044	0.042	0.033	0.041	0.054	0.059	0.059	0.019	0.002
1.26	0.036	0.036	0.039	0.031	0.037	0.040	0.064	0.030	0.003
1.58	0.033	0.032	0.033	0.036	0.029	0.028	0.054	0.041	0.005
2.00	0.030	0.032	0.030	0.032	0.033	0.032	0.035	0.051	0.007
2.51	0.028	0.029	0.029	0.028	0.028	0.030	0.026	0.056	0.009
3.16	0.026	0.027	0.028	0.028	0.025	0.027	0.031	0.052	0.013
3.98	0.026	0.027	0.028	0.027	0.028	0.028	0.031	0.038	0.020
5.01	0.030	0.028	0.030	0.029	0.029	0.029	0.032	0.031	0.031
6.31	0.035	0.034	0.035	0.035	0.035	0.035	0.039	0.047	0.050
7.94	0.044	0.044	0.044	0.044	0.043	0.045	0.048	0.061	0.078
10.00	0.056	0.055	0.055	0.056	0.051	0.058	0.060	0.068	0.110
12.59	0.071	0.070	0.069	0.068	0.065	0.073	0.074	0.089	0.138
15.85	0.088	0.089	0.087	0.088	0.081	0.090	0.091	0.102	0.154
19.95	0.109	0.110	0.111	0.111	0.116	0.112	0.117	0.131	0.169
25.12	0.138	0.139	0.137	0.137	0.174	0.137	0.143	0.167	0.206

70

Table 3c 2046 - Linear Extrapolation

Tape # 0 File #107
Date 5/15/78 Time 20:46

Averaging time = 20 minutes

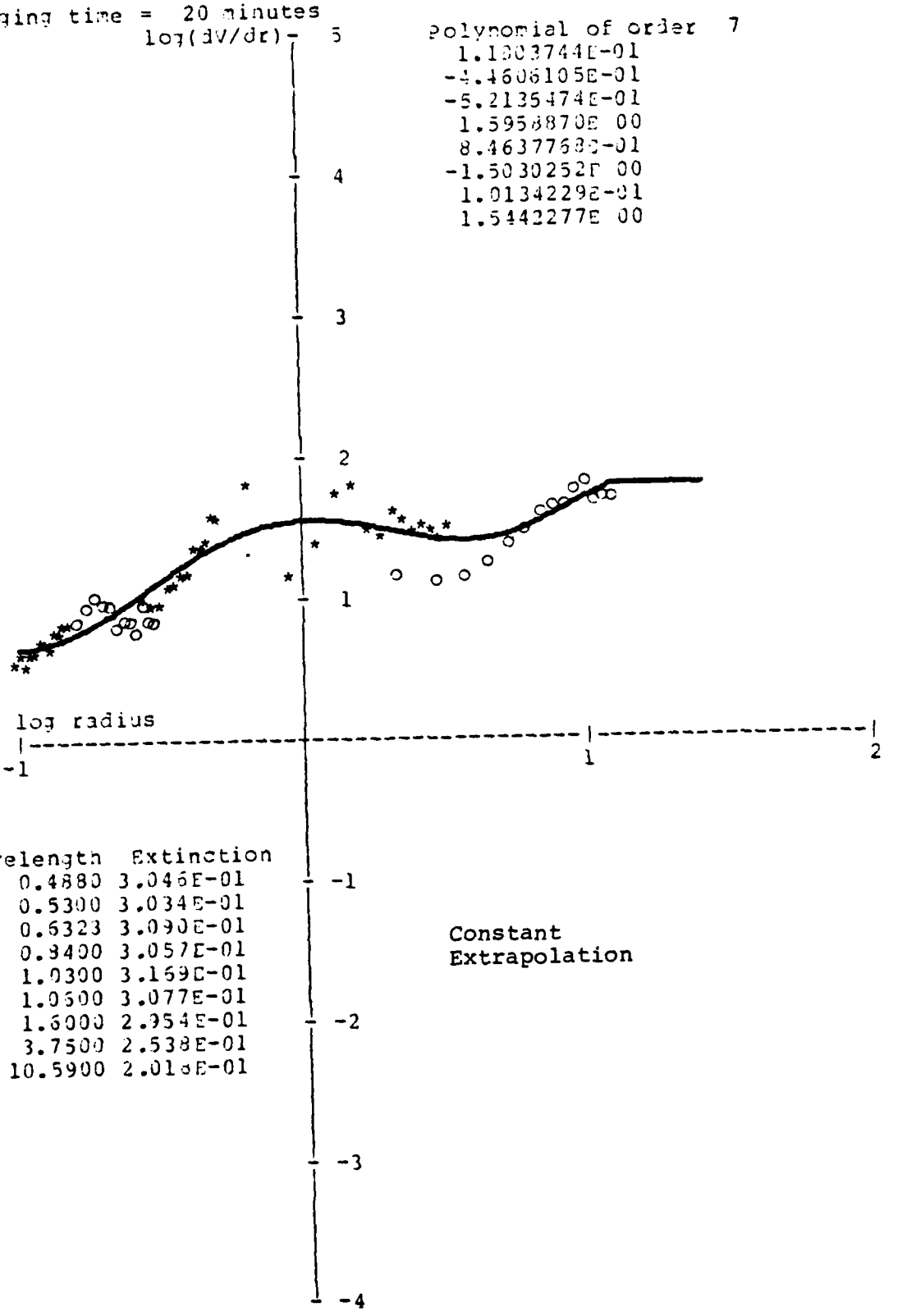

Polynomial of order 7
1.1303744E-01
-4.4606105E-01
-5.2135474E-01
1.5958870E 00
8.4637768E-01
-1.5030252E 00
1.0134229E-01
1.5442277E 00

Wavelength	Extinction
0.4880	3.046E-01
0.5300	3.034E-01
0.6323	3.090E-01
0.8400	3.057E-01
1.0300	3.169E-01
1.0600	3.077E-01
1.6000	2.954E-01
3.7500	2.538E-01
10.5900	2.016E-01

Constant
Extrapolation

Figure 25c

Functional Extinction Contribution

radius	0.49	0.53	0.63	0.84	1.03	1.06	1.60	3.75	10.59	λ
0.10	0.001	0.001	0.000	0.000	0.000	0.000	0.000	0.000	0.000	
0.13	0.002	0.002	0.001	0.000	0.000	0.000	0.000	0.000	0.000	
0.16	0.005	0.004	0.003	0.001	0.001	0.001	0.000	0.000	0.000	
0.20	0.010	0.009	0.006	0.003	0.002	0.001	0.000	0.000	0.000	
0.25	0.020	0.018	0.013	0.007	0.004	0.004	0.001	0.000	0.000	
0.32	0.033	0.032	0.026	0.016	0.010	0.010	0.003	0.000	0.000	
0.40	0.045	0.046	0.042	0.031	0.021	0.020	0.008	0.001	0.001	
0.50	0.046	0.049	0.057	0.052	0.039	0.038	0.017	0.002	0.001	
0.63	0.036	0.040	0.057	0.068	0.059	0.059	0.033	0.006	0.002	
0.79	0.043	0.040	0.042	0.066	0.072	0.073	0.053	0.012	0.002	
1.00	0.052	0.050	0.039	0.048	0.064	0.069	0.070	0.023	0.003	
1.26	0.043	0.043	0.046	0.037	0.045	0.047	0.076	0.036	0.004	
1.58	0.039	0.038	0.038	0.042	0.035	0.033	0.063	0.050	0.006	
2.00	0.035	0.038	0.035	0.038	0.040	0.038	0.041	0.062	0.008	
2.51	0.033	0.034	0.034	0.033	0.034	0.035	0.030	0.068	0.012	
3.16	0.031	0.032	0.033	0.033	0.031	0.032	0.037	0.063	0.017	
3.98	0.031	0.032	0.033	0.032	0.033	0.034	0.036	0.046	0.026	
5.01	0.035	0.033	0.035	0.035	0.035	0.034	0.038	0.038	0.041	
6.31	0.041	0.040	0.041	0.041	0.042	0.042	0.047	0.057	0.065	
7.94	0.051	0.051	0.052	0.052	0.051	0.053	0.057	0.074	0.101	
10.00	0.066	0.065	0.064	0.066	0.062	0.069	0.071	0.083	0.143	
12.59	0.076	0.075	0.074	0.073	0.072	0.078	0.080	0.100	0.164	
15.85	0.075	0.076	0.075	0.075	0.071	0.077	0.078	0.090	0.148	
19.95	0.075	0.076	0.076	0.076	0.080	0.077	0.081	0.093	0.129	
25.12	0.076	0.076	0.075	0.075	0.099	0.075	0.079	0.095	0.125	

Table 3d 2046 - Constant Extrapolation

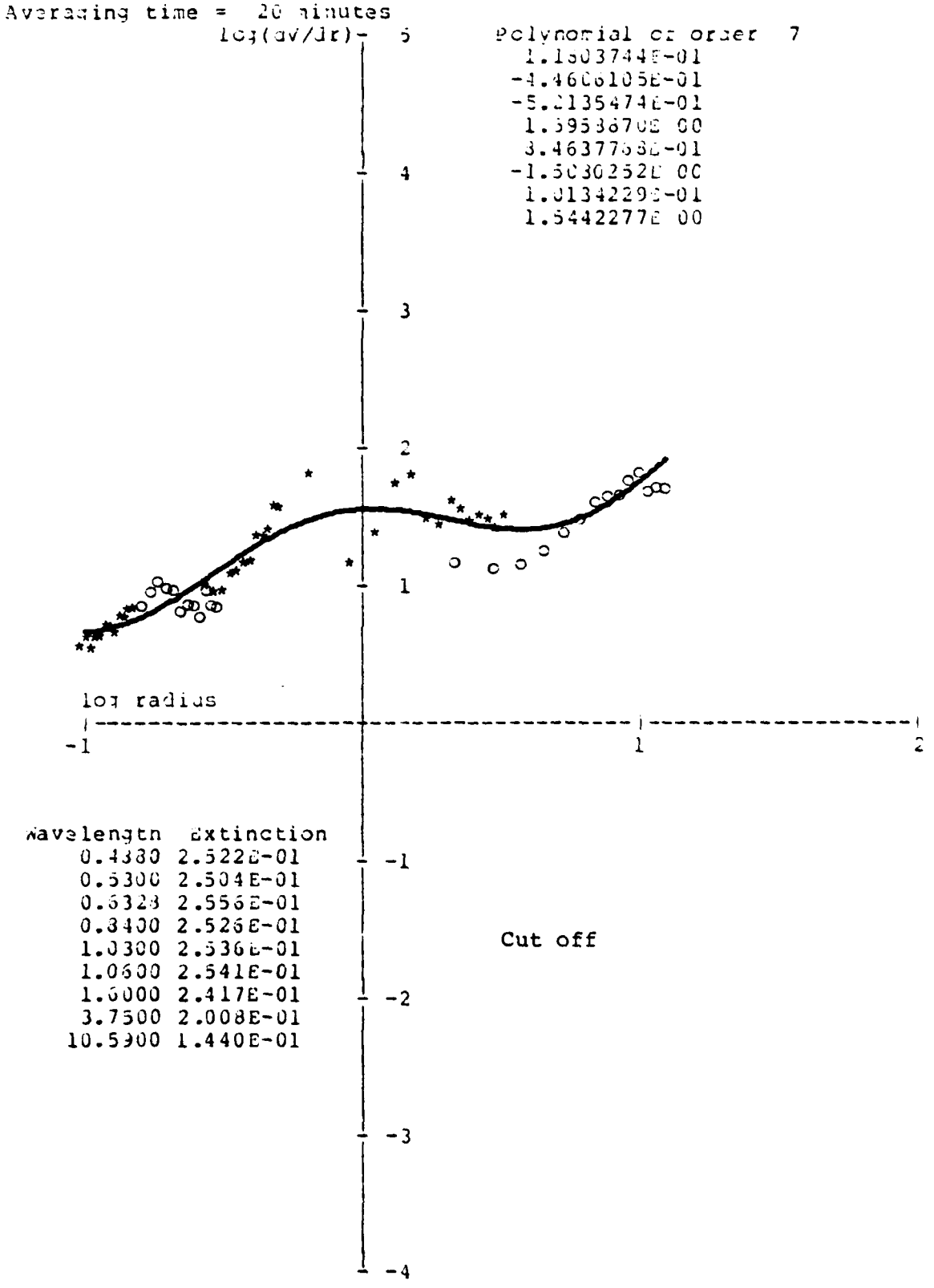
Date # 0 File #107
Date 5/15/78 Time 20:45
Averaging time = 20 minutes
log(dv/dr)
Polynomial of order 7
1.1503744E-01
-4.4606105E-01
-5.2135474E-01
1.3953870E 00
3.4637768E-01
-1.5030252E 00
1.0134229E-01
1.5442277E 00
log radius
Wavelength Extinction
0.4380 2.522E-01
0.5300 2.504E-01
0.6328 2.556E-01
0.8400 2.526E-01
1.0300 2.536E-01
1.0600 2.541E-01
1.5000 2.417E-01
3.7500 2.008E-01
10.5900 1.440E-01
Cut off

Figure 25d

Fractional Extinction Contribution

radius	0.49	0.53	0.63	0.84	1.03	1.06	1.60	3.75	10.59	λ
0.10	0.001	0.001	0.001	0.000	0.000	0.000	0.000	0.000	0.000	
0.13	0.003	0.002	0.001	0.001	0.000	0.000	0.000	0.000	0.000	
0.16	0.006	0.005	0.003	0.001	0.001	0.001	0.000	0.000	0.000	
0.20	0.013	0.011	0.007	0.004	0.002	0.002	0.000	0.000	0.000	
0.25	0.024	0.022	0.016	0.009	0.005	0.005	0.001	0.000	0.000	
0.32	0.040	0.039	0.031	0.019	0.012	0.012	0.004	0.000	0.000	
0.40	0.054	0.055	0.051	0.038	0.026	0.025	0.010	0.001	0.001	
0.50	0.055	0.060	0.069	0.062	0.048	0.046	0.021	0.003	0.001	
0.63	0.044	0.049	0.069	0.082	0.074	0.072	0.040	0.007	0.002	
0.79	0.052	0.048	0.051	0.080	0.090	0.089	0.064	0.015	0.003	
1.00	0.062	0.060	0.047	0.058	0.080	0.084	0.086	0.029	0.004	
1.26	0.052	0.052	0.056	0.045	0.056	0.057	0.093	0.046	0.006	
1.58	0.047	0.046	0.046	0.051	0.044	0.040	0.078	0.063	0.009	
2.00	0.043	0.045	0.042	0.045	0.050	0.045	0.051	0.079	0.012	
2.51	0.039	0.042	0.041	0.040	0.042	0.043	0.037	0.087	0.017	
3.16	0.037	0.039	0.040	0.040	0.038	0.039	0.045	0.079	0.024	
3.98	0.037	0.039	0.040	0.038	0.042	0.041	0.044	0.059	0.037	
5.01	0.042	0.040	0.043	0.042	0.043	0.042	0.046	0.048	0.057	
6.31	0.050	0.049	0.050	0.050	0.052	0.051	0.057	0.072	0.092	
7.94	0.066	0.066	0.067	0.067	0.068	0.068	0.073	0.099	0.151	
10.00	0.095	0.093	0.092	0.094	0.092	0.099	0.103	0.126	0.239	
12.59	0.138	0.136	0.135	0.133	0.134	0.142	0.146	0.188	0.344	
15.85	0.000	0.000	0.000	0.000	0.000	0.000	0.000	0.000	0.000	
19.95	0.000	0.000	0.000	0.000	0.000	0.000	0.000	0.000	0.000	
25.12	0.000	0.000	0.000	0.000	0.000	0.000	0.000	0.000	0.000	

Table 3e 2046 - Cut off Extropolation

created end point.

2. Linear: The polynomial is cut off at the middle of the last range and the remainder of the fit is given by a linear extrapolation from the cutoff point to the created end point.
3. Constant: The polynomial is cut off at the radius of the last data point (12 μm) and log(dV/dr) is assumed constant out to log(r) = 1.4.
4. Cutoff: The extinction calculation is cut off at the radius of the last data point.

A plot of log(dN/dr) for these data is shown in Figure 24. The 7th order fit looks very good and even the extrapolation region shows no apparent problems. On the other hand the volume plots show that the extrapolation technique has serious consequences. The volume plots for these techniques are presented in Figures 25 and the corresponding extinction calculation results are listed in Tables 3. The results are summarized below:

Technique	Percent Extrapolation Contribution	0.488 μm Extinction (km^{-1})
Polynomial (25a)	41%	0.432
Linear (25b)	34%	0.358
Constant (25c)	23%	0.305
Cutoff (25d)	0	0.252

Table 4

Shown are calculated aerosol contribution to the optical extinction at .4880 μm. The percent contribution due to extrapolated sizes for the various extrapolation techniques is also shown.

The actual aerosol contribution to the optical extinction should lie somewhere within the range given in Table 4. (Recall, however, that all values are computed using a 25 μm particle radius cutoff.) There is no unambiguous way to choose one of the methods, but certain guidelines do clarify the situation:

1. The cutoff method assumes that there are no particles with sizes larger than 12 μm, which is unrealistic.
2. The polynomial method can give an unrealistically high estimate of large particle sizes concentration for some circumstances.
3. The linear and constant methods will give results which are nearly the same for cases where dV/dr is nearly constant but the results will diverge when dV/dr is not constant.

We reject the cutoff and polynomial methods. The linear method could overestimate extinction when the number of large size particles is large (such as in a fog) and the constant method will lead to overestimation for relatively clear air. Whichever technique is chosen will lead to errors for some circumstances, and this must be accepted. The best overall compromise is as follows: Use the linear method for all cases where the slope of log(dV/dr) vs log(r) is less than or equal to zero. For positive slope the constant method is used.

The combination method will be used for future reduction of NPS data, but has not been used in the past. Almost all past data has been obtained during fairly clear conditions for which the large size particles have a small overall effect. For such

conditions the polynomial method, which was used, is expected to give good results. This is born out by the close agreement between NPS calculations and optical measurements. Data which was obtained during low visibility will be reprocessed. An example of the type of data normally obtained is shown in Figures 26 and Tables 3f and 3g for a period during 5/8 - 0835. log(dV/dr) generally decreases with particle size and the large size conbribution to the 0.488 μm extinction is small. The polynomial extrapolation looks terrible while the linear looks good. The 0.488 μm extinctions and % contribution from extrapolated sizes are:

polynomial	0.064	km^{-1}	7%
linear	0.058	km^{-1}	0.4%

The 7% contribution from the polynomial extrapolation could produce an error of that magnitude, but that is acceptable. The difference in the large size extrapolation does change the calculated extinction at longer wavelengths appreciably. At 10.59 μm the polynomial extrapolation gives 0.016 km^{-1} and the linear 0.008 km^{-1} with 35% and 4% contribution due to extrapolated sizes, respectively. Again this is not serious since for this high visibility the molecular extinction is dominant at longer wavelengths.

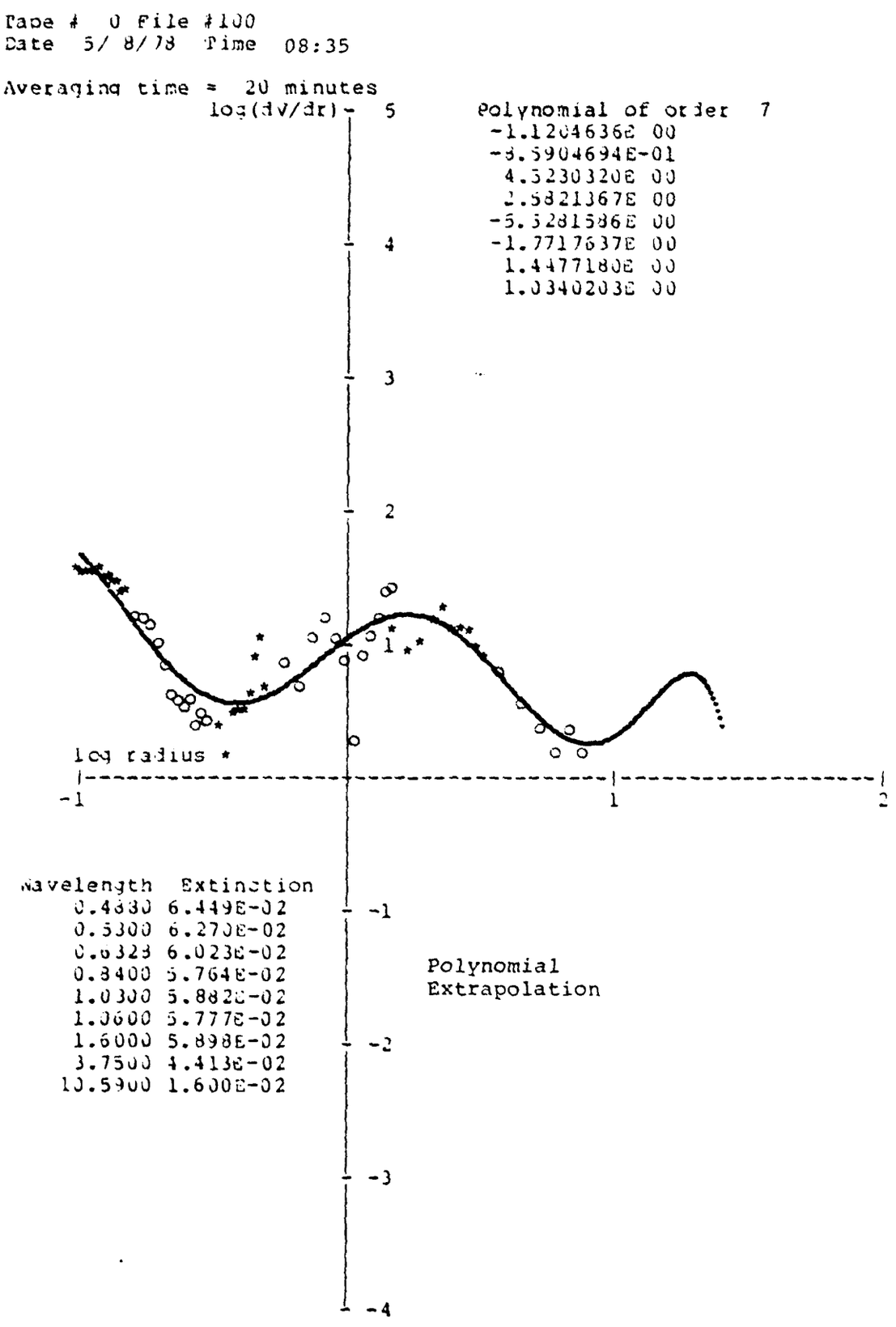
Tape # 0 File #100
Date 5/ 8/78 Time 08:35
Averaging time = 20 minutes
log(dV/dr)
Polynomial of order 7
-1.12046362 00
-8.5904694E-01
4.52303208 00
2.58213678 00
-5.52815868 00
-1.77176378 00
1.44771808 00
1.03402038 00
log radius *
Wavelength Extinction
0.4880 6.449E-02
0.5300 6.270E-02
0.6328 6.023E-02
0.8400 5.764E-02
1.0300 5.882E-02
1.0600 5.777E-02
1.6000 5.898E-02
3.7500 4.413E-02
10.5900 1.600E-02
Polynomial
Extrapolation

Figure 26a

Fractional Extinction Contribuition

radius	0.49	0.53	0.63	0.84	1.03	1.06	1.60	3.75	10.59	λ
0.10	0.037	0.030	0.018	0.007	0.003	0.003	0.001	0.000	0.003	
0.13	0.039	0.032	0.020	0.008	0.004	0.004	0.001	0.000	0.002	
0.16	0.038	0.032	0.020	0.009	0.005	0.004	0.001	0.000	0.001	
0.20	0.034	0.031	0.022	0.010	0.006	0.005	0.001	0.000	0.001	
0.25	0.034	0.032	0.024	0.013	0.008	0.007	0.002	0.000	0.001	
0.32	0.036	0.035	0.029	0.019	0.012	0.011	0.003	0.000	0.001	
0.40	0.038	0.040	0.039	0.029	0.020	0.019	0.007	0.001	0.001	
0.50	0.038	0.042	0.052	0.048	0.037	0.036	0.015	0.002	0.002	
0.63	0.035	0.040	0.060	0.074	0.067	0.066	0.035	0.007	0.004	
0.79	0.057	0.053	0.057	0.094	0.105	0.106	0.073	0.019	0.008	
1.00	0.088	0.087	0.074	0.089	0.123	0.131	0.128	0.049	0.015	
1.26	0.092	0.093	0.108	0.090	0.108	0.113	0.175	0.097	0.026	
1.58	0.094	0.094	0.100	0.115	0.096	0.091	0.163	0.148	0.040	
2.00	0.081	0.088	0.087	0.098	0.104	0.096	0.102	0.173	0.051	
2.51	0.059	0.064	0.067	0.066	0.072	0.074	0.058	0.151	0.056	
3.16	0.038	0.040	0.044	0.046	0.041	0.043	0.047	0.095	0.054	
3.98	0.022	0.024	0.026	0.026	0.028	0.028	0.029	0.043	0.048	
5.01	0.015	0.014	0.016	0.016	0.017	0.016	0.016	0.020	0.044	
6.31	0.011	0.011	0.012	0.012	0.012	0.012	0.013	0.017	0.045	
7.94	0.010	0.011	0.012	0.012	0.012	0.012	0.012	0.019	0.055	
10.00	0.014	0.014	0.015	0.016	0.015	0.016	0.016	0.022	0.081	
12.59	0.022	0.022	0.023	0.024	0.023	0.025	0.024	0.034	0.125	
15.85	0.031	0.032	0.033	0.034	0.033	0.035	0.034	0.045	0.159	
19.95	0.028	0.029	0.031	0.032	0.032	0.033	0.032	0.042	0.130	
25.12	0.010	0.011	0.011	0.012	0.017	0.012	0.012	0.016	0.046	

Table 3f 0835 Polynomial Extrapolation

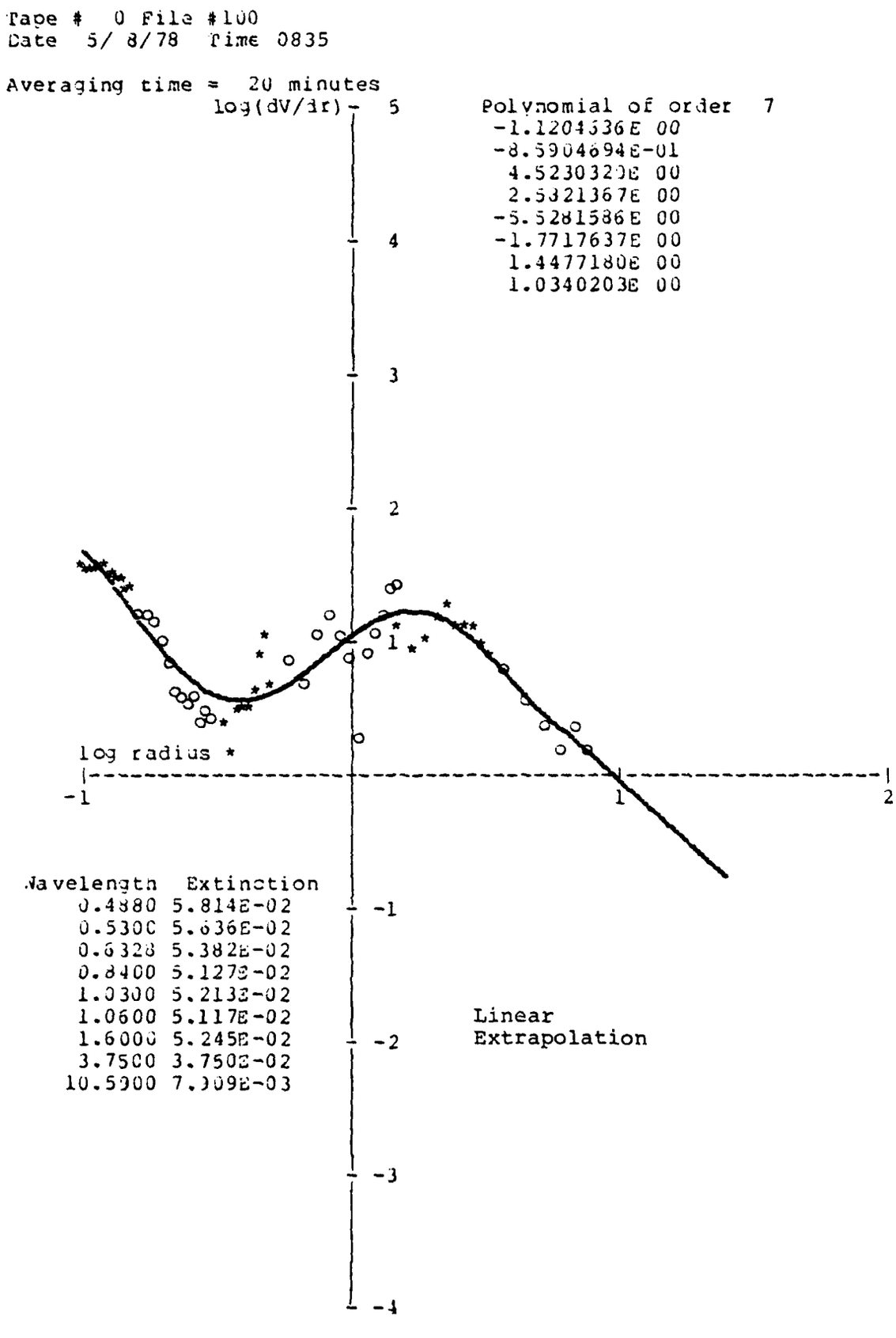
Tape # 0 File #100
Date 5/ 8/78 Time 0835
Averaging time = 20 minutes
log(dV/dr)
Polynomial of order 7
-1.1204536E 00
-8.5904694E-01
4.5230320E 00
2.5321367E 00
-5.5281586E 00
-1.7717637E 00
1.4477180E 00
1.0340203E 00
log radius *
Wavelength Extinction
0.4880 5.814E-02
0.5300 5.636E-02
0.6328 5.382E-02
0.8400 5.127E-02
1.0300 5.213E-02
1.0600 5.117E-02
1.6000 5.245E-02
3.7500 3.750E-02
10.5900 7.309E-03
Linear
Extrapolation

Figure 26b

Fractional Extinction Contribution

radius	0.49	0.53	0.63	0.84	1.03	1.06	1.60	3.75	10.59 λ
0.10	0.041	0.033	0.020	0.008	0.003	0.003	0.001	0.000	0.006
0.13	0.043	0.035	0.022	0.009	0.004	0.004	0.001	0.000	0.004
0.16	0.042	0.036	0.023	0.010	0.005	0.005	0.001	0.000	0.003
0.20	0.038	0.034	0.024	0.012	0.006	0.006	0.001	0.000	0.002
0.25	0.038	0.035	0.027	0.015	0.008	0.008	0.002	0.000	0.002
0.32	0.039	0.039	0.033	0.021	0.013	0.013	0.004	0.000	0.002
0.40	0.042	0.044	0.043	0.033	0.023	0.022	0.008	0.001	0.003
0.50	0.042	0.046	0.058	0.054	0.042	0.040	0.017	0.003	0.004
0.63	0.039	0.044	0.067	0.083	0.075	0.075	0.039	0.008	0.008
0.79	0.063	0.059	0.063	0.105	0.118	0.120	0.082	0.022	0.016
1.00	0.097	0.097	0.083	0.100	0.139	0.148	0.144	0.058	0.030
1.26	0.102	0.104	0.121	0.101	0.122	0.128	0.197	0.114	0.052
1.58	0.104	0.104	0.112	0.129	0.109	0.102	0.183	0.174	0.081
2.00	0.090	0.098	0.098	0.110	0.117	0.109	0.115	0.203	0.104
2.51	0.066	0.072	0.075	0.074	0.082	0.084	0.065	0.177	0.113
3.16	0.042	0.045	0.050	0.052	0.047	0.049	0.052	0.112	0.109
3.98	0.024	0.027	0.029	0.029	0.031	0.032	0.033	0.051	0.098
5.01	0.016	0.016	0.018	0.018	0.019	0.018	0.018	0.023	0.089
6.31	0.011	0.011	0.012	0.012	0.012	0.012	0.013	0.018	0.081
7.94	0.007	0.007	0.008	0.008	0.008	0.008	0.009	0.014	0.067
10.00	0.005	0.005	0.005	0.006	0.005	0.006	0.006	0.008	0.051
12.59	0.003	0.003	0.003	0.004	0.004	0.004	0.004	0.006	0.034
15.85	0.002	0.002	0.002	0.002	0.002	0.003	0.002	0.003	0.021
19.95	0.001	0.001	0.002	0.002	0.002	0.002	0.002	0.002	0.012
25.12	0.001	0.001	0.001	0.001	0.002	0.001	0.001	0.002	0.008

Table 3g 0835 Linear Extrapolation

IX. CTQ-79 Comparison with NPS Optics

In June of 1979 NPS conducted a research cruise on Monterey Bay. The purpose of the operation was to determine the proper scaling expressions for overwater water vapor transport to be used in optical propagation models.[16] Coincident overwater optical measurments were made in order to compare measured and calculated extinction and scintillation. Since the ship was not dedicated to optical comparisons, these data were obtained as targets of opportunity and the number of comparisons is not large.

The Knollenberg ASASP and CSASP spectrometers were mounted on the access platform of the RV/ACANIA meteorological mast at a height of approximately 10 m above mean sea level. This is higher than the average height of the optical path. Optical measurements were made on the NPS 13.6 km optical range which has end points at Pt. Pinos and Marina. Both end points are immediately adjacent to the shoreline.

Optical extinction was measured at 0.4880, 0.6328, 0.84, 1.03, 1.06, and 11.05 μm. The molecular contribution to the extinction was computed using LOWTRAN III B[17] adapted for use on a Hewlett Packard 9835 computer. Meteorological input data for the calculation was obtained on board the ship. Subtracting the calculated molecular component from the optically measured extinction yielded the aerosol extinction. The wavelengths used for the comparison were chosen because the optical filters used are narrow which simplifies the LOWTRAN calculation. Rather than integrate over the width of the filter, it was possible to simply calculate the molecular component

for a 5 cm^{-1} wide region at the center of the filter band. This was the method used for the results presented here.

The aerosol contribution to the extinction was also calculated from the measured aerosol spectra by the methods outlined earlier in this report. Due to the method of obtaining the data, it was not possible to use the new binning method, but the combined linear-constant extrapolation to larger sizes was used.

The results are presented in Table 4. The extinction in units of 10^{-2} km^{-1} as measured optically, the calculated molecular contribution, their difference, and the values calculated from the aerosol spectra are shown. A comparison of the aerosol extinctions as determined from the two methods is also shown in Figure 27. The figure shows that the aerosol spectra determined values are higher than optical for all wavelengths except 11 μm. (The optically measured values for 0.4880 μm appear to be in error.) The systematic error is approximately 40% comparing to the optical value. The comparison is expected to be poorest for long wavelengths where the molecular extinction is dominant since the difference between two large numbers is expected to yield large errors. However, this is not true for these data. The percent error at 11 μm is not significantly different and, in addition, the systematic difference is not present.

It is not possible to identify the source of the systematic difference. Five sources are possible: (1) aerosol measurements, (2) optical measurements, (3) LOWTRAN calculation, (4) aerosol calculation, (5) path average different from point measurement. The extrapolation method of the aerosol calculation is suspect but the

Table 4. Extinction (10^{-2} km^{-1})

Date/Time	λ (μm)	Optics	Lowtran	Difference	Aerosol
6/5 1830	11.0	18.3	13.8	4.5	8.0
6/6 1620	11.0	15.1	9.4	5.7	8.1
1720	0.49	22.9	1.9	21	33
"	0.63	22.5	0.7	22	33
"	0.84	22.1	4.1	18	32
"	1.03	19.4	0.1	19	33
"	1.06	21.7	0.1	22	32
"	1.6	22.7	0.5	22	32
1805	11.0	15.0	9	6	8.2
6/7 1405	11.0	19.7	18	2	7.6
1430	1.03	43.9	0.1	44	49
"	1.06	35.4	0.1	35	49
1550	11.0	20.0	17.6	2.4	7.8
1630	0.63	43.2	0.7	42	52
"	0.84	40.1	5.0	35	51
"	1.03	35.0	0.1	35	51
"	1.06	38.3	0.1	38	51
"	1.6	35.3	0.5	35	49
1715	11.	19.9	16	4	4.7
1730	1.6	26.6	0.5	26	37
1740	0.49	62.0	1.9	60	30
"	0.84	30.0	4.4	26	30
"	1.03	28.8	0.1	29	30
"	1.06	30.3	0.1	30	30
1900	0.49	52.6	1.9	51	26
"	0.63	21.9	0.7	21	26
"	0.84	20.6	4.1	17	26
"	1.03	18.5	0.1	18	26
"	1.00	20.1	0.1	20	26
"	1.6	19.7	0.5	19	25
"	11.0	14.9	8.6	6	4.8
2000	11.0	14.0	9.0	5	5.9
2020	0.49	50.2	1.9	48	25
"	0.63	19.5	0.7	19	25
"	0.84	18.4	2.1	16	25
"	1.03	17.5	0.1	17	25
"	1.06	18.3	0.1	18	25

Date/Time	λ (μm)	Optics	Lowtran	Difference	Aerosol
6/7 2040	11	15.0	9.0	6	5.9
6/8 0900	0.63	25.6	0.7	25	31
"	0.84	24.2	4.9	19	30
"	1.03	22.4	0.1	22	30
"	1.00	24.0	0.1	24	30
0920	1.6	21.5	0.5	21	28
0930	11	21.2	14.9	6	4.7
0950	0.49	58.2	1.9	56	33
"	0.63	27.0	0.7	26	33
"	0.84	25.2	4.9	20	32
"	1.03	22.7	0.1	23	32
"	1.06	24.2	0.1	24	32
"	1.6	24.5	0.5	24	31
1015	11	25.4	14.9	11	5.9

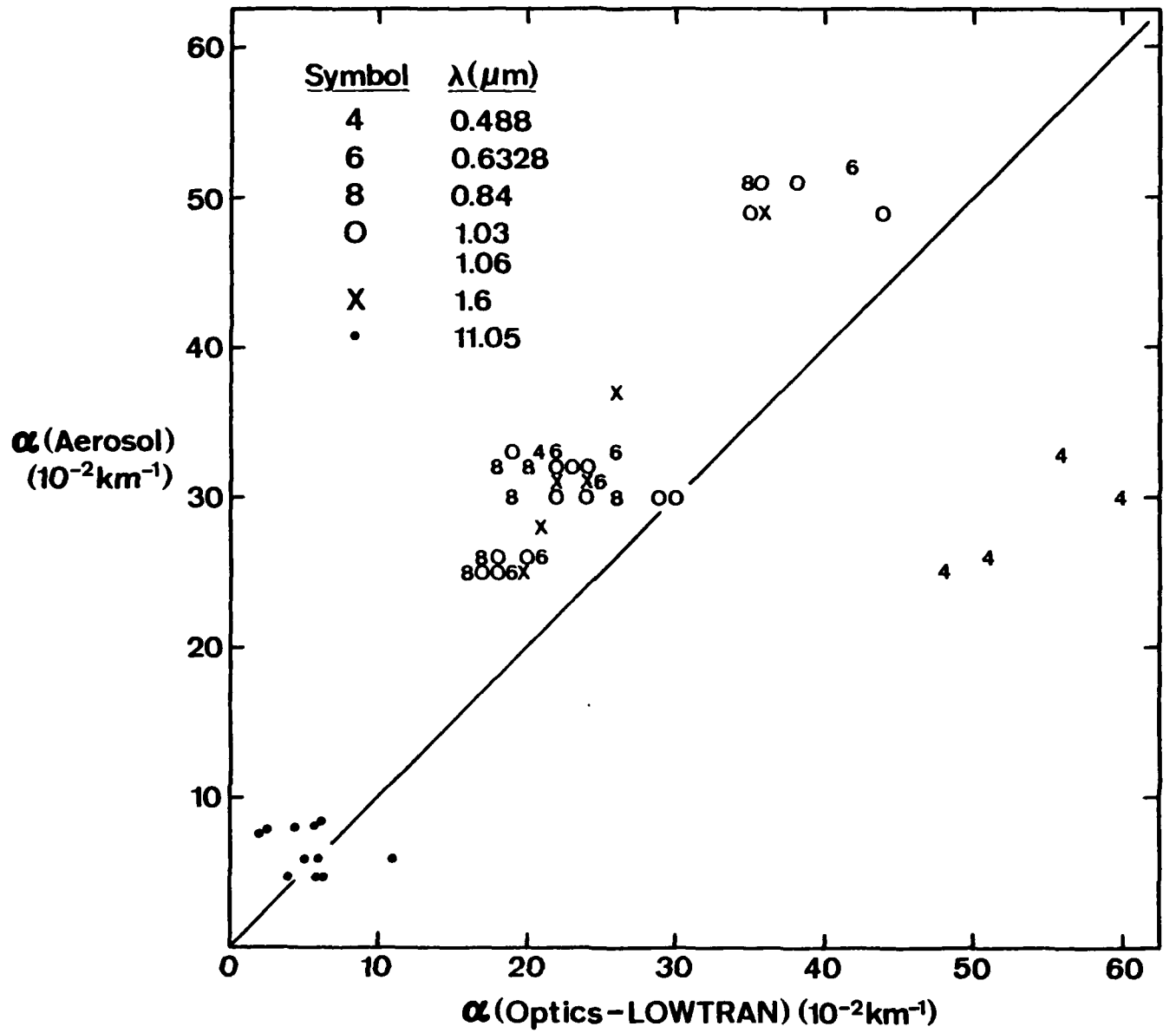
Symbol λ(μm)
4 0.488
6 0.6328
8 0.84
O 1.03
1.06
X 1.6
• 11.05
α(Aerosol) (10⁻²km⁻¹)
α(Optics-LOWTRAN) (10⁻²km⁻¹)
0
10
20
30
40
50
60

Figure 27

long wavelength results are most sensitive to the extrapolation and it is here that the comparison is best. Apparently, the extrapolation technique works reasonably well. Even with the systematic difference these results are quite good since a 40% error is within acceptable bounds for EO/MET applications.

LOWTRAN note: The LOWTRAN III B and LOWTRAN IV codes were found to have an error which produces erroneous results for 1.06 μm. This is due to peculiarities in the division of the wavelength spectrum into bands. For details, contact NPS.

X. Summary and Recommendations

The PMS spectrometers owned and operated by NPS have been calibrated and operated under a wide range of conditions. Comparisons have been made with other aerosol spectrometers and with optical equipment. No systematic instrument errors were observed that couldn't be accounted for by external conditions, or by the ambiguity zones.

In general the units performed quite well, but certain problem areas exist, which are listed below:

1. For wind directions greater than 30° away from the inlet the number of counts decreases.
2. At high wind speeds it appears that the air flow rate in the scattering chamber increases, thereby increasing the apparent particle density.
3. Noise counts are registered in the small size bins of each range and the magnitude of this effect depends on system cleanliness[15]
4. The percentage of the counting time for large sizes is too small, giving poor statistics.
5. Ambiguity zones cause incorrect sizing within some ranges.

These problems do not make the spectrometers ineffective but mean that they must be used with care. We recommend the following:

1. Provisions must be made for keeping the spectrometer pointed into the wind.
2. Delete at least the first 3 size lines from each range for the ASASP.

3. Fit all data with a low order polynominal in order to smooth over ambiguity zone errors and expected data fluctuations.
4. Don't use a spectrometer for a purpose for which it was not designed (interchanging aircraft/ground based units) without insuring correct mean and turbulent flow through the sample chamber.

Changing the counting time fraction would require a factory modification and is not an option available to the operator.

Laboratory measurements should be made to determine the sampling chamber flow rate under various wind conditions, particularly high winds. This would enable corrections to be made to the data for high wind conditions.

Note that method 2 used for NPS data is essentially the same as that used by Trusty of NRL. He replaces all data for range 0 of the ASASP with a single point.

Note that there is an error in the LOWTRAN code as described in section IX.

Finally, in our opinion, the types of spectrometers used by NPS perform sufficiently well to be used to determine the aerosol contribution to optical extinction for EO/MET applications.

References

1. Pinnick, R. G. and H. J. Auvermann, J. Aerosol Science 10, 55 (1979).

2. "Experimental Aspects of a Shipboard System Used in Investigations of Overwater Turbulence and Profile Relationships," T. M. Houlihan, K. L. Davidson, C. W. Fairall, and G. E. Shacher, NPS-61-78-001.

3. "Atmosphere Marine Boundary Layer Measurements in the Vicinity of San Nicolas Island during CEWCOM-78," G. W. Fairall, G. E. Schacher, K. L. Davidson, and T. M. Houlihan, NPS 61-78-007.

4. Results calculated and made available by D. Jensen, NOSC.

5. "Results of Naval Postgraduate School Aerosol Measurements for San Nicolas Island Spectrometer Intercomparison," G. E. Schacher, C. W. Fairall, and K. L. Davidson, NPS 61-79-011 PR.

6. Jaenicke, R. J. Aerosol Science 3, 95 (1972).

7. R. Knollenberg, private communication.

8. "Reduced Data from Calspan's Participation in the CEWCOM-78 Field Experiment of the Coast of Southern California during May 1978," E. J. Mack and T. A. Niziol, Calspan Report #6232-M-2.

9. Gene Mack, Calspan Corporation, private communication.

10. "Optical Experiments in the Marine Boundary Layer," E. C. Crittenden, A. Cooper, E. Milne, W. Rodeback, R. Armstead and S. Kalmbach, NPS 61-78-006.

11. Wells, W. C. and M. W. Munn, Applied Optics 16, 654 (1977)

12. "On the Growth of Aerosol Particles with Relative Humidity," J. W. Fitzgerald, NRL Memorandum Report 3847, 1978

13. G. Mathews, unpublished data, Pacific Missile Test Center.

14. G. Trusty, Proc. Workshop on Remote Sensing of the Marine Boundary Layer, p.53 (1977)

15. Particle Measurement Systems, ASASP instruciton manual

16. "Measurements of the Humidity Structure Function Parameters, c_q^2 and c_{tq}, over the ocean", C. W. Fairall, G. E. Schacher, and K. L. Davidson, accepted Boundary Layer Meteorology.

17. "Naval Weapons Center Version of the Atmospheric Transmittance Computer Code LOWTRAN: User's Manual and Program Listing," W. M. Cornette, NWC Technical Memorandum 3107, 1977.

DISTRIBUTION LIST

		No. of Copies
1.	Defense Documentation Center Cameron Station Alexandria, Virginia 22314	2
2.	Library, Code 0142 Naval Postgraduate School Monterey, California 93940	2
3.	Dean of Research, Code 012 Naval Postgraduate School Monterey, California 93940	1
4.	Dr. C. W. Fairall BDM Corporation, 1340 Munras St. Monterey, California 93940	4
5.	Professor J. Dyer, Code 61Dy Naval Postgraduate School Monterey, California 93940	1
6.	Professor G. J. Haltiner, Code 63Ha Naval Postgraduate School Monterey, California 93940	1
7.	Assoc. Professor K. L. Davidson, Code 63Ds Naval Postgraduate School Monterey, California 93940	4
8.	Professor G. Schacher, Code 61Sq Naval Postgraduate School Monterey, California 93940	10
9.	Professor E. C. Crittenden, Code 61Ct Naval Postgraduate School Monterey, California 93940	1
10.	Dr. J. H Richter Code 532 Naval Oceans Systems Center San Diego, California 92152	1
11.	Dr. Lothar Rohnke Code 8320 Naval Research Laboratory Washington, D. C. 20375	1
12.	Dr. D. Jensen Code 5322 Naval Oceans Systems Center San Diego, California 92152	1

13. Mr. H. Hughes — 1
Code 5332
Naval Ocean System Center
San Diego, California 92152

14. Dr. J. Fitzgerald — 1
Code 8326
Naval Research Laboratory
Washington, D. C. 20375

15. Mr. Jeck — 1
Code 8323
Naval Research Laboratory
Washington, D. C. 20375

16. Dr. G. Trusty — 1
Code 5568
Naval Research Laboratory
Washington, D. C. 20375

17. Dr. A. Shlanta — 1
Code 3173
Naval Weapons Center
China Lake, California 93555

18. Dr. Barry Katz — 1
Code R42
Naval Surface Weapons Center
White Oak Laboratory
Silver Spring, Maryland 20362

19. Mr. Eugene J. Mack — 1
Calspan Corporation
Buffalow, New York 14221

20. Dr. R. Knollenberg — 1
Particle Measurements, Inc.
1855 S. 57th Ct.
Boulder, Colorado 80301

21. Mr. G. Mathews — 1
Code 1232
Pacific Missile Test Center
Point Mugu, California 93042

22. Mr. J. Rosenthal — 1
Code 3253
Pacific Missile Test Center
Point Mugu, California 93042

23. CDR K. Van Siekle — 1
Code Air-370
Naval Air Systems Command
Washington, D. C. 20360

AD-A087 656 NAVAL POSTGRADUATE SCHOOL MONTEREY CA F/G 4/1
OPTICAL AEROSOL SPECTROMETERS FACTORS AFFECTING OPTICAL EXTINCT--ETC(U)
APR 80 G E SCHACHER, K L DAVIDSON
UNCLASSIFIED NPS-61-80-013 NL

2 - 2

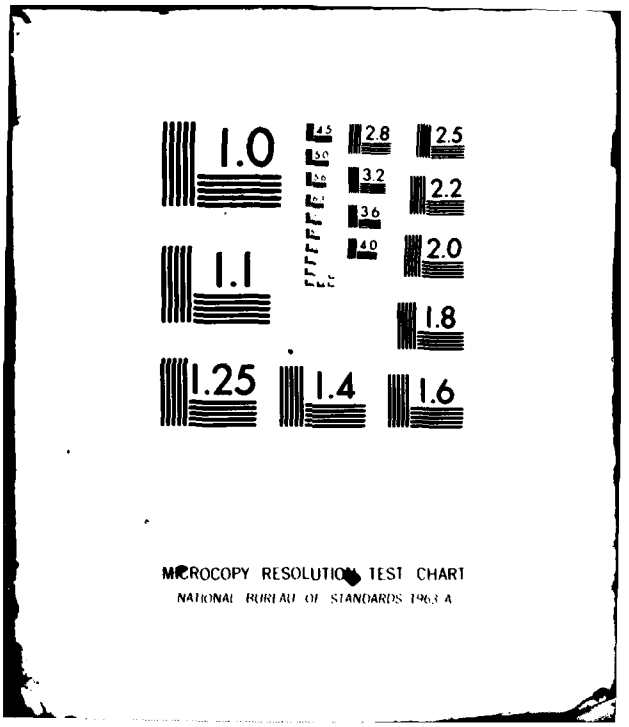
1.0
1.1
1.25
1.4
1.6
1.8
2.0
2.2
2.5
2.8
3.2
3.6
4.0
MICROCOPY RESOLUTION TEST CHART
NATIONAL BUREAU OF STANDARDS 1963 A

24. Lt. Gary Ley 1
PMS-405
Naval Sea Systems Command
Washington, D. C. 20360

25. Dr. A. Goroch 1
Naval Environmental Research Prediction Facility
Monterey, California 93940

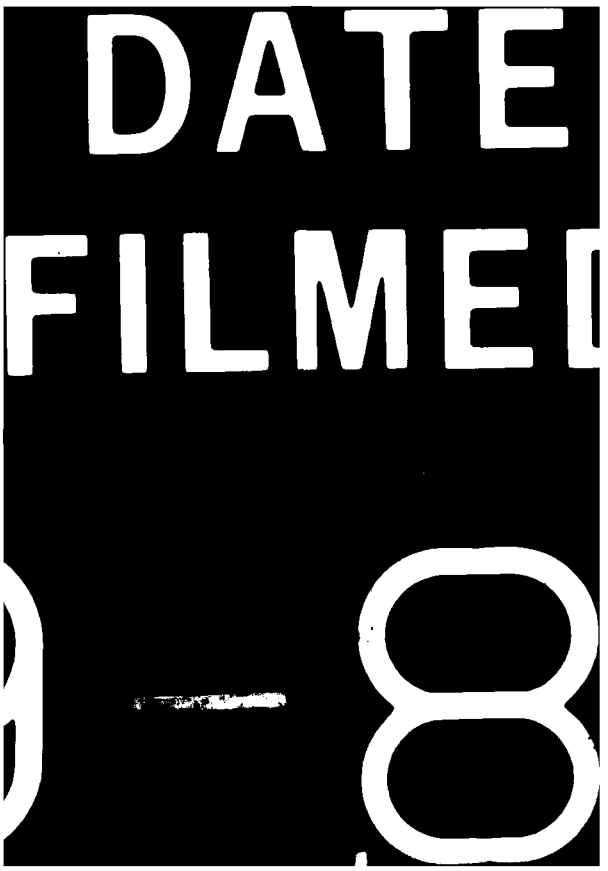
DATE
FILME
8